

Preparation of Acrylic Monomer Grafted PET Films by γ ray Irradiation for Selective Adsorption of Hazardous Metal Ions

ナジア, ラーマン

<https://doi.org/10.15017/1470558>

出版情報 : Kyushu University, 2014, 博士 (工学), 課程博士
バージョン :
権利関係 : 全文ファイル公表済

**Preparation of Acrylic Monomer Grafted PET
Films by γ Ray Irradiation for Selective
Adsorption of Hazardous Metal Ions**

Nazia Rahman

**Preparation of Acrylic Monomer Grafted PET
Films by γ Ray Irradiation for Selective
Adsorption of Hazardous Metal Ions**

by

Nazia Rahman

Supervisor

Prof. Dr. Kazuhiro HARA

A thesis submitted to the Kyushu University in accordance with the requirements for the degree of Doctor of Philosophy in the Graduate School of Engineering

June, 2014

CONTENTS

	Page
CHAPTER 1: General Introduction	1
1.1. Heavy metals in industrial waste waters and their adverse effect on human health	1
1.2. Heavy metal removal from industrial waste water: Permissible limits and recovery methods	2
1.3. Polyethylene terephthalate (PET), and the reasons behind choosing PET as the base material to prepare metal ion adsorbents	6
1.4. Grafting of functional monomers on PET to improve metal adsorption property: Grafting methods	9
1.5. Previous studies on the adsorption of heavy metals by the monomer grafted PET and present approach of selective adsorption	15
1.6. Investigation of metal adsorption process: Isotherms and kinetics	17
1.6.1. Modeling of metal adsorption isotherms	17
1.6.2. Modeling of metal adsorption kinetics	18
1.7. Objectives of present study	19
CHAPTER 2: The effect of hot DMSO treatment on γ-ray induced grafting of acrylamide onto PET film	23
2.1. Introduction	23
2.2. Materials and Methods	27
2.2.1. Materials	27

2.2.2.	Sorption of AAm solution to the DMSO-treated PET films	27
2.2.3.	Grafting of AAm onto the DMSO-pretreated PET films	28
2.2.4.	Optical micrograph	29
2.2.5.	X-ray diffraction	29
2.2.6.	Infrared (IR) spectroscopy	30
2.2.7.	Scanning electron microscopy (SEM)	30
2.2.8.	Water uptake measurements	30
2.2.9.	Hydrolysis of AAm-grafted PET film And Hg(II) uptake measurements	31
2.2.9.1.	Determination of hydrolysis percentage of AAm	31
2.2.9.2.	Determination of Hg(II) uptake efficiency	31
2.3.	Experimental results	32
2.3.1.	DMSO-assisted grafting of AAm onto the PET films by γ irradiation	32
2.3.1.1.	Effect of DMSO treatment temperature on grafting of AAm	33
2.3.1.2.	Effect of FeCl ₃ on AAm grafting	35
2.3.1.3.	Effect of monomer concentration on grafting of AAm	35
2.3.1.4.	Effect of dose and dose rate on grafting of AAm	36
2.3.2.	Optical micrographs of the PET films	39
2.3.3.	X-ray diffraction analysis of PET films	42

2.3.4.	FTIR spectroscopic analysis of PET films	45
2.3.5.	Scanning electron microscopic analysis of PET films	47
2.3.6.	Water uptake measurements	51
2.3.7.	Hg(II) uptake	52
2.4.	Discussion	53
CHAPTER 3: Selective Hg(II) adsorption from aqueous solutions of Hg(II) and Pb(II) by hydrolyzed acrylamide-grafted PET films		58
3.1.	Introduction	58
3.2.	Experimental	59
3.2.1.	Materials and Reagents	59
3.2.2.	Instrument and Apparatus	60
3.2.3.	Grafting of AAm onto the PET films by γ -ray irradiation	60
3.2.4.	Hydrolysis of AAm-grafted PET films	61
3.2.5.	Metal ion adsorption by the hydrolyzed AAm-grafted PET film	61
3.2.6.	Determination of metal ion uptake capacity	61
3.2.7.	Desorption of metal ions	62
3.3.	Results and discussion	62
3.3.1.	Preparation and characterization of the adsorbent film	62
3.3.2.	Selective adsorption of Hg(II) ions by the adsorbent film from aqueous solutions containing Hg(II) and Pb(II)	67
3.3.3.	Adsorption kinetics of selective Hg(II) adsorption	68

3.3.4.	Equilibrium adsorption isotherms of selective Hg(II) adsorption	73
3.3.5.	Effect of pH on selective Hg(II) adsorption	75
3.3.6.	Desorption of Hg(II) and reuse of the adsorbent	77
3.4.	Conclusion	79
CHAPTER 4: Selective Cu(II) adsorption from aqueous solutions including Cu(II), Co(II) and Ni(II) by modified acrylic acid grafted PET film		80
4.1.	Introduction	80
4.2.	Experimental	82
4.2.1.	Materials and Reagents	82
4.2.2.	Instrument and Apparatus	82
4.2.3.	Grafting of AAc onto the PET films by gamma radiation	83
4.2.4.	KOH treatment of the AAc grafted film	83
4.2.5.	Metal ion adsorption by the modified AAc grafted PET film	84
4.2.6.	Determination of metal ion uptake capacity	84
4.2.7.	Desorption of metal ions	84
4.3.	Results and discussion	85
4.3.1.	Preparation and characterization of the adsorbent film	85
4.3.2.	Selective Cu(II) ion adsorption by the adsorbent film	93
4.3.3.	Equilibrium adsorption isotherm of selective Cu(II) ion adsorption	94

4.3.4.	Adsorption kinetic of selective Cu(II) ion adsorption	99
4.3.5.	Effect of pH on selective Cu(II) ion adsorption	105
4.3.6.	Desorption and reuse of the adsorbent	105
4.4.	Conclusion	107
CHAPTER 5: Summary and future study		108
5.1.	Summary of present study	108
5.2.	Suggestion of future study	111
References		113
Appendix A		126
List of publications		128
Acknowledgments		129

List of Tables

	Page
CHAPTER 1	
Table 1.1: Permissible limits for industrial effluent discharge	3
Table 1.2: Brief description of the previous studies on grafting of vinyl and acrylic monomers on PET through γ-ray induced grafting	13
CHAPTER 2	
Table 2.1: A comparison of graft yield and/or graft density derived in the present study (γ-ray) with the results obtained using other methods	38
Table 2.2: The removal of Hg(II) ions by the pristine PET and the hydrolyzed, AAm-grafted PET films.	52
CHAPTER 3	
Table 3.1. Hg(II) and Pb(II) adsorption capacity of AAm-grafted PET and hydrolyzed AAm-grafted PET compared with those of other adsorbents (from single metal solutions)	63
Table 3.2. Pseudo-first-order and pseudo-second-order rate constants for selective Hg(II) adsorption	69
CHAPTER 4	
Table 4.1: Metal ion adsorption capacity of AAc grafted PET, modified AAc grafted PET compared with some other adsorbents	86
Table 4.2: Langmuir and Freundlich isotherm parameters for selective Cu(II) adsorption	96
Table 4.3: The pseudo-first-order and pseudo-second-order rate constants for selective Cu(II) adsorption	102

List of Figures

	Page
CHAPTER 1	
Figure 1.1: (a) A short section of a PET polymer chain (b) The repeating unit of PET	6
Figure 1.2: Functionalization of PET through grafting with acrylic monomers.	10
Figure 1.3: General mechanism of grafting of acrylic monomers on PET film.	14
CHAPTER 2	
Figure 2.1. Weight gain (× after soaking in DMSO for 0.5 h, ○ after soaking in 50 wt % AAm solution for 24 h) and graft yield (● after grafting at 50 wt % AAm monomer concentration, with a 50-kGy dose at a dose rate of 1 kGy/h, and at 1 wt % FeCl₃) as a function of the DMSO pretreatment temperature.	34
Figure 2.2. The AAm monomer concentration dependence of the AAm-graft yield onto the 140 °C DMSO pretreated PET films while maintaining the other grafting conditions: a 50-kGy total dose, a 1-kGy/h dose rate and the presence of 1 wt % FeCl₃.	36
Figure 2.3. The total γ-ray dose dependence of the AAm-graft yield on the 140 °C DMSO-pretreated PET films with all other grafting conditions held constant: 50 wt % AAm, a 1-kGy/h dose rate and the presence of 1 wt % FeCl₃.	37
Figure 2.4. Optical micrographs of (a) the pristine PET film, (b) the DMSO-pretreated (at 140 °C) wet film, (c) the wet AAm-solution-soaked DMSO-pretreated film (DMSO pretreated at 140 °C and soaked in 50 wt % AAm solution) and (d) AAm grafted PET film (DMSO pretreated at 140 °C and γ-ray irradiated with a	40

50-kGy dose at a 1-kGy/h dose rate in the presence of 1 wt % FeCl₃ after soaking in 50 wt % AAm solution)

Figure 2.5. Optical micrographs of the wet PET films with (a) DMSO pretreatment at 100 °C, (b) AAm sorption (50 wt % AAm solution) after (a), (c) DMSO pretreatment at 140 °C, (d) AAm sorption (50 wt % AAm solution) after (c), (e) DMSO pretreatment 160 °C, and (f) AAm sorption (50 wt % AAm solution) after (e) 41

Figure 2.6.(a). X-ray diffractogram of pristine PET film 43

Figure 2.6.(b). X-ray diffractogram of wet PET films with DMSO pretreatment at 140 °C 43

Figure 2.6.(c). X-ray diffractogram of AAm soaked (50 wt % AAm solution) wet film after DMSO pretreatment at 140 °C 44

Figure 2.6.(d). X-ray diffractogram of AAm grafted PET film (DMSO pretreated at 140 °C and γ -ray irradiated with a 50-kGy dose at a 1-kGy/h dose rate in the presence of 1 wt % FeCl₃ after soaking in 50 wt % AAm solution) 44

Figure 2.7. FTIR spectra in the (a) higher and (b) lower wavenumber regions for (1) pristine PET, (2) the AAm grafted PET with an 8.6 % graft yield, and (3) with a 12.9 % graft yield. (c) The graft yield dependence of the absorbance ratio of the IR peak at 3200 cm⁻¹ to that at 3054 cm⁻¹ 46

Figure 2.8.(a). SEM micrograph of pristine PET film surface 48

Figure 2.8.(b). SEM micrograph of the AAm grafted PET film 49

Figure 2.8.(c). The contrast-enhanced image of Figure 2.8.(b). 50

Figure 2.9. The graft yield dependence of the water uptake in the AAm-grafted PET films. 51

CHAPTER 3

Figure 3.1. FTIR spectra of (1) ungrafted PET film, (2) AAm-grafted PET film, (3) hydrolyzed AAm-grafted PET film, and (4) Hg(II)-loaded hydrolyzed AAm-grafted PET film. 65

Figure 3.2. SEM images of hydrolyzed AAm-grafted PET films (a) before Hg(II) loading, and (b) after Hg(II) loading. 66

Figure 3.3. Adsorption kinetics for competitive adsorption of Hg(II) and Pb(II) by hydrolyzed AAm-grafted films with the same initial concentration of metal ions (pH 4.5; initial concentration = 100 mg/L). 70

Figure 3.4.1. Pseudo-first-order plot for selective Hg(II) adsorption. 71

Figure 3.4.2 Pseudo-second-order plot for selective Hg(II) adsorption. 72

Figure 3.5. Equilibrium adsorption isotherm for competitive adsorption of Hg(II) and Pb(II) by the hydrolyzed AAm-grafted films with the same initial concentrations of metal ions (pH 4.5; $t = 40$ min). 74

Figure 3.6. Langmuir isotherm plot for selective Hg(II) adsorption. 75

Figure 3.7. Effect of pH on the competitive adsorption of Hg(II) and Pb(II) by the hydrolyzed AAm-grafted films with the same initial concentration of metal ions (initial concentration = 500 mg/L; $t = 40$ min). 76

Figure 3.8. Repeated use of a hydrolyzed AAm-grafted film for adsorption of Hg(II) from a mixture of Hg(II) and Pb(II) (pH 4.5; $t = 40$ min; $C_i = 100$ mg/L). 78

CHAPTER 4

Figure 4.1. (a) AAc grafted PET (b) AAc grafted PET after 85

modification by KOH treatment (c) Modified AAc grafted PET film after Cu(II) loading (d) Modified AAc grafted PET film after Co(II) loading (e) Modified AAc grafted PET film after Ni(II) loading.

Figure 4.2. FTIR spectra of (1) ungrafted PET film (2) AAc grafted PET film (3) KOH treated film AAc grafted PET film. The spectra are split into the two figures at 1900 cm^{-1} . 88

Figure 4.3.(a). SEM micrograph of ungrafted PET film. 90

Figure 4.3.(b). SEM micrograph of AAc grafted PET film, (b-1) graft chains are attracted by hydrogen bonding and the functional groups are inaccessible to the metal ions. 91

Figure 4.3.(c). SEM micrograph modified AAc grafted PET, (c-1) graft chains are repulsed by electrostatic force of $-\text{COO}^-$ group and the functional groups are accessible to the metal ions 92

Figure 4.4. Equilibrium adsorption isotherm for competitive adsorption of Cu(II), Ni(II) and Co(II) by the modified graft films under the same initial concentrations of metal ions. (pH 4; $t = 60$ min; $G = 40\%$) 95

Figure 4.5.1. Langmuir isotherm plot for selective Cu(II) adsorption 97

Figure 4.5.2. Freundlich isotherm plot for selective Cu(II) adsorption 98

Figure 4.6: Adsorption kinetics for competitive adsorption of Cu(II), Ni(II) and Co(II) by the modified graft films under the same initial concentrations of metal ions. (pH 4; Initial concentration, $C_i = 2000\text{ mg/L}$; $G = 40\%$) 101

Figure 4.7.1. Pseudo-first order plot for selective Cu(II) adsorption 103

Figure 4.7.2. Pseudo-second order plot for selective Cu(II) adsorption 104

Figure 4.8: Effect of pH on the competitive adsorption of Cu(II), Ni(II) and Co(II) by the modified graft films under the same initial concentrations of metal ions. (t =60 min; Initial concentration = 500 mg/L; G = 40 %) 106

Figure 4.9. Repeated use of modified AAc grafted film for adsorption of Cu(II) from mixture of Cu(II), Co(II) and Ni(II) [pH 4; t = 60 min; C_i = 500 ppm; G = 40 %] 107

CHAPTER 1

General Introduction

1.1. Heavy metals in industrial waste waters and their adverse effect on human health

Elements which have atomic weights between 63.5 and 200.6, and a specific gravity greater than 5.0 are termed as heavy metals [Srivastava et al., 2008]. With the rapid development of industries such as metal plating facilities, mining operations, fertilizer industries, tanneries, batteries, paper industries and pesticides, etc., the discharge of toxic heavy metals into the environment as industrial wastewaters increased excessively and became one of the most serious environmental problems.

Toxic heavy metals often detected in industrial wastewaters include copper, nickel, mercury, lead, cadmium, zinc, and chromium. Copper is important for animal metabolism, but excessive ingestion of copper causes adverse health effects, such as vomiting, cramps, convulsions, or even death [Paulino et al., 2006]. The most common effect of nickel is skin dermatitis. It can also cause lung and kidney problems, gastrointestinal distress and pulmonary fibrosis [Borba et al., 2006]. Nickel is known as human carcinogen. Mercury may have toxic effects on the central nervous system. High concentrations of mercury may result in damage to the gastrointestinal tract, the nervous system, and the kidneys [Namasivayam et al., 1999]. Lead poisoning can cause a number of adverse human health effects such as damage of the central nervous system, the kidney, liver and reproductive system, basic cellular processes and brain

functions. The noxious symptoms include anemia, insomnia, headache, dizziness, irritability, weakness of muscles, hallucination and renal damages [Naseem et al., 2001]. The acute (short-term) inhalation exposure of cadmium may cause pulmonary irritation. Chronic (long-term) inhalation or oral exposure to cadmium leads to Kidney dysfunction. U.S. Environmental Protection Agency classified cadmium as a probable human carcinogen. Zinc is a trace element necessary for proper functioning of human body and is commonly found in nutritional supplements. However, taking too much zinc into the body can bring about health problems, such as stomach cramps, skin irritations, vomiting, nausea and anemia [Oyaro et al., 2007]. Chromium occurs in the environment mainly in two valence states, trivalent chromium Cr(III) and hexavalent chromium Cr(VI). The respiratory tract is the major target organ for Cr(VI) and Cr(III) toxicity. Cr(VI) is more toxic than Cr(III). Cr(VI) inhalation exposure can cause lung tumors [Khezami et al., 2005].

1.2. Heavy metal removal from industrial waste water: Permissible limits and recovery methods

Heavy metals are non-biodegradable, so unlike many organic pollutants, toxic metals discharged in aquatic streams are not decomposed by microbiological activity; rather these tend to accumulate in lower plants and animals and thereby enter the food chain. Furthermore the polluted areas can become widened by diffusion in the environment [D'Itri et al., 1998]. Well known environmental destruction cases due to the contamination of heavy metals in aquatic streams are Minamata tragedy (organic mercury poisoning) and Itai-itai disease (cadmium poisoning) in Japan. In 1968 the

government of Japan recognized that the Minamata disease was caused by the discharge of mercury containing wastes by a nearby industry. At the same time Japanese Ministry of Health and Welfare declared that the *Itai-Itai* disease was suspected to be caused by the cadmium eluted off to the upstream of Jintsu River from Kamioka Mine [Ui, 1992]. These disasters ignited public interest in heavy metals as potential hazards for human life and health. With recent advances in the understanding of the behavior of heavy metals in the environment and their toxicity, various regulatory bodies have set the maximum prescribed limits for the discharge of toxic heavy metals in the aquatic systems (Table 1.1) [National effluent standards at Ministry of the Environment, Government of Japan; Sud et al., 2008].

Table 1.1. Permissible limits for industrial effluent discharge [National effluent standards at Ministry of the Environment, Government of Japan; Sud et al., 2008]

Metal Contaminant	Permissible limits in Japan (mg/L)	Permissible limits by international bodies (µg/L)	
		WHO	USEPA
Cadmium	0.1 ^a	3	5
Lead	0.1 ^b	10	5
Hexavalent chromium compounds	0.5	-	-
Arsenic	0.1 ^c	10	50
Mercury	0.005	1	2
Copper	3	-	-
Zinc	2	-	1300
Chromium	2	50	100

^aCadmium and its compounds, ^bLead and its compounds, ^cArsenic and its compounds.

To maintain the regulation standard of toxic heavy metals in the industrial effluents, the availability of the recovery agent at low cost and their easy handling is important. Again the recovery process should be such that it can be accomplished with simple equipments and low energy consumption. Another important consideration is the easy separation of the hazardous heavy metal ion from the recovery agent and in this case, incineration which may generate carbon dioxide and detrimental gas should be avoided [Hara et al., 2004].

Most commonly used methods for removal of hazardous metal ions from industrial waste water includes precipitation, ion exchange, electrochemical method, activated carbon adsorption etc. But these methods have some disadvantages.

Chemical precipitation methods in which chemicals react with heavy metal ions to form insoluble precipitates are the most widely used process in industry [Ku et al., 2001]. However, the precipitation methods do not always provide a satisfactory removal rate to meet the pollution control limits and produces toxic sludge along with the difficulty in recovering metals from the sludge.

In ion-exchange processes active groups of the resins are exchanged with metal ions. These methods have high treatment capacity and removal efficiency. But the high cost of resins and high operational costs are the demerits of these methods.

Electrochemical methods can recover metals in the elemental metal state through the plating-out of metal ions on a cathode surface. However, electrochemical wastewater technologies require relatively large capital investment and the expensive electricity supply.

Now-a-days adsorption is recognized as one of the most effective and economic method for heavy metal wastewater treatment. The advantages of

adsorption process include flexibility in design and operation.

Activated carbon (AC) adsorbents were commonly used in the heavy metal waste water treatment due to its large micropore and mesopore volumes and the resulting high surface area [Fu et al., 2011]. But currently the exhausted source of commercial coal-based AC caused increase of price of these adsorbents. Again these adsorbents are difficult to regenerate and reuse.

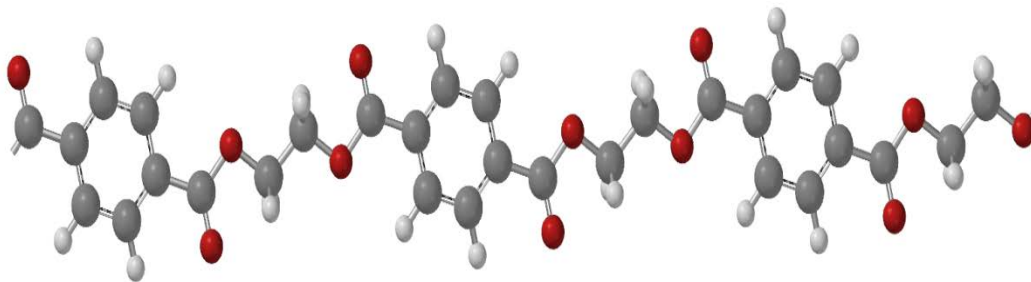
Many types of alternative low cost adsorbents have been studied for the adsorption of metal ions from aqueous solutions including sawdust [Sciban et al., 2006], sporopollenin [Ünlü et al., 2006; Arslan et al., 2004], chitosan [Schmuhl et al., 2001], peat [Ho et al., 2001], cellulose [Shukla et al., 1992] clay mineral [Al-Degs et al., 2006] etc. However, some of these adsorbents do not have high adsorption capacities or need long adsorption equilibrium times while others are not suitable for reuse.

To circumvent these limitations, numerous approaches have been studied. A recent development in the field of heavy metal removal is the use of functional monomer grafted synthetic polymers as adsorbent. This is advanced by the availability of a variety of cheap host polymers and grafting monomers [Hegazy et al., 1999]. Such functionalized materials have relatively high metal ion loading capacities and strong binding affinities for selected metal ions. In many cases these adsorbents can produce high-quality treated effluent. In addition, adsorption to these adsorbents is often reversible and the adsorbents can be regenerated by suitable desorption process.

1.3. Polyethylene terephthalate (PET), and the reasons behind choosing PET as the base material to prepare metal ion adsorbents

Polyethylene terephthalate, (PET) is a thermoplastic polymer resin of the polyester family which is exclusively used in films, textile fiber, packaging materials, and biomaterials [Ping et al., 2011]. The natural state of PET is colorless, semi-crystalline resin. The monomer unit of PET is ethylene terephthalate, $C_{10}H_8O_4$ (Figure 1.1).

(a)



(b)

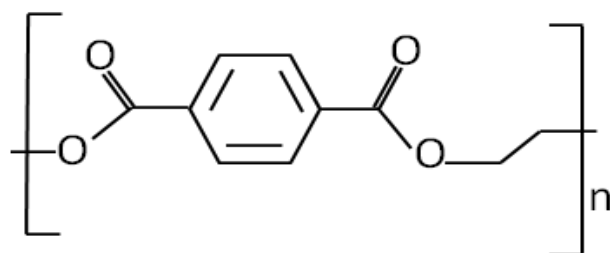


Figure 1.1. (a) A short section of PET polymer chain (b) The repeating unit of PET

PET have excellent mechanical and thermal property, and chemical stability including resistance to mineral acids (weak acids even at boiling temperature, and most strong acids at room temperature), oxidizing agents, sunlight, and micro organisms. Besides the excellent properties of PET, the need of recycling of waste PET materials such as PET bottles has attracted our attention.

Although a PET bottle is a newly invented container it has expanded market share among the beverage containers attracting with its advantages such as it is unbreakable, lightweight, transparent and resealable. In recent years a PET bottle has become one of the most commonly consumed and disposed plastic products in daily life in Japan. In 2010 the share of beverage bottled in PET bottle was 64.9 % and total consumed PET bottles were about 600,000 tons in Japan. Consequently recycling of PET bottles has turned out to be a vital issue. This is because, recycling of PET bottles can not only contribute to reduce the volume of municipal solid waste to be disposed which is an urgent necessity as the remaining capacity of final disposal sites is rapidly diminishing, but it can also convert the large amount of post-consumer PET bottles to products due to the easy recyclability of PET, which can then serve the need of the society and lower the consumption of natural resource [PET bottle recycling in Japan, at CPBR, Japan, 2012].

The PET bottle recycling in Japan is assisted by the initiation of 3R activities, where the 3Rs refer to restraining generation (Reduce), reuse (Re-use) and regeneration (Recycle) and the enforcement of several laws for the promotion of sorted collection and recycling of containers and packaging improved the PET bottle recycling in Japan. Japan's success with PET recovering is highly recognized worldwide. In 2010 the collection rate of recyclable PET bottles was 72 % in Japan

compared with 48 % in Europe and 29 % in the US [PET bottle recycling in Japan, at CPBR, Japan, 2012; The world in transition, and Japan's efforts to establish a sound material-cycle Society at Ministry of Environment Government of Japan, 2008; Controlling transboundary movements of hazardous wastes printed as part of the 2009-2011 work programme of the Basel Convention Committee]

However, the worry was that about 52.5% of the total collected volume of PET bottles were exported, the vast majority of them to China. Such transboundary movement of recovered PET is associated with several important challenges. One of these challenges is that an increase in the export of recovered PET from a country can lead to a slowdown or a hollowing out of the domestic PET recycling industry. In addition, PET recycling business in some importing countries can spread pollution potential due to improper handling of those resources. Besides these, the products produced from recovered PET in the importing country can turn into wastes after a short time of use due to inappropriate utilization. Export of any waste causing environmental pollution or increasing environmental burden in importing countries is against the spirit of the Basel Convention. The Basel Convention stipulates countries to take appropriate measures to ensure that the transboundary movement of hazardous wastes and other wastes is reduced to the minimum consistent with the environmentally sound and efficient management of such wastes. [PET bottle recycling in Japan, at CPBR, Japan, 2012; The world in transition, and Japan's efforts to establish a sound material-cycle Society at Ministry of Environment Government of Japan, 2008; Controlling transboundary movements of hazardous wastes printed as part of the 2009-2011 work programme of the Basel Convention Committee].

Hence the export of the recovered PET cannot ensure effective utilization of the PET bottles collected by the investment of an enormous amount of time and energy, rather it may hinder Japan's ability to steadily maintain and strengthen its PET waste collection structures that have been built up over the years. In order to establish a sustainable PET recycling structure it is essential to develop appropriate application areas of reclaimed PET materials. It is expected that the utilization of waste PET materials in hazardous metal ion removal can be an effective way of PET recycling because the extensive refinement of the substance is not necessarily required for such applications. Thus future prospect of recycling of waste PET materials in heavy metal removal encouraged us to study preparation of heavy metal adsorbent from PET materials.

1.4. Grafting of functional monomers on PET to improve metal adsorption property: Grafting methods

Although PET has outstanding basic properties, the strong hydrophobic character, and poor wettability and reactivity of its surface is not suitable for its application in heavy metal adsorption. The hazardous-metal-ion capturing property of PET can be improved by grafting with different functional monomers such as acrylamide, acrylic acid, methacrylic acid, itaconic acid, glycidyl methacrylate, 4-vinyl pyridine, 2-hydroxyethylmethacrylate, etc [Coşkun et al., 2006 J. Polym. Res.; Karakısla, 2003; Bağ et al., 2000; Bozkaya et al., 2012; Coşkun et al., 2006 Sep. Purif. Tehnol, Coşkun et al., 2006 React. Funct. Polym., Tehnol Soykan et al., 2006, Arslan, 2010; Yiğitoğlu et al., 2005; Yiğitoğlu et al., 2009].

‘Grafting’ is a method wherein monomers are covalently bonded (modified) onto the polymer chain. The advantage of graft polymerization onto a polymer film is that a variety of functions possessed by the grafted polymer can be given to the films while maintaining the mechanical properties of the parent films [Hsieh et al., 1986; Abdel-Bary et al., 1986; Saçak et a., 1993, Saçak et al., 1992, Şanlı et al., 1997; Rao et al., 1979]. The process of grafting of functional monomers on PET to bring metal adsorption property is depicted in Figure 1.2.

Several methods have been used to initiate graft copolymerization including ionizing radiation, ultraviolet light, plasma treatment, decomposition of chemical initiators, and oxidation of polymers. Most commonly used method for grafting of monomers is conventional chemical method. In the chemical process, free radicals are produced from the initiators and transferred to the substrate to react with monomer to form the graft co-polymers. Chemical initiation process is not free from contamination, and often brings about problems arising from local heating of the initiator [Bhattacharya et al., 2004]. Toxic chemical initiators also have risk of environmental pollution.

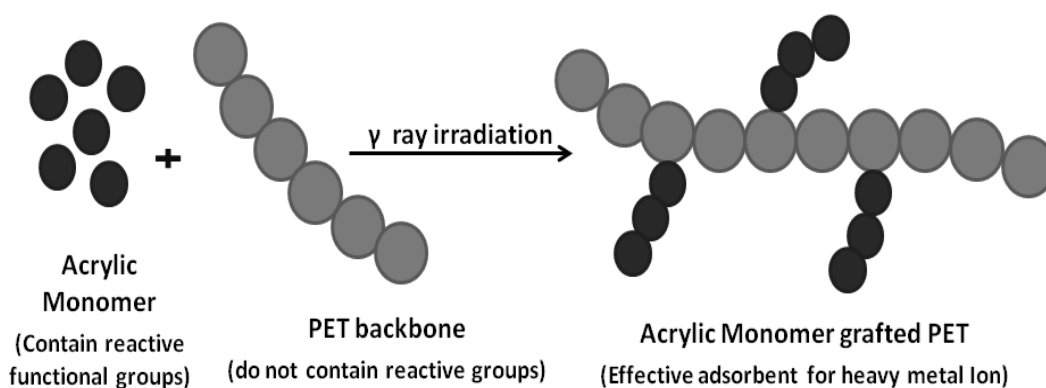


Figure 1.2. Functionalization of PET through grafting with acrylic monomers.

Among the grafting methods, radiation-induced grafting is the most advantageous technique. The major advantages of radiation grafting are (a) in a radiation technique no initiator is required; free radical formation is on the backbone polymer/monomer, so the purity of the processed products may be maintained, (b) the widespread penetration of ionizing radiation through the polymer matrix ensures rapid and uniform formation of radicals for initiating grafting throughout the whole polymer matrix, (c) the reactions can be conducted at room temperatures and in gaseous, liquid, or even solid-state phase and (d) radiation technique offers less environmental pollution than chemical method [Nasef, 2000; Brandrup et al., 1975].

Radiation induced grafting usually proceeds in two different ways: (a) pre-irradiation and (b) mutual irradiation technique. In the pre-irradiation technique, the polymer backbone is first irradiated in vacuum or in the presence of an inert gas to form free radicals. Then the irradiated polymer material is allowed to react with the monomer. On the other hand, in the mutual irradiation technique, the polymer and the monomers are irradiated simultaneously to form free radicals for subsequent reactions. Since in the pre-irradiation technique the monomers are not exposed to radiation, this method is relatively free from homopolymer formation that takes place in the simultaneous technique. However, the disadvantage of the preirradiation technique is scission of the base polymer due to its direct irradiation, which can result in the formation of block co-polymers. [Campbell et al., 1966]

Most of the earlier studies on grafting of vinyl monomers on PET have been conducted by using chemical method of initiation [Coşkun et al., 2006 J. Polym. Res.; Karakısla, 2003; Bağ et al., 2000; Bozkaya et al., 2012; Çoşkun et al., 2006, Sep. Purif. Technol.; Coşkun et al., 2006, React. Funct. Polym; Arslan 2010; Yiğitoğlu et al.,

2005; Yiğitoğlu et al., 2009, Abdel-Bary et al., 1986; Saçak et al., 1993; Saçak et al., 1992; Şanlı et al., 1997; Rao et al., 1979]. This is because, presence of many aromatic rings on PET backbone endow PET good radiation resistance. The radiation chemical yields $G(R)$ of PET is only 0.02 (G value is defined as the occurrence of individual atomic or molecular events for absorption of 100 eV in the system. $G(R)$ stands for the yields of free radicals per 100 eV absorbed) [Brandrup et al., 1975; Campbell et al., 1966]. Thus, theoretically, grafting of vinyl monomers onto PET backbone through radiation-induced graft copolymerization is difficult. But it is possible to graft vinyl and acrylic monomers onto PET backbone under high energy radiation if the reaction conditions, such as homo-polymerization inhibitor, solvent, monomer concentration, dose and dose rate are selected carefully [Gupta et al., 2009; El-Arnaouty et al., 2008, Gupta et al., 2010; Gupta et al., 2008; El-Gendy et al., 2006; Kattan et al., 2006; Ping et al., 2011; Ping et al., 2010]. Brief description of the previous studies on grafting of vinyl and acrylic monomers on PET through γ -ray induced grafting is presented in Table 1.2. The possible main mechanism involved in γ induced graft copolymerization of vinyl monomers on PET films can be represented as Figure 1.3 according to previous studies [Campbell et al., 1966; Ping et al., 2011, Buxbaum et al., 1968].

Table 1.2. Brief description of the previous studies on grafting of vinyl and acrylic monomers on PET through γ -ray induced grafting

Monomer, form of PET [reference]	Method	Dose rate (kGy/h)	Dose (kGy)	Inhibitor	Solvent	Graft yield (%)
AAc, PET fiber [Gupta et al., 2009]	PIT ^a	0.18	0-80	FeSO ₄	MEK/H ₂ O	0-8
AAc/AN, PET fiber [El-Arnaouty et al., 2008]	SIT ^b	4.3	0-20	Mohr's salt	DMF/H ₂ O	0-133
AAc/NVP, PET fiber [Gupta et al., 2010]	PIT	0.16	0-40	-	THF/H ₂ O	0-6
AAc/NIPAAm, PET fiber [Gupta et al., 2008]	PIT	0.18	0-40	FeSO ₄	H ₂ O	0-11
NVP, PET fiber [El-Gendy et al., 2006]	SIT	4.72	0-14	-	CH ₃ OH/H ₂ O	0-15
AAc, PET film [Kattan et al., 2006]	SIT	2.15	0-100	FeCl ₃	H ₂ O	0-85
St, PET film [Nasef et al., 2000]	SIT	1.32-15.00	0-30	-	CH ₂ Cl ₂	0-240
NBA, PET film [Ping et al., 2011]	SIT	0.83-2.53	0-35	FeSO ₄	CH ₃ OH	0-22.1
NBA/St, PET film [Ping et al., 2010]	SIT	1.46	10-35	-	DCM	103.7

(St: styrene; AAc: acrylic acid; AN: acrylonitrile; NIPAAm: N-isopropylacrylamide; NVP: N-vinylpyrrolidone; AAm: acrylamide; CH₂Cl₂: methylenechloride; MEK: methyl ethyl ketone; DMF: N,N-Dimethylformamide; THF: tetrahydrofuran; DCM: dichloromethane).

^a Preirradiation technique and ^b Simultaneous irradiation technique.

1.5. Previous studies on the adsorption of heavy metals by the monomer grafted PET and present approach of selective adsorption

Adsorbents prepared by grafting of different monomers such as acrylamide (AAM), acrylic acid (AAc), methacrylic acid (MAA), methacrylic acid(MAA)/acrylamide(AAM), itaconic acid (IA)/acrylamide (AAM), glycidyl methacrylate (GMA), 4-vinyl pyridine (4-VP), 4-vinyl pyridine (4-VP)/2-hydroxyethylmethacrylate (HEMA) on PET fibers and films have been investigated for the adsorption of hazardous heavy metal ion from water [Coşkun et al., 2006, J. Polym. Res.; Saçak et al., 1993; Karakısla, 2003; Bağ et al., 2000; Bozkaya et al., 2012; Çoşkun et al, 2006, Sep. Purif. Technol.; Çoşkun et al, 2006, React. Funct. Polym., Arslan, 2010; Yiğitoğlu et al., 2005; Yiğitoğlu et al., 2009; Hamada et al., 2012].

A reactive fibrous adsorbent prepared by graft copolymerization of AAM onto PET fibers has been examined for the adsorption properties of Pb(II) ion from aqueous solution [Coşkun et al., 2006, J. Polym. Res.]. AAc grafted PET fiber has been investigated for adsorption of Cu(II) from aqueous solutions [Karakısla, 2003]. Zinc, cadmium, cobalt and nickel adsorption by PET fibers grafted with MAA has been determined using flame atomic absorption spectrometry [Bağ et al., 2000]. PET fibers have been grafted with 4-VP monomer using benzoyl peroxide as initiator in aqueous media and the removal of Hg(II) ions from aqueous solution by the reactive fiber was examined [Bozkaya et al., 2010]. A reactive fibrous adsorbent has been prepared by graft copolymerization of MAA/AAM monomer mixture onto PET fiber and the

adsorption of Cu(II), Ni(II) and Co(II) ions from aqueous solution by the reactive fiber has been studied [Çoşkun et al, 2006, Sep. Purif. Technol.]. Grafting of IA/AAM co-monomers onto PET fibers has been carried out and the removal of Cu(II), Ni(II) and Co(II) metal ions from aqueous solution by the grafted fiber has been studied [Çoşkun et al., 2006 React. Funct. Polym.]. PET fibers have been grafted with GMA using benzoyl peroxide as initiator and 1,6-diaminohexane (HMDA) was covalently attached to this GMA grafted PET fibers. The prepared HMDA-GMA-g-PET fibers have been used as a sorbent for removal of Cr(VI) ions from aqueous solutions [Arslan, 2010]. Adsorption of hexavalent chromium from aqueous solutions using 4-VP grafted PET fibers has been investigated [Yiğitoğlu et al., 2005]. A fibrous adsorbent has been prepared by grafting 4-VP and HEMA monomer mixture onto PET fibers and the grafted fiber showed high affinity to bind with Cr(VI) ions in the mixed solution of Cr(VI)–Cu(II), Cr(VI)–Cd(II) and Cr(VI)–Cu(II)–Cd(II) at pH 3 [Yiğitoğlu et al., 2009]. Amidoximated diaminomaleodinitrile grafted PET films has been studied for removal of Cu(II), Ni(II) and Zn(II) [Hamada et al., 2012]. All these adsorbents showed considerable metal ion adsorption capacities and re-usability. Thus monomer grafted PET adsorbents have good potential in heavy metal removal.

However, most of the previous studies on PET based adsorbents focused on metal ion adsorption from single metal solution while less results appeared on metal ion adsorption from multi metal solution. Generally various heavy metal ions are often present in industrial effluents, hence it is important to develop methods that can effectively and, at the same time, selectively recover a specific heavy metal to allow reuse of the recovered metal. Otherwise even if the heavy metals are removed from the waste water to a certain regulated level, there will remain risk of secondary

pollutions of these heavy metals in a more concentrated form. Consequently the present study focused on selective metal ion adsorption from binary or ternary metal solution.

1.6. Investigation of metal adsorption process: Isotherms and kinetics

In order to properly understand the adsorption process of metal ions, it is necessary to understand two basic ingredients: equilibrium and kinetics. An adsorption isotherm represents the relationship between the equilibrium metal adsorption capacity of the adsorbent and the equilibrium concentration of metal ions in solution. And kinetic deals with changes of adsorption in time and is concerned especially with rates of adsorption. Hence isotherm and kinetic models are often used to understand the mechanism of heavy metal adsorption by the adsorbent.

1.6.1. Modeling of metal adsorption isotherms

Two isotherm models namely Langmuir model and Freundlich model are often used to study metal ion adsorption from aqueous systems [Langmuir, 1918; Freundlich, 1906].

The Langmuir model assumes monolayer adsorption of adsorbate on a structurally homogeneous adsorbent where all adsorption sites are identical.

The linear form of the Langmuir isotherm is presented by

$$C_e/Q_e = C_e/Q_o + 1/(Q_o b) \quad \dots\dots\dots (1.1)$$

where C_e is the equilibrium concentration (mg L^{-1}), Q_o the monolayer saturation adsorption capacity of adsorbent (mg g^{-1}), Q_e is the equilibrium adsorption capacity and b is Langmuir adsorption constant (Lmg^{-1}).

The Freundlich model is an empirical model that was shown to be consistent with exponential distribution of active centers, characteristic of heterogeneous surfaces. The Freundlich isotherm is described by the following equation

$$\log Q_e = \log K_F + (1/n) \log C_e \quad \dots\dots\dots (1.2)$$

where C_e is the equilibrium concentration (mg L^{-1}), Q_e is the equilibrium adsorption capacity, K_F the sorption capacity (mg g^{-1}) and n is an empirical parameter.

1.6.2. Modeling of metal adsorption kinetics

Various kinetic models have been suggested to investigate the mechanisms of adsorption. A simple kinetic model of adsorption is the pseudo-first order equation of form (1.3) [Ho et al., 2006].

$$dQ_t/dt = k_1 (Q_e - Q_t) \quad \dots\dots\dots (1.3)$$

where Q_t and Q_e are the amount of ions adsorbed (mg g^{-1}) at any specific time and equilibrium time, respectively, k_1 is the rate constant (min^{-1}) of first-order adsorption. After definite integration of eq. (1.3) by applying boundary conditions, $Q_t = 0$ at $t = 0$ and $Q_t = Q_t$ at $t = t$ and rearrangement to linear form gives

$$\log (Q_e - Q_t) = \log Q_e - (k_1/2.303) t \quad \dots\dots\dots (1.4)$$

The pseudo-first-order rate constants could be determined experimentally by plotting $\log (Q_e - Q_t)$ against t .

Another commonly used model, pseudo-second-order eq. is expressed as

$$dQ_t/dt = k_2 (Q_e - Q_t)^2 \quad \dots\dots\dots (1.5)$$

where k_2 ($\text{g min}^{-1} \text{mg}^{-1}$) is the rate constant of second-order adsorption [Freundlich, 1906]. After definite integration of eq. (1.5) by applying boundary conditions and rearrangement to liner form gives

$$t/Q_t = (1/ k_2 Q_e^2) + t/ Q_e \quad \dots\dots\dots (1.6)$$

The pseudo second-order rate constants could be determined experimentally by plotting t/Q_t against t

According to many earlier literature reviews, majority of adsorption studies can be represented as a pseudo-first-order rate mechanism. However, in recent years, the wide application of pseudo-second-order rate expression to the adsorption of pollutants from aqueous solutions revealed that the pseudo-second-order equation can better describe the chemisorption process involving sharing or exchange of electrons between the adsorbent and adsorbate [Ho, 2006].

1.7. Objectives of present study

In the present study selective adsorption of hazardous heavy metals by the acrylic monomer grafted PET films prepared through γ ray induced grafting were investigated in order to explore the potential reuse of waste PET materials. Specifically present study concentrates on the following objectives:

I. Preparation of low cost and effective adsorbents for hazardous metal ion removal from industrial waste water

Considering the urgent need of alternative low cost and effective recovery agents to prevent heavy metal pollution as discussed in section 1.1. and 1.2., in the present study preparation of low cost, effective adsorbents for hazardous metal ion removal is targeted.

II. Explore effective re-use of waste PET materials

From the view point of effective recycling of waste PET materials as discussed in section 1.3., in the present research preparation of hazardous metal ion adsorbents from PET film is examined.

III. Grafting of acrylic monomers on PET film by γ -ray irradiation to impart metal adsorption property to PET

Although PET have outstanding basic properties, it is necessary to graft PET with functional monomers to impart metal adsorption property to PET (Figure 2). γ -ray induced grafting is a powerful and environment friendly method to prepare polymers with desired property which is more advantageous than the other grafting techniques as mentioned in section 1.4. But due to the radiation resistant property of PET, it is necessary to select the appropriate grafting conditions to achieve grafting of monomers on PET through γ -ray irradiation. In the present study appropriate grafting conditions for γ -ray induced grafting of two commonly used acrylic monomers, acrylamide (AAM) and acrylic acid (AAc) were investigated. Simultaneous irradiation technique is used in the present study

considering the drawback of scission of the base polymer due to direct irradiation in the preirradiation technique as mentioned in section 1.4. Chapter 2 represents a new method for γ ray induced grafting of AAm on PET film by treatment with a swelling agent, dimethyl sulfoxide (DMSO) prior to grafting. Grafting of AAc on PET film by γ ray irradiation and the characterization of the AAc grafted films are described in Chapter 4.

IV. Application of the acrylic monomer grafted PET films in selective heavy metal adsorption

Acrylic monomer grafted PET adsorbents have promising heavy metal removal efficiency as discussed in section 1.5. However, it is more realistic to develop selective recovery method for a specific metal ion from mixture of metal ions to allow re-use of the recovered metal ion. Therefore in the present work acrylic monomer grafted PET films were examined for selective adsorption of metal ions. Chapter 3 describes the use of AAm grafted PET films in selective Hg(II) adsorption from mixture of Hg(II) and Pb(II). Mercury and lead which appear in industrial effluents are hazardous for human life and health. Both Hg(II) from Pb(II) are soft acids and structurally similar, consequently selective recovery of Hg(II) from mixture of Hg(II) and Pb(II) is important. Chapter 4 demonstrates the application of AAc grafted PET films in selective adsorption of Cu(II) from mixture of Cu(II), Co(II) and Ni(II). Cu(II), Co(II) and Ni(II) are of environmental concern and have structural similarity. So selective adsorption of Cu(II) from mixture of Cu(II), Co(II) and Ni(II) can be useful for waste water treatment.

V. Investigation of selective metal adsorption process, desorption of metal ions and reusability of the adsorbent

Isotherm and kinetic models are useful to understand the mechanism of heavy metal adsorption by the adsorbent as discussed in section 1.6. Therefore in the present study isotherm and kinetic models were used to investigate the selective heavy metal adsorption processes. In chapter 3 isotherm and kinetics of selective Hg(II) adsorption by the AAm grafted PET films were analyzed by using isotherm and kinetic models. In chapter 4 isotherm and kinetics of selective Cu(II) adsorption by the AAc grafted PET films were investigated by using isotherm and kinetic models. It is known that pH has a significant influence on the adsorption process because it determines the surface behavior of the adsorbent and the availability of metal ions in solution. Therefore the effect of pH on the selective Hg(II) adsorption by the AAm grafted PET films (chapter 3) and selective Cu(II) adsorption by the AAc grafted PET films (chapter 4) was investigated. Another concern is the easy separation of the heavy metal ions from the recovery agent and reusability of the adsorbent. Hence desorption of metal ions from the monomer grafted PET films and reusability of the adsorbent films were also examined (desorption of Hg(II) ions and reusability of AAm grafted PET films are shown in chapter 3, desorption of Cu(II) ions and reusability of AAc grafted PET films are shown in chapter 4).

CHAPTER 2

The effect of hot DMSO treatment on the γ -ray-induced grafting of acrylamide onto PET films

2.1. Introduction

In addition to the conventional applications, PET has been used as a functional material by attaching amino, carboxylic or other reactive groups to its surface to expand its applications to many fields, such as conductive films, biocompatible materials and recovery agents for heavy metals [Arslan, 2010; Wirse'n et al., 2005; Zhang et al., 2012; Coşkun et al., 2006; Yiğitoğlu et al., 2005; Yiğitoğlu et al., 2009]. To fabricate such highly functional PET, graft copolymerization is a useful technique that causes the covalent bonding of functional monomers onto the polymer surface while maintaining the properties of parent polymer [Hsieh et al., 1986; Abdel-Bary et al., 1986; Saçak et al., 1993; Saçak et al., 1992; Şanlı et al., 1997; Rao et al., 1979].

In this study, we attempted to bind acrylamide ($\text{CH}_2=\text{CH}-\text{CO}-\text{NH}_2$, AAm), a highly water soluble vinyl monomer well known as the monomer of polyacrylamide (PAAm), to the surface of PET. PAAm has been widely used as a water-soluble thickener in wastewater treatment, gel electrophoresis, papermaking, ore processing, tertiary oil recovery and the manufacture of permanent press fabrics. In addition to its

usage as the starting material for PAAm, AAm has been known to functionalize the surfaces of many polymers by grafting and as an environmental purifying material [Coşkun et al., 2006, Ibrahim et al., 2006, Gupta et al., 2003; Maziad et al., 2002; Raji et al., 1998; Latha et al., 1991]: A reactive fibrous adsorbent prepared using graft copolymerization of AAm onto PET fibers has been studied for the adsorption of Pb(II) ions from aqueous solution, and the capacity of the adsorbent has been reported to be 39.57 mg/g of fiber for a graft yield of 15.7 % [Coşkun et al., 2006]. The graft copolymerization of the AAm monomer onto the non-woven, polyethylene-coated polypropylene (PE-co-PP) fabric was carried out using an irradiation method and the uptake of Cu(II), Co(II), and Ni(II) by the grafted fabrics was evaluated [Ibrahim et al., 2006]. Ion-exchange membranes have been prepared via the alkaline hydrolysis of radiation-grafted polyethylene grafted AAm membranes and an excellent binding capacity of the membranes for mercury ions has been reported [Gupta et al., 2003]. AAm has been grafted onto poly(vinyl chloride) using γ -ray irradiation to prepare ion exchange membranes with a strong tendency to remove ^{60}Co from radioactive liquid waste containing both ^{60}Co and ^{137}Cs [Maziad et al., 2002]. AAm-grafted sawdust, converted to anion exchanger via treatment with ethylenediamine followed by HCl, has been used effectively for the removal of Cr(VI) from aqueous solutions [Raji et al., 1998]. AAm-based chelating resins prepared using *N,N'*-methylene-bis-acrylamide as the crosslinking agent has been studied for the adsorption of Fe(III), Fe(II), Ni(II), and Cu(II) [Latha et al., 1991].

As mentioned in the preceding paragraphs, the grafting of AAm on PET has been performed through various methods to combine the excellent properties of PET and the characteristic functionality of AAm. Most of the earlier studies used chemical

methods of initiation for the grafting of AAm [Şanlı et al., 1997, Coşkun et al., 2006, Saçak et al., 1993, Şanlı et al., 1993] or other vinyl monomers [Coşkun et al., 2006; Yiğitoğlu et al., 2005; Yiğitoğlu et al., 2009; Abdel-Bary et al., 1986; Saçak et al., 1993, Saçak et al., 1992; Rao et al., 1979; Karakisla et al., 2003; Bağ et al., 2000; Bozkaya et al., 2012; Coşkun et al., 2006; Arslan, 2010] on PET as mentioned in chapter 1 section 1.4. Although the chemical method produced AAm grafted PET with high graft yield, it is known that the chemical initiation method is not free from contamination and also that chemical initiation often brings about problems arising from the local heating of the initiator [Bhattacharya et al., 2004]. Toxic chemical initiators also have the risk of the environmental pollution. Therefore, the grafting of AAm through methods other than chemical initiation, such as photografting [Wirseń et al., 2005; Yao et al., 1990; Uchida et al., 1990], CO₂ laser-induced graft copolymerization [Dadsetsan et al., 2000] and surface-initiated atom transfer radical polymerization (SI-ATRP) [Zhang et al., 2012; Zhou et al., 2011] has also been investigated. However, the low graft yield obtained using these methods is not suitable for the application of grafted products in the field of heavy metal adsorption or other uses described in the preceding paragraph.

From this point of view, the radiation-induced grafting can be the most suitable method for the grafting of AAm on PET films. The major advantages of radiation grafting are as follows. (a) In a radiation technique, no initiator is required; as free radicals are formed on the polymer/monomer backbone, the purity of the processed products may be maintained. (b) The widespread penetration of ionizing radiation through the polymer matrix ensures rapid and uniform formation of radicals to initiate the grafting process throughout the entire polymer matrix. (c) The reactions can be

conducted at room temperatures. (d) The radiation technique generates less environmental pollution than chemical methods [Bhattacharya et al., 2004; Nasef et al., 2000]. The radiation-induced graft copolymerization of various vinyl monomers, such as acrylic acid [Gupta et al., 2009], acrylic acid/acrylonitrile [El-Arnaouty et al., 2008], acrylic acid/*N*-vinyl pyrrolidone [Gupta et al., 2010], acrylic acid/*N*-isopropyl acrylamide [Gupta et al., 2008] and *N*-vinyl pyrrolidone [El-Gendy et al., 2006] onto PET fibers and acrylic acid [Kattan et al., 2006], styrene [Nasef et al., 2000], *n*-butyl acrylate [Ping et al., 2011] and *n*-butyl acrylate/styrene [Ping et al., 2010] on the PET films demonstrated the high quality of the product generated using radiation induced grafting for different applications.

However, to the best of the authors' knowledge, no previous studies have reported on the powerful γ -ray induced graft copolymerization of acrylamide onto PET films or fibers. This lack of study is due to serious difficulties in grafting of AAm onto PET films:

- (1) the strong propensity of AAm to homopolymerize,
- (2) the low diffusion of AAm through PET.

Although homopolymerization (condition 1) is known to be suppressed by some transition metal salts [Gupta et al., 2009], condition 2 has been difficult to overcome because the origins lie in the nature of the PET: the high degree of crystallization and ordering of the amorphous regions retard the AAm monomer permeation into the interior of the PET.

Under these conditions, in this study we adopted γ -ray-induced grafting assisted by *dimethyl sulfoxide* (DMSO) pretreatment to attain a higher graft yield of AAm on PET while maintaining the product purity. The effects of grafting on the surface structures

and on the mercury (Hg(II)) adsorption properties of the AAm-grafted PET were comparatively investigated to examine their relationship. Hg(II) is a well-known toxic material classified as a priority pollutant in spite of being commonly used in many industries [Molinari et al., 2004]; therefore, the Hg(II) capturing property is important from the view point of environmental protection.

2.2. Materials and Methods

2.2.1. Materials

Commercial PET films (Teijin DuPont films, G2) with thicknesses of 50 μm were kindly provided by Teijin Co. Ltd (Osaka, Japan). These films were cut into small pieces (2 cm \times 2 cm), washed with acetone, and dried in a vacuum oven before use. AAm and FeCl_3 were procured from Sigma Aldrich. DMSO and KOH were supplied by Wako pure chemical industries Ltd. Hg(II) acetate (anhydrous, Chameleon Reagent) and Hg(II) standard solution (Merck) were used as the source of the adsorbate and for the calibration of the metal concentrations, respectively.

2.2.2. Sorption of AAm solution to the DMSO- pretreated PET films

Dry PET films (weighing W_{pristine}) were soaked in DMSO for 0.5 h at different temperatures (from 60 to 160 $^{\circ}\text{C}$). After withdrawing the PET films from the DMSO, the excess liquid on the PET surface was removed by blotting between filter papers and the weights of the films (W_{DMSO}) were recorded. Then, the films were kept in the

AAM aqueous solution (50 wt %) for 24 h. Again, after withdrawing the PET films from the AAM solution, the surface fluid was absorbed using filter paper, and the film weights ($W_{\text{AAM sol}}$) were recorded. Following the previous study [You et al., 1984], the ratios of the adsorbed DMSO (δW_{DMSO}) and AAM ($\delta W_{\text{AAM sol}}$) to PET were calculated using the equations below:

for the DMSO absorption ratio,

$$\delta W_{\text{DMSO}} (\%) = (W_{\text{DMSO}} - W_{\text{pristine}}) / W_{\text{pristine}} \times 100, \quad \dots\dots\dots (2.1)$$

for the AAM absorption ratio,

$$\delta W_{\text{AAM sol}} (\%) = (W_{\text{AAM sol}} - W_{\text{pristine}}) / W_{\text{pristine}} \times 100. \quad \dots\dots\dots (2.2)$$

2.2.3. Grafting of AAM onto the DMSO-pretreated PET films

The DMSO-pretreated PET films were put into several glass bottles containing aqueous AAM solutions with different concentrations (25, 40, 50 and 70 wt %). After 24 h, FeCl₃ was added to the bottles at a constant concentration (1 wt %) to minimize homopolymer formation. Then, the bottles with specimens were γ -ray irradiated for different periods in a 1.0 kGy/h field (the total doses were 20, 50, 70, or 100 kGy) in the ⁶⁰Co γ -ray irradiation facility at the Research Reactor Institute, Kyoto University (the grafting reactions were conducted without deoxygenating the AAM aqueous solutions following previous studies [Goel et al., 2009; Tuhin et al., 2012; Martinovich et al., 2006] to keep the process convenient and economical). The PET films were removed from the bottles after the irradiation and, then, soaked in 60 °C distilled water for 24 h to remove the AAM homopolymers from the films. The rinsed films were dried in a 60 °C vacuum oven for 24 h, and finally, the weights of the PET films

were measured ($W_{\text{AAm grafted}}$).

The graft yields of the specimens were calculated from the percentage increase in weight ($\delta W_{\text{AAm grafted}}$) as in the previous study [You et al., 1984] using the equation,

$$\delta W_{\text{AAm grafted}} (\%) = (W_{\text{AAm grafted}} - W_{\text{pristine}}) / W_{\text{pristine}} \times 100. \quad \dots\dots\dots (2.3)$$

Again, following Ref. [Coşkun et al., 2006], the AAm graft densities (D) were derived using the equation,

$$D (\mu\text{g}/\text{cm}^2) = (W_{\text{AAm grafted}} - W_{\text{pristine}}) / S, \quad \dots\dots\dots (2.4)$$

where S is the surface area of the pristine PET sample.

2.2.4. Optical micrograph

The optical micrographs of the wet and dry PET films after different pretreatments were observed using an optical microscope (Nikon, Inverted microscope, Eclipse TE 300) with a magnification of 40×.

2.2.5. X-ray diffraction

X-ray diffraction (XRD) measurements were performed using a SmartLab X-ray diffractometer (Rigaku. ID no: FKOD 12-001). The diffractograms were measured over 2θ in the range of 5–60° using Cu- K_{α} radiation monochromated with a nickel filter.

2.2.6. Infrared (IR) spectroscopy

The vibrational spectroscopic analyses of the specimens were performed using a Fourier transform infrared (FTIR) spectrophotometer (Jasco FTIR 620) over a wavenumber range from 400 to 4000 cm^{-1} to investigate the interactions between the PET matrix and the grafted AAm and, also, to estimate the amount of AAm grafted to PET.

2.2.7. Scanning electron microscopy (SEM)

In addition to the optical microscopic observations over a 100- μm range, the minute surface morphologies of the pristine and AAm-grafted PET films were observed using a scanning electron microscope (SEM, Zeiss Ultra55) operated at 10 KeV after carbon coating.

2.2.8. Water uptake measurements

After weighing (W_0), each of the pristine and dried AAm-grafted PET films was kept in a beaker filled with distilled water at 25 °C for 24 h. After this period, the specimens were removed from the containers, and their weight (W_s) were measured immediately after blotting their surfaces. From the measured weights, the water-uptake percentage was calculated using the equation,

$$\text{Water uptake (\%)} = (W_s - W_0) / W_0 \times 100. \quad \dots\dots\dots (2.5)$$

2.2.9. Hydrolysis of AAm-grafted PET film and Hg(II) uptake measurements

The films with a 14 % graft yield were hydrolyzed by 10 % KOH at 60 °C for 1 h (Sec. 2.2.9.1). Then, each of the 20 mg hydrolyzed AAm grafted PET films was soaked in 5 ml of an aqueous 100.0 mg/L-Hg(II) solution (pH~4.5) for 40 minutes at room temperature (25 °C) to examine the Hg(II) uptake ability of the hydrolyzed AAm-grafted PET (Sec. 2.2.9.2).

2.2.9.1. Determination of hydrolysis percentage of AAm

Following the previous study [Faterpeker et al., 1981], the hydrolysis percentage of the amide groups to carboxylate groups was calculated from the IR absorbance using the equation,

$$\text{Hydrolysis (\%)} = (B - C) / (B - A) \times 100 \dots\dots\dots (2.6)$$

where *A*, *B* and *C* are the absorbance ratios of [3200 cm⁻¹ (assigned to –NH₂ groups of AAm) / 3054 cm⁻¹ (aromatic –CH stretching vibration of PET)] of the non-grafted, AAm-grafted and hydrolyzed AAm-grafted PET films, respectively.

2.2.9.2. Determination of Hg(II) uptake efficiency

Before and after the adsorption, the Hg(II) concentrations of the aqueous solutions were analyzed using an inductively coupled plasma mass spectrometer

(ICP-MS, Agilent7700 Series). The Hg(II) uptake efficiencies of the films were calculated using the equation,

$$Uptake\ efficiency\ (\%) = (C_1 - C_2) / C_1 \times 100, \quad \dots\dots\dots (2.7)$$

where C_1 and C_2 are the Hg(II) concentrations (mg/L) before and after the adsorption, respectively.

2.3. Experimental Results

2.3.1 DMSO-assisted grafting of AAm onto the PET films by γ -ray irradiation

The pristine PET films showed no AAm-grafting despite the fact that those films had been γ -ray irradiated in the AAm solution in the usual manner. In this situation, the authors attempted to investigate the AAm-grafting onto DMSO-pretreated PET films under various conditions: at several DMSO pretreatment temperatures (Sec. 2.3.1.1), in the presence and absence of a polymerization inhibitor (Sec. 2.3.1.2), at several AAm-monomer concentrations (Sec. 2.3.1.3) and at several γ -ray total doses and dose rates (Sec. 2.3.1.4).

2.3.1.1 Effect of DMSO pretreatment temperature on grafting of AAm

Before the AAm-solution adsorption, the PET films were pretreated with DMSO at temperatures over the range 60–160 °C. It was found that the specimens pretreated with DMSO over the temperature range 60–140 °C showed increases in both the DMSO and AAm adsorption (Figure 2.1), while the samples pretreated at 160 °C showed lower AAm adsorption than that at 140 °C despite the greater DMSO adsorption. It should also be noted that no significant weight loss was observed for the DMSO-pretreated PET films over the range 60–140 °C.

The γ -ray grafting of AAm was performed on the DMSO-pretreated PET films at 100, 140 and 160 °C, which showed significant amounts of DMSO and AAm adsorption. The graft yield was observed to increase as the DMSO-pretreatment temperature increased up to 140 °C (Figure 2.1): 5 % at 100 °C and 14 % at 140 °C and decreased to 8 % at 160 °C.

Based on these results for graft yields, the subsequent investigations were performed on the PET films pretreated with DMSO at 140 °C.

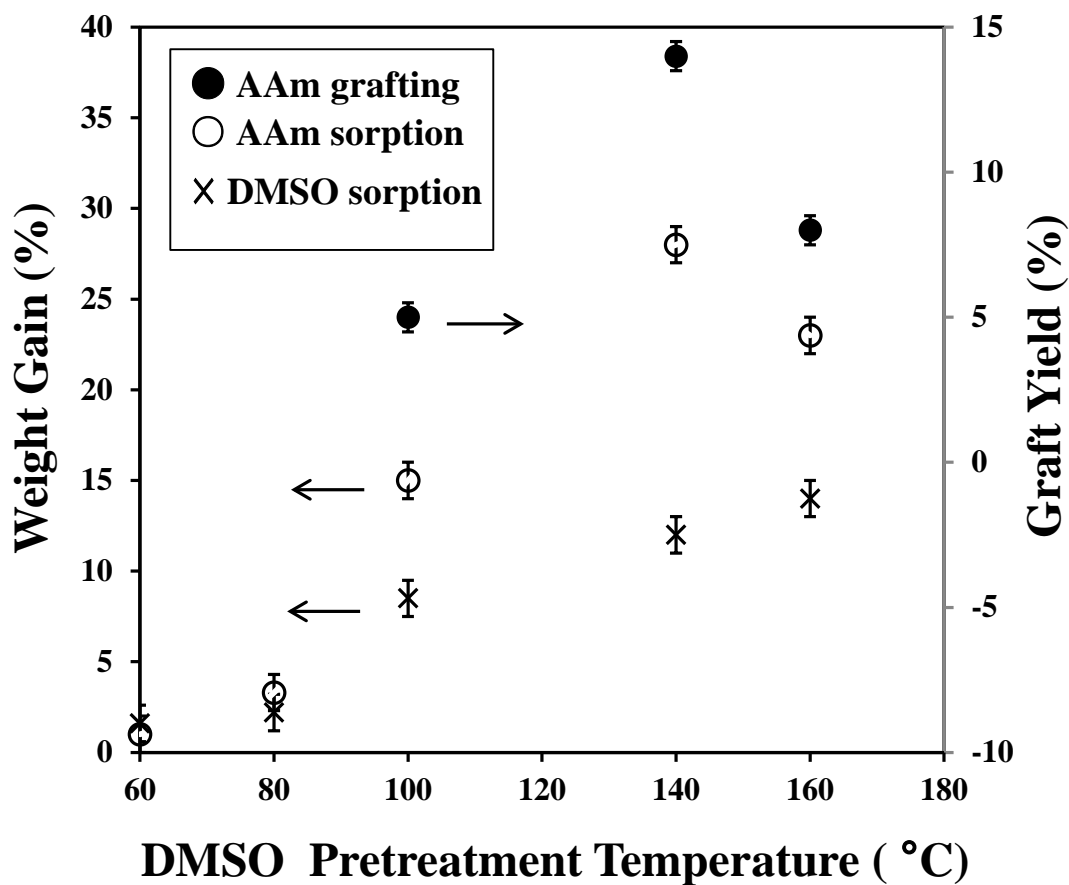


Figure 2.1. Weight gain (\times after soaking in DMSO for 0.5 h, \circ after soaking in 50 wt % AAm solution for 24 h) and graft yield (\bullet after grafting at 50 wt % AAm monomer concentration, with a 50-kGy dose at a dose rate of 1 kGy/h, and at 1 wt % FeCl_3) as a function of the DMSO pretreatment temperature.

2.3.1.2. Effect of FeCl₃ on AAm grafting

To examine the effect of a polymerization inhibitor (FeCl₃), the AAm-graft yields derived after γ -ray grafting process in the presence and absence of FeCl₃ were compared while keeping the other conditions the same (140 °C DMSO-pretreated PET films, grafting at 50 wt % AAm concentration and 50 kGy radiation dose at a 1-kGy/h dose rate). The obtained graft-yield was 11 % without FeCl₃, which increased to 14 % in the presence of FeCl₃. It was also observed that the AAm solution surrounding the AAm grafted PET film in the absence of FeCl₃ formed a hard gel of homopolymerized PAAms during irradiation, while the AAm solution formed a soft gel (for high AAm concentration) or remained liquid (for low AAm concentration) in presence of FeCl₃.

2.3.1.3. Effect of monomer concentration on grafting of AAm

To investigate the dependence of the graft yields on the AAm-monomer concentration, the yields obtained after grafting with different monomer concentrations from 25 to 50 wt % were investigated with the other conditions kept the same (140 °C DMSO-pretreated PET films, γ -ray grafting with a 50-kGy radiation dose at a 1-kGy/h dose rate in the presence of 1 wt % FeCl₃).

The graft yield increased as the monomer concentration increased from 25 to 50 wt % (Figure 2.2): 8 % graft yield at 25 wt % AAm and 14 % for 50 wt %, while the graft yield slightly decreased at 70 wt % of monomer (Figure 2.2).

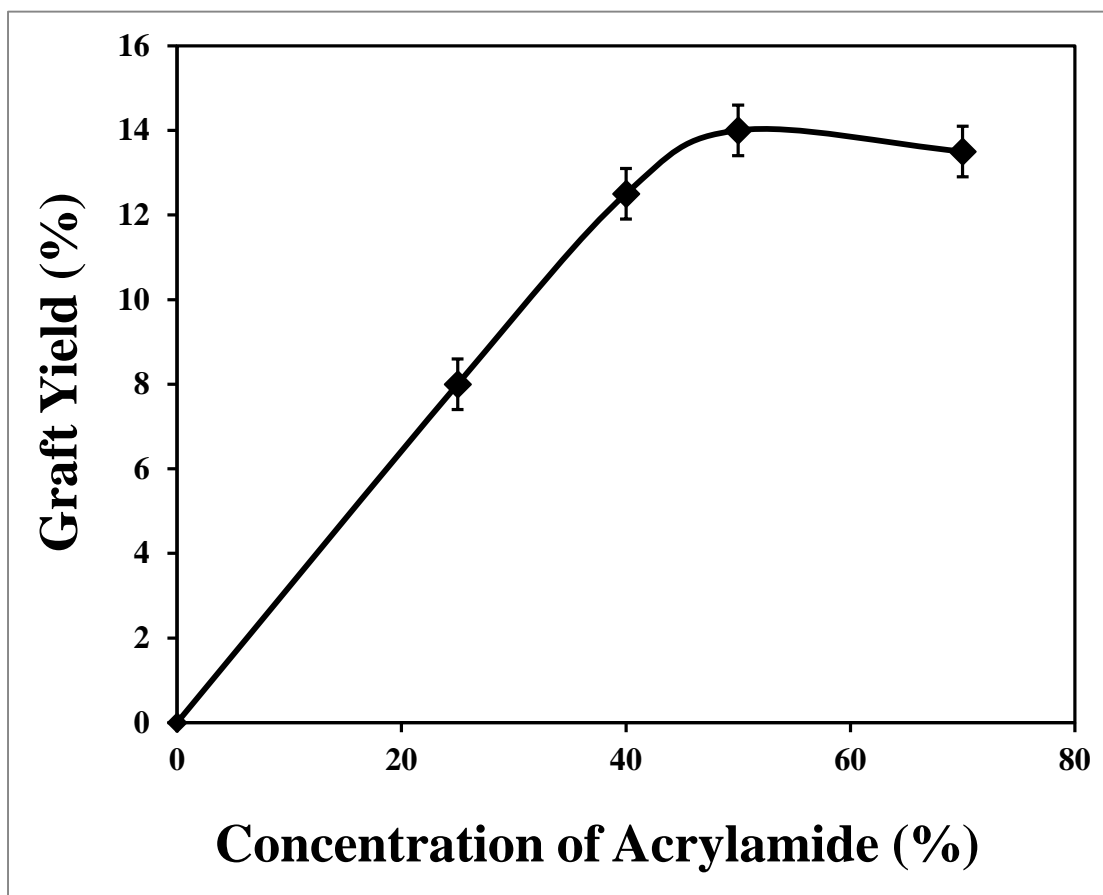


Figure 2.2. The AAm monomer concentration dependence of the AAm-graft yield onto the 140 °C DMSO pretreated PET films while maintaining the other grafting conditions: a 50-kGy total dose, a 1-kGy/h dose rate and the presence of 1 wt % FeCl₃.

2.3.1.4. Effect of dose and dose rate on grafting of AAm

To study the total γ -ray dose dependence of the graft yield, the graft yields acquired using total doses that varied from 20 to 100 kGy were obtained under the same conditions (140 °C DMSO-pretreated PET films, γ -ray grafting at 50 wt % of AAm and a 1-kGy/h dose rate in the presence of 1 wt % FeCl₃) (Figure 2.3).

The graft yield increased as the total dose increased, while the rate of increase decreased as the total dose increased (Figure 2.3).

In addition to the total γ -ray dose dependence, the graft yields obtained using two dose rates, 1.02 and 2.40 kGy/h, were investigated while keeping the other conditions the same (140 °C DMSO-pretreated PET films, γ -ray grafting at 50 wt % of AAm and a 50-kGy total dose in the presence of 1 wt % FeCl_3); however, the graft yield was found to be almost unchanged.

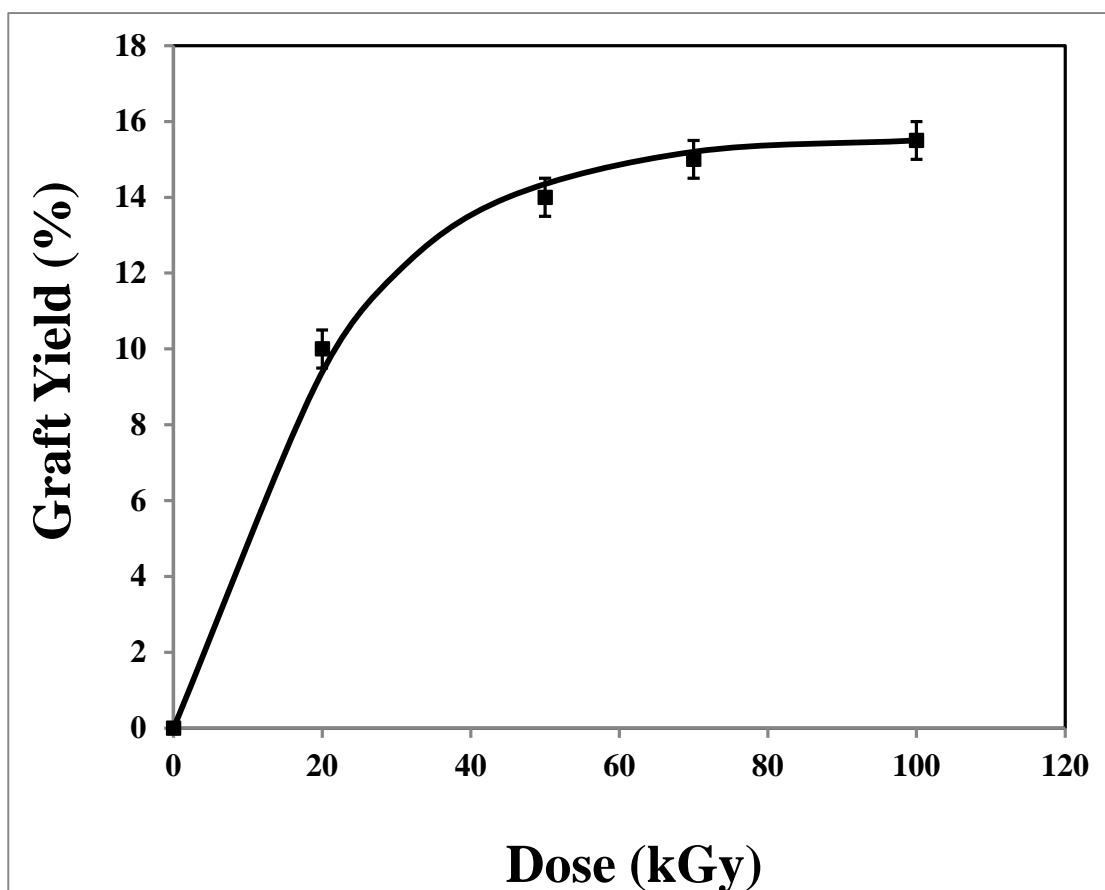


Figure 2.3. The total γ -ray dose dependence of the AAm-graft yield on the 140 °C DMSO-pretreated PET films with all other grafting conditions held constant: 50 wt % AAm, a 1-kGy/h dose rate and the presence of 1 wt % FeCl_3 .

The highest graft yield obtained was 15.5 % for the 140 °C DMSO-pretreated PET films under the following grafting conditions: 50 wt % AAm monomer, a 100-kGy total dose at a rate of 1 kGy/h, and 1 wt % FeCl₃.

In Table 2.1, the γ -ray graft yield and/or graft density derived in the present study is compared with those obtained from some other methods [Zhang et al., 2012, Uchida et al., 1990, Dadsetan et al., 2000; Zhou et al., 2011].

Table 2.1. A comparison of graft yield and/or graft density derived in the present study (γ -ray) with the results obtained using other methods.

Grafting method	Graft yield (%)	Graft density ($\mu\text{g}/\text{cm}^2$)
UV radiation [Coşkun et al., 2006]	0.3 ^a	-
UV radiation [Bäg et al., 2000]	-	10 ^a
CO ₂ laser [Bozkaya et al., 2012]	-	359 ^a
SI-ATRP [Coşkun et al., 2006]	1.37 ^a	-
SI-ATRP [Zhang et al., 2010]	2.52 ^a	-
γ -ray irradiation [present study]	15.5 (\pm 0.5)	1125 (\pm 25)

SI-ATRP: surface-initiated atom transfer radical polymerization; UV: ultraviolet.

^a the values are described as they appear in the references.

2.3.2. Optical micrographs of the PET films

The optical micrographs of the surface of the pristine PET films after the different pretreatments are shown in Figure 2.4. More pores are observed in the micrograph of wet DMSO-pretreated films (Figure 2.4 (b)) than the pristine PET films (Figure 2.4 (a)), indicating the formation of micropores on the PET surface by the DMSO pretreatment. The pore structure of the DMSO-pretreated film changed after soaking in an AAm solution, which became more significant in the wet AAm-solution-soaked PET film (Figure 2.4 (c)). The surface structure of the AAm-grafted film resembled that of the wet AAm-solution-soaked DMSO-pretreated film (Figure 2.4 (d)).

The optical micrographs of the PET films were also studied to investigate the effect of the DMSO-pretreatment temperatures on the surface structure. Figure 2.5 shows the optical micrographs of the PET films after DMSO-pretreatment at 100 °C (Figure 2.5(a)), 140 °C (Figure 2.5(c)) and 160 °C (Figure 2.5(e)) as well as the samples soaked in AAm solution after the DMSO treatment (Figures 2.5(b), (d) and (f), respectively).

As shown in Figure 2.5, the number of pores and their diameters increased with increasing pretreatment temperature, which promoted monomer diffusion into the polymer matrix.

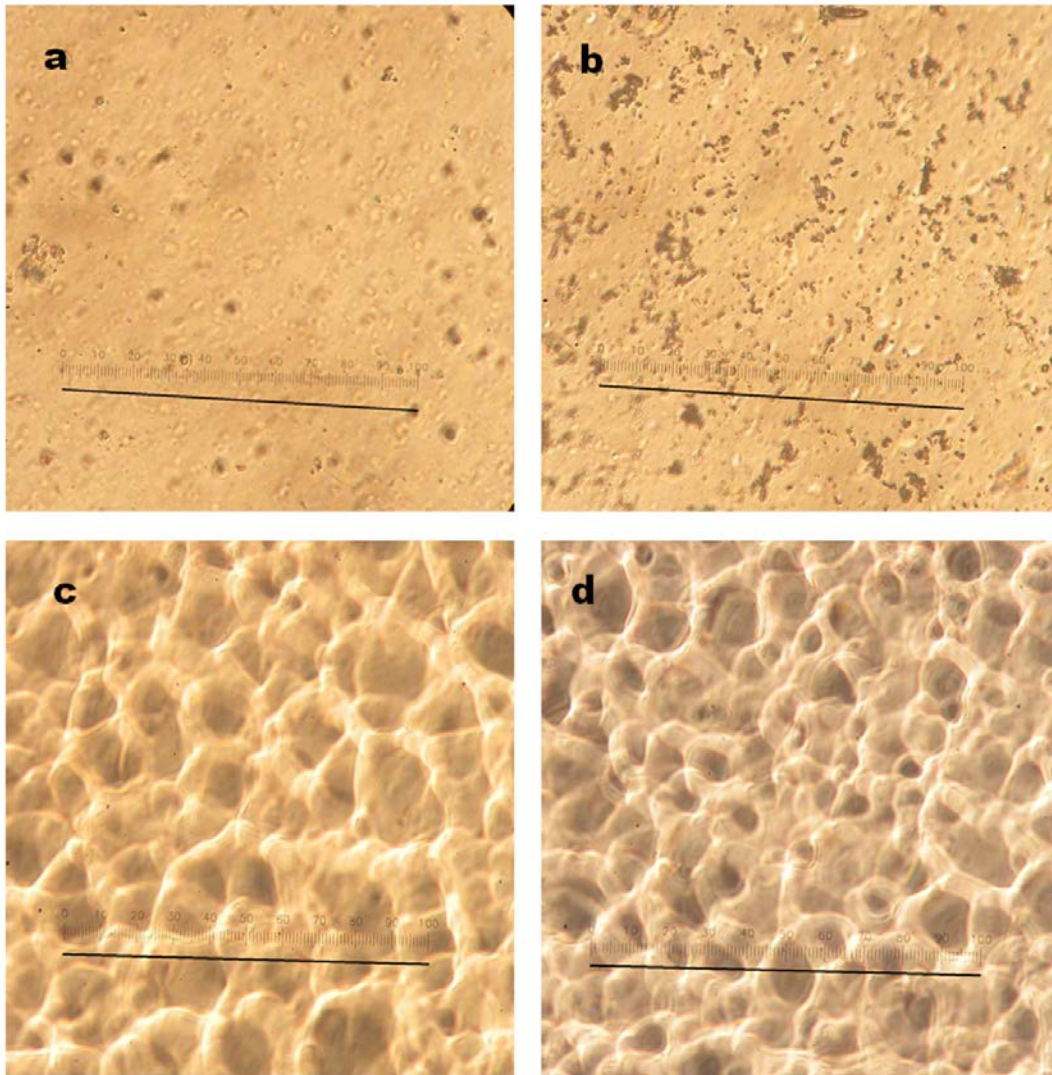


Figure 2.4. Optical micrographs of (a) the pristine PET film, (b) the DMSO-pretreated (at 140 °C) wet film, (c) the wet AAm-solution-soaked DMSO-pretreated film (DMSO pretreated at 140 °C and soaked in 50 wt % AAm solution) and (d) AAm grafted PET film (DMSO pretreated at 140 °C and γ -ray irradiated with a 50-kGy dose at a 1-kGy/h dose rate in the presence of 1 wt % FeCl_3 after soaking in 50 wt % AAm solution) [The black line inside each figure represents 100 micrometers].

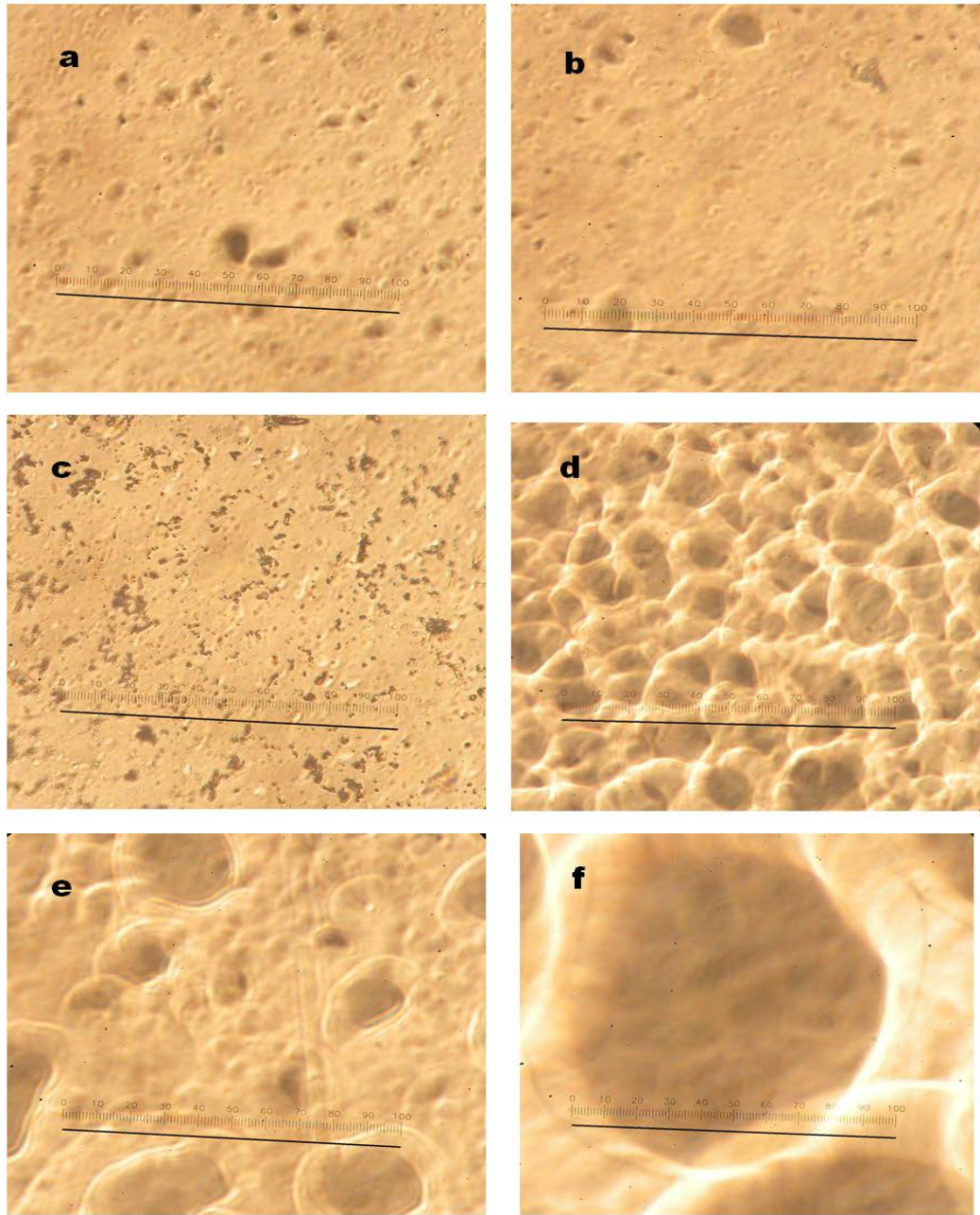


Figure 2.5. Optical micrographs of the wet PET films with (a) DMSO pretreatment at 100 °C, (b) AAm sorption (50 wt % AAm solution) after (a), (c) DMSO pretreatment at 140 °C, (d) AAm sorption (50 wt % AAm solution) after (c), (e) DMSO pretreatment 160 °C, and (f) AAm sorption (50 wt % AAm solution) after (e) [The black line inside each figure represents 100 micrometers].

2.3.3. X-ray diffraction analysis of PET films

X ray diffraction analyses were performed on the pristine PET film, the DMSO pretreated wet PET film (pretreated at 140 °C), the AAm-soaked (50 wt % AAm solution) wet film (after DMSO pretreatment at 140 °C) and the AAm grafted PET film (DMSO-pretreated at 140 °C and γ -ray irradiated with a 50-kGy dose at a 1-kGy/h dose rate in the presence of 1 wt % FeCl₃ after soaking in 50 wt % AAm solution). The investigation showed that the amount of the crystalline phase in the PET film increased significantly after the treatment with DMSO (figure 2.6b). The AAm-soaked wet film showed little increase in the degree of crystallinity compared to the DMSO treated film (figure 2.6c). However, the AAm-grafted film showed a significant decrease in the degree of crystallinity compared to the AAm-soaked wet film (figure 2.6d).

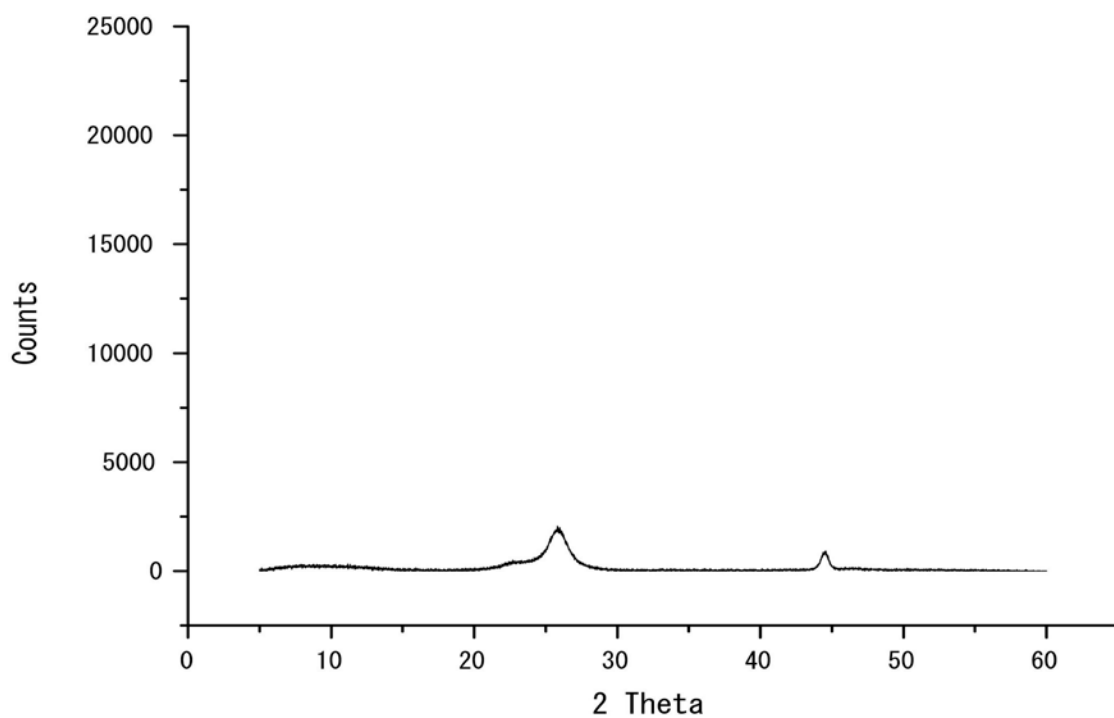


Figure 2.6.(a). X-ray diffractogram of pristine PET film

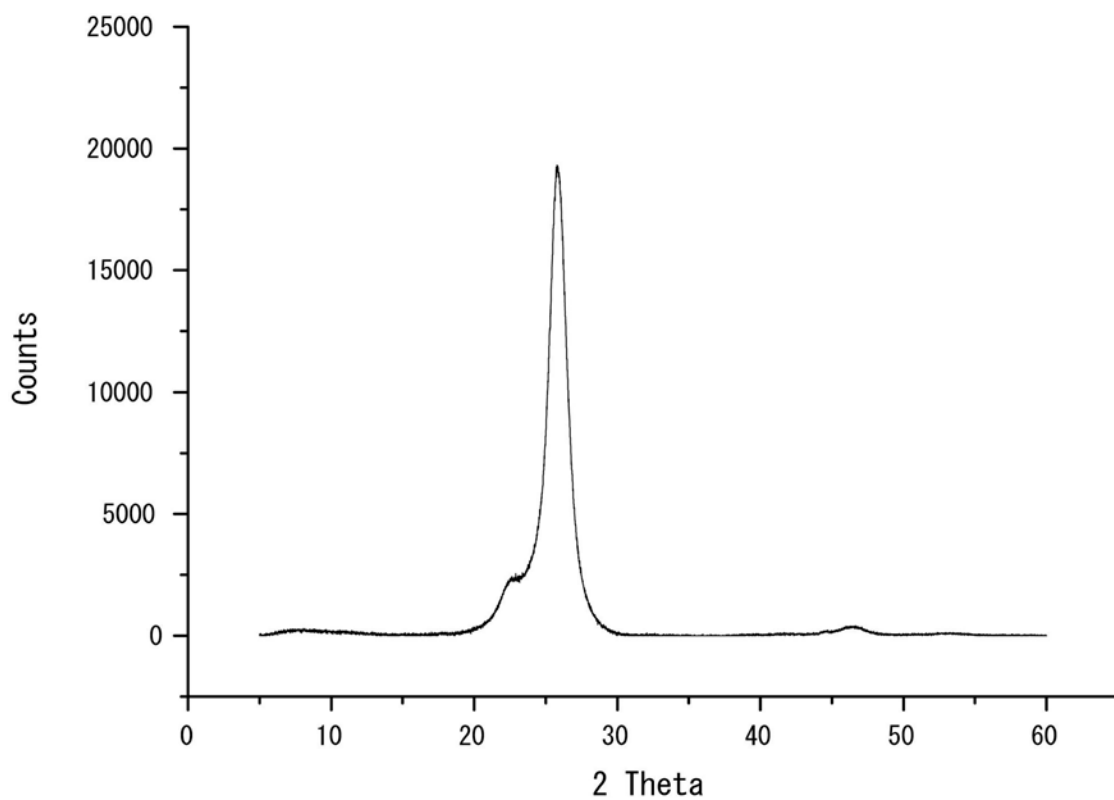


Figure 2.6.(b). X-ray diffractogram of wet PET films with DMSO pretreatment at 140 °C

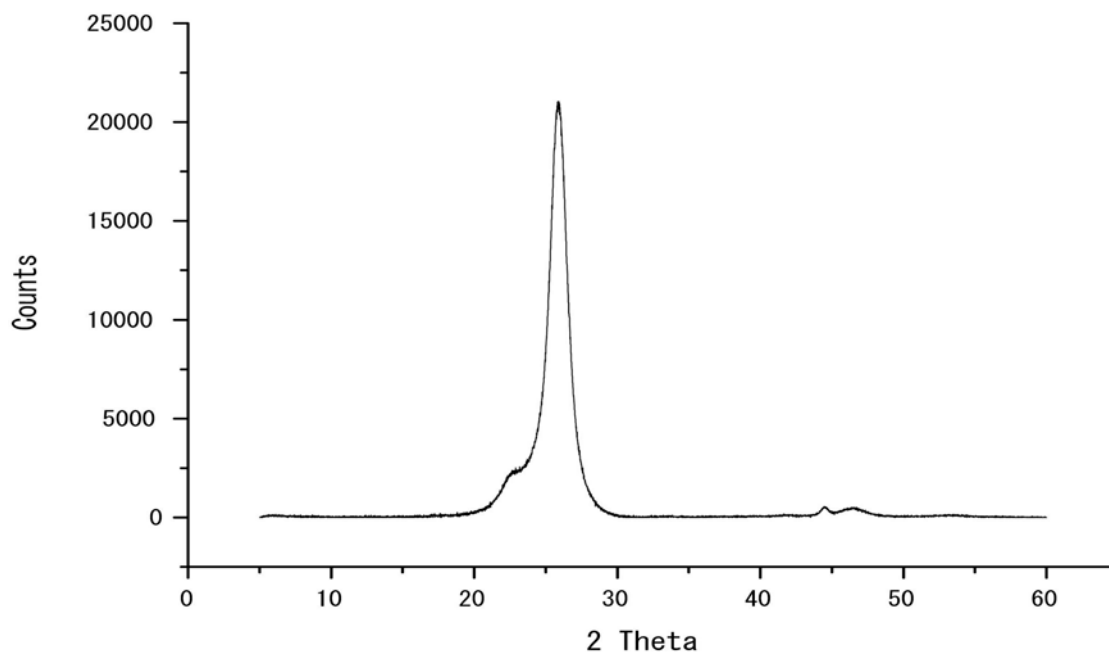


Figure 2.6.(c). X-ray diffractogram of AAm soaked (50 wt % AAm solution) wet film after DMSO pretreatment at 140 °C

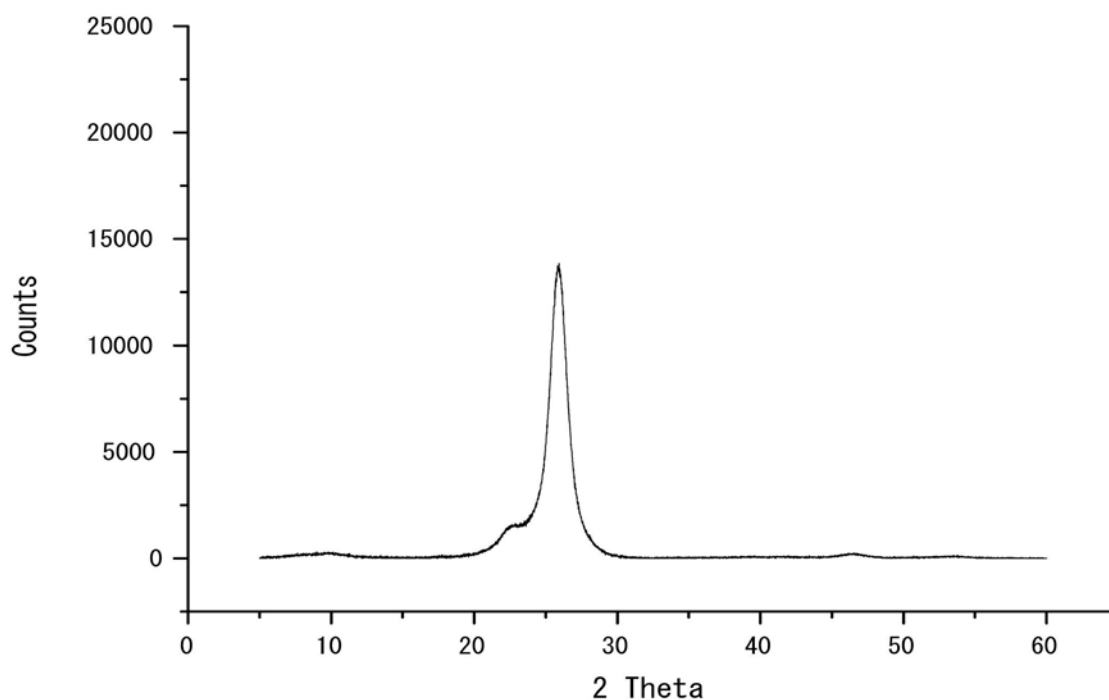


Figure 2.6.(d). X-ray diffractogram of AAm grafted PET film (DMSO pretreated at 140 °C and γ -ray irradiated with a 50-kGy dose at a 1-kGy/h dose rate in the presence of 1 wt % FeCl_3 after soaking in 50 wt % AAm solution)

2.3.4. FTIR spectroscopic analysis of PET films

To investigate the effects of the AAm grafting, the IR spectra of pristine PET and the AAm-grafted PET films were investigated and compared over the wavenumber ranges from 3800 to 2400 cm^{-1} (Figure 2.7(a)) and 1700-1450 cm^{-1} (Figure 2.7(b)). The grafted films used for the IR analyses were DMSO-pretreated at 140 °C and immersed in 25, 40 and 50 wt % AAm solutions. They were γ -ray irradiated with a 50-kGy total dose at a 1-kGy/h dose rate in the presence of 1 wt % FeCl_3 . New peaks appeared which indicated grafting onto PET and were assigned to the AAm groups, while the other characteristic peaks of PET remained almost unchanged. Specifically, in the spectra of the AAm-grafted PET films, the newly observed peaks at 3350 and 3200 cm^{-1} were assigned to the asymmetric and symmetric stretching vibrations of the $-\text{NH}_2$ groups of AAm, respectively. The intensity of the peaks related to the $-\text{NH}_2$ groups increased with the graft-yield percentage as shown in Figure 2.7(a); in addition, a new shoulder peak also appeared at 1672 cm^{-1} , which was assigned to the vibration of carbonyl amide (Figure 2.7(b)). The characteristic peaks of PET and AAm observed in the present study agreed well with the values reported in the literature [Zhang et al., 2010; Coşkun et al., 2006].

As shown in Figure 2.7(c), the ratio of the IR absorption intensity of the 3200 cm^{-1} peak (assigned to the NH_2 symmetric stretching of AAm) to the 3054 cm^{-1} peak (assigned to the aromatic CH stretching of PET) showed a linear dependence on the AAm-graft yield (calculated from the gravimetric data).

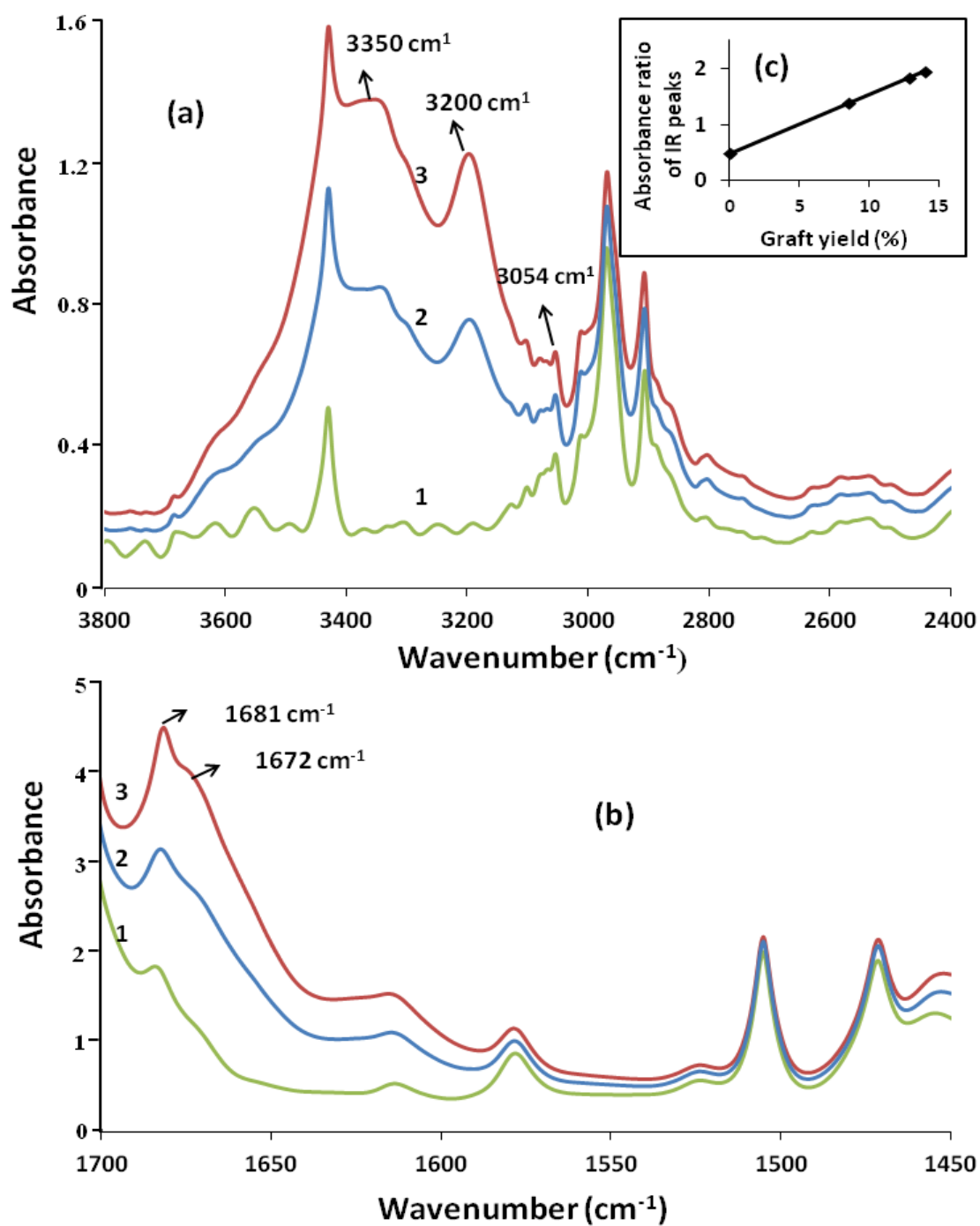


Figure 2.7. FTIR spectra in the (a) higher and (b) lower wavenumber regions for (1) pristine PET, (2) the AAm grafted PET with an 8.6 % graft yield, and (3) with a 12.9 % graft yield. (c) The graft yield dependence of the absorbance ratio of the IR peak at 3200 cm⁻¹ to that at 3054 cm⁻¹.

2.3.5. Scanning electron microscopic analysis of PET films

The surface textures of the pristine PET and AAm-grafted-PET films were observed using SEM to probe the morphological changes after AAm grafting at a smaller scale than the optical microscopy. The grafted films used for the SEM analyses were DMSO-pretreated at 140 °C and γ -ray irradiated with a 50-kGy dose at a 1-kGy/h dose rate in the presence of 1 wt % FeCl₃ after soaking in a 50 wt % AAm solution. An SEM micrograph of the pristine PET film is shown in Figure 2.8(a) and an image of the AAm-grafted PET film and its contrast-enhanced image are shown in Figure 2.8(b) and Figure 2.8(c), respectively. From the micrographs, it is clear that the AAm grafting caused significant changes in the surface morphologies of the PET films.

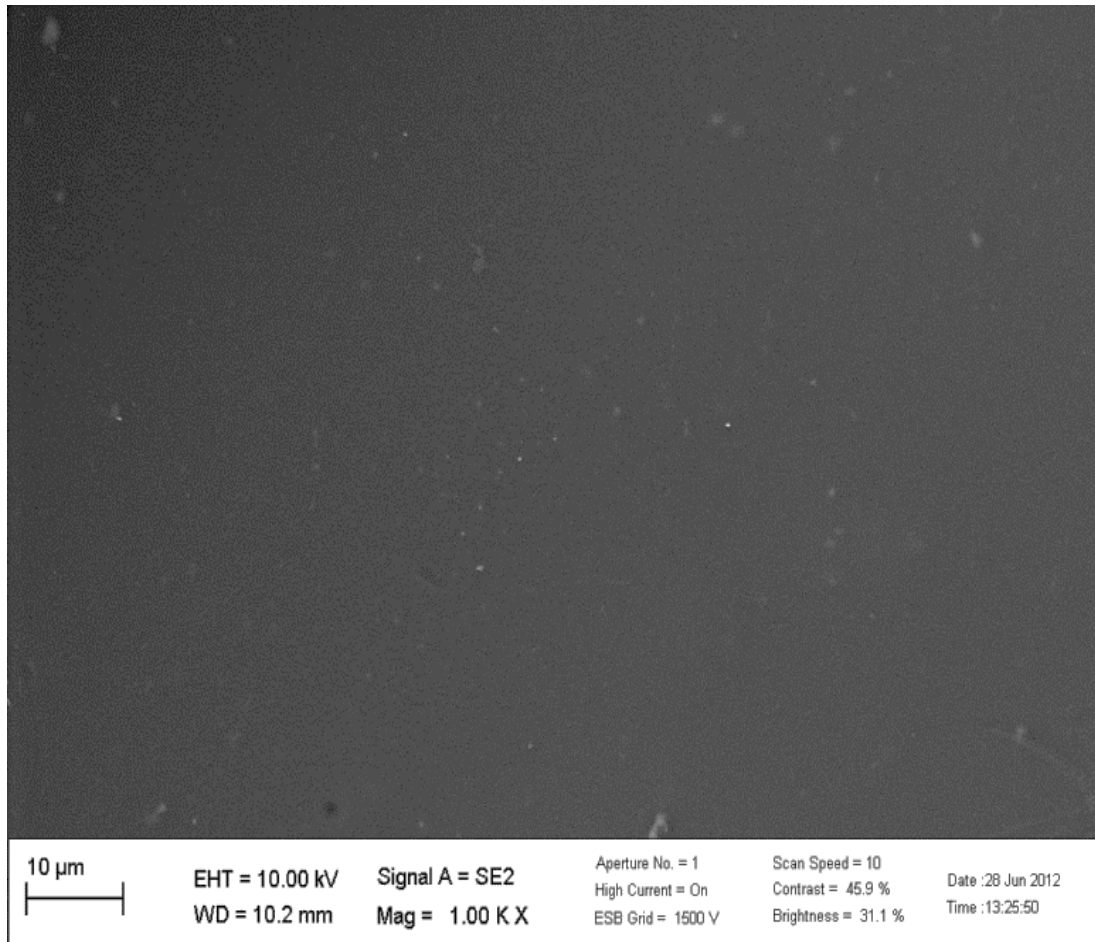


Figure 2.8.(a). SEM micrograph of pristine PET film surface

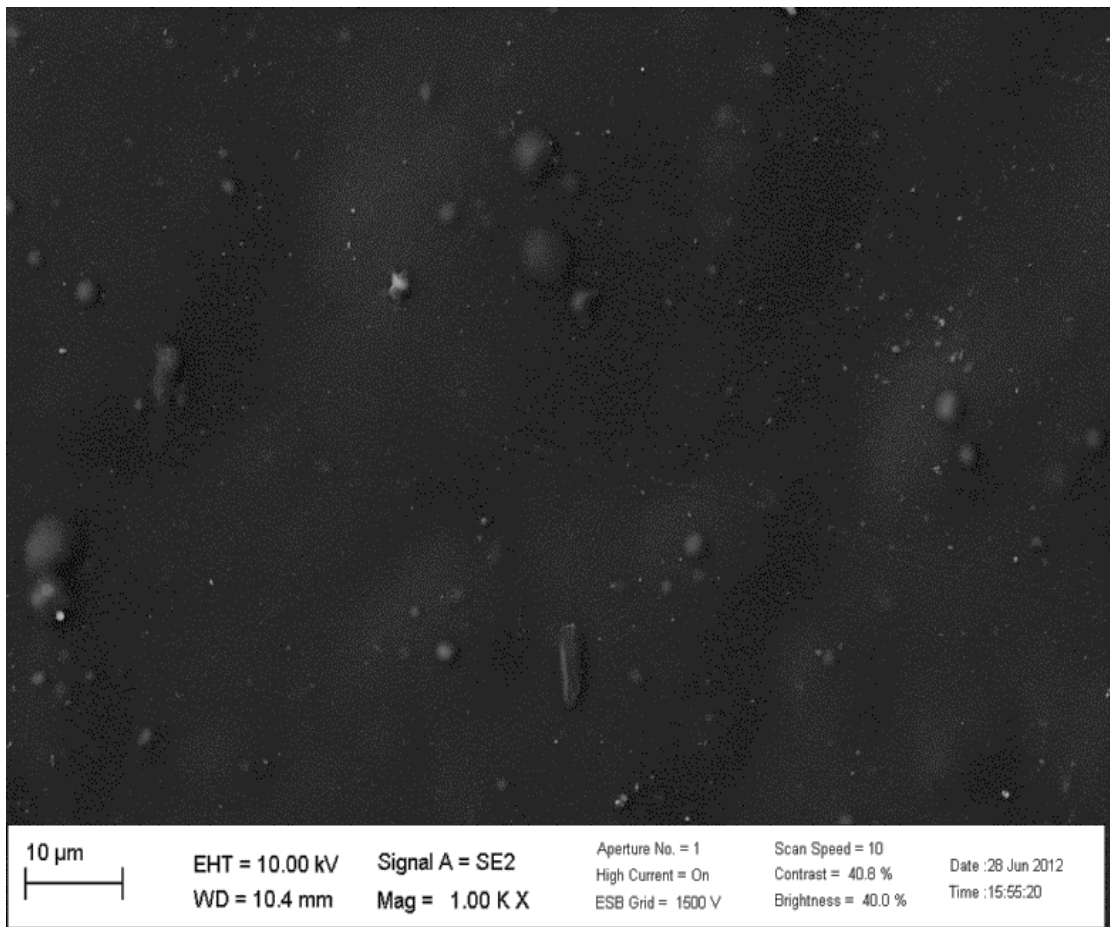


Figure 2.8.(b). SEM micrograph of the AAm grafted PET film

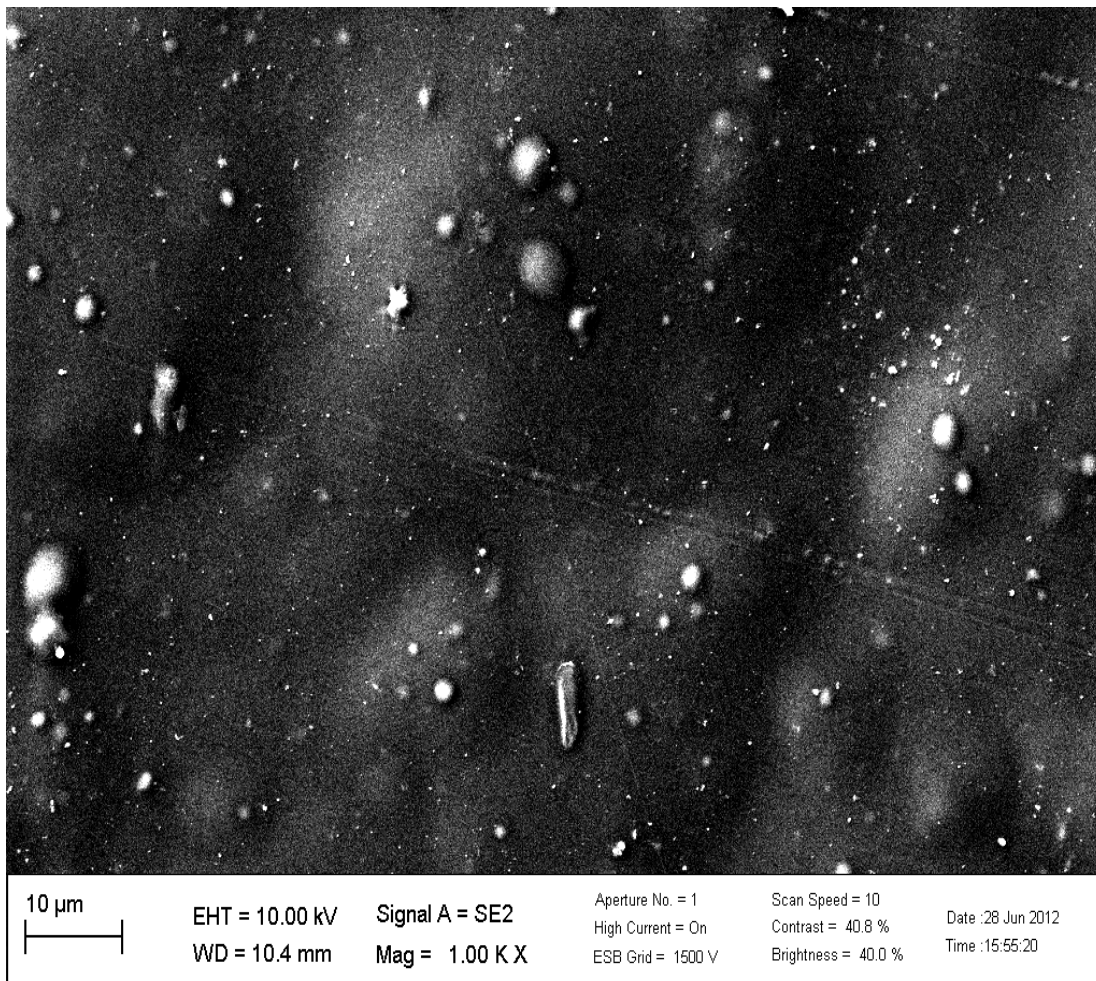


Figure 2.8.(c). The contrast-enhanced image of Figure 2.8.(b).

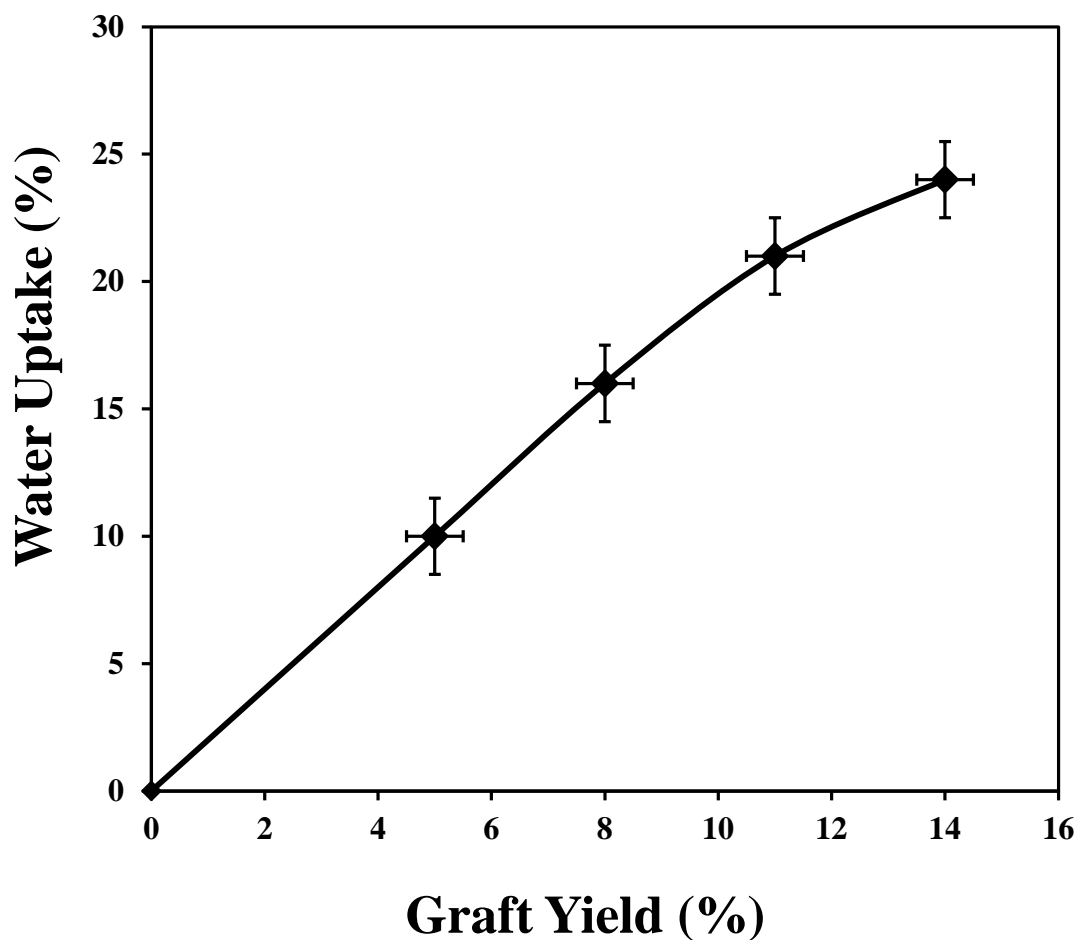


Figure 2.9. The graft yield dependence of the water uptake in the AAm-grafted PET films.

2.3.6. Water uptake measurements

AAm-grafted PET films with different yields (from 0 to 14 %) were prepared for experiments that measured the water uptake (after DMSO pretreatment at 100 or 140 °C, immersion in a 25 or 50 wt % AAm solution, and γ -ray irradiation with a 50-kGy total dose at a 1-kGy/h dose rate in the presence or absence of 1 wt % FeCl₃). The water uptake percentages of the AAm-grafted PET films in distilled water are shown in Figure 2.9. The water uptake percentage simply increased with the graft

yield despite the various preparation conditions.

2.3.7. Hg(II) uptake

The pristine PET film showed no Hg(II) adsorption. To increase the accessibility of the metal ions to the amide groups, the AAm-grafted films (DMSO pretreated at 140 °C, γ -ray irradiated with a 50-kGy dose at a 1-kGy/h dose rate in the presence of 1 wt % FeCl₃ after soaking in 50 wt % AAm solution) with a 14 % graft yield were partially hydrolyzed by KOH (the hydrolysis percentage was approximately 30 %) [Gupta et al., 2003] and the hydrolyzed films were used to examine the Hg(II) adsorption capacity. The hydrolyzed, AAm-grafted PET films showed high removal efficiency for Hg(II) ions (Table 2.2).

Table 2.2. The removal of Hg(II) ions by the pristine PET and the hydrolyzed, AAm-grafted PET films.

Initial Hg(II) concentration (mg/L)	Sample adsorbent	Hg(II) removal (%)
100.0 (\pm 0.5)	Pristine PET film	0
	Hydrolyzed AAm grafted PET film	96 (\pm 1)

2.4. Discussions

In this study, we investigated the γ -ray-induced grafting of AAm onto PET films. During the AAm-grafting, the SEM photographs demonstrated changes in the morphology of the PET surface, indicating the emergence of graft chains on its surface. This observation is the most fundamental condition necessary for water and Hg(II) uptake because the water uptake is related to the hydrophilicity of the AAm group and the Hg(II) uptake is expected to come from the ability of the AAm amide groups to form covalent bonds with Hg(II) ions. In addition to the SEM images, the FTIR spectra of the AAm-grafted PET films also showed peaks that were not observed in the pristine PET film, which were assigned to the symmetric and asymmetric stretching of AAm NH_2 group. We confirmed a linear relationship between the graft yield (obtained using the gravimetric method) and the normalized absorbance at 3200 cm^{-1} (assigned to the NH_2 symmetric stretching of AAm) divided by the absorbance at 3054 cm^{-1} (assigned to the aromatic CH stretching of PET). These features demonstrate the evolution of the AAm graft in the PET matrix. It is very difficult to distinguish between PAAms covalently bonded to PET or firmly entangled in PET, but by taking into account the water solubility of the monomeric AAm or homopolymerized PAAms, it is expected that almost all of the non-bonded PAAm was partitioned into the water after a 24 h washing of the AAm-grafted PET films at high temperature, as described in section 2.2.3. Actually, the water- and Hg(II)-uptake capacities of the grafted films were considerably larger than those of the pristine PET film, reflecting the emergence of grafted AAm-chains in the PET matrix.

During the investigations, we found that the graft yield and, correspondingly,

the adsorption capabilities were increased considerably by the DMSO treatments of the PET surfaces at high temperatures (100-140 °C) prior to the grafting procedure. The highest graft yield obtained in the present work was 15.5 % under conditions of 140 °C for the DMSO-pretreatment temperature, 50 wt % of the AAm monomer and a 100-kGy total dose (dose rate: 1 kGy/h) in 1 wt % of FeCl₃ solution, which is much higher than that achieved using other non-chemical grafting techniques, such as UV irradiation, a CO₂ laser or the SI-ATRP method (Table 2.1). In addition to the increase in the graft yield, the optical micrographs observed after the high-temperature DMSO pretreatments demonstrated the formation of micropores on the PET surfaces. These pores are hypothesized to facilitate the permeation of the AAm-monomers into the PET matrix and to assist the subsequent AAm grafting as well as increase the graft-possible surface area. Because no significant weight losses were measured in the PET specimens after the DMSO pretreatments, the pore formation is not believed to occur via the dissolution or extraction of PET but due to the dislocation of PET polymer chains caused by the interaction between DMSO and PET. The details on this phenomenon are described in the following paragraphs.

As is often experienced, AAm grafting on the pristine PET film was not successful, which might be due to the high degree of crystallization and ordering of the amorphous regions of PET that retards monomer diffusion. In this work, we attempted to treat the PET films with DMSO prior to the AAm- γ -induced grafting, which considerably increased the graft yield. The reasons for adopting DMSO is hypothesized as follows: Solvents with similar solubility parameters to PET will swell the PET's surface, which will provide enough energy to disrupt the intermolecular cohesive forces between the polymer chains and will permit chain mobility [Ribnick

et al., 1972; Knox et al., 1981]. During this process, surface pore formation can occur, depending on the interaction degree between the solvent and the polymer [Jameel et al., 1982]. PET is an (AB) alternating copolymer, where A is the semirigid aromatic segment $-\text{CO}-\text{C}_6\text{H}_4-$ with 9.5 as the solubility parameter (δ) and B is a flexible aliphatic ester $-\text{CO}-\text{O}-\text{CH}_2-\text{CH}_2-$ with $\delta=12.0$. Because the δ of the aliphatic ester portion is very close to that of DMSO ($\delta=12.9$), the situation is favorable for AAm diffusion into PET and the subsequent grafting onto it [Şanlı et al., 1993].

The pretreatment of the PET film with DMSO at high temperatures may increase the interaction between PET and DMSO, and consequently, this interaction can promote pore formation on the PET surface, which facilitates the diffusion of AAm into the polymer matrix. While negligible for the pristine PET film, the AAm solution adsorption increased with increasing DMSO pretreatment temperature over the range from 60 to 140 °C and reached a maximum value, 28 %, for a film treated at a temperature of 140 °C (Fig. 2.1). Although this trend can be explained by the preceding discussion, there were also different features observed for the specimen pretreated at 160 °C (Fig. 2.1): the AAm solution adsorption decreased, which is most likely due to the extraction of the low-molecular-weight PET and partial dissolution of PET in DMSO at 160 °C [Hsieh et al., 1986; Jameel et al., 1981]. The DMSO pretreatment temperature dependence of the AAm-grafting degree agrees with the AAm adsorption, which indicates a close relationship between the AAm absorption amount and the grafting yield.

The effect of the DMSO pretreatment on the structure of the PET film that aids the diffusion of AAm is further revealed via XRD analysis of the films. The XRD results show an increase in the crystalline phase after DMSO treatment. It is

hypothesized that DMSO penetration into the PET matrix enhanced the segmental mobility of the macromolecules in the amorphous phase, which made the diffusion of the AAm monomer into the PET matrix easier. As a result of the enhancement of the segmental mobility of the macromolecules in the amorphous phase induced by DMSO, the volume of the crystallites that existed in PET before the DMSO treatment increased [Martinovich et al., 2006]. Again, the reduction in the degree of crystallinity after AAm grafting might be due to the disordering of the chain structures of the PET matrix caused by the amorphous AAm grafts. Dilution of the crystalline structure of PET after graft co-polymerization is also reported in previous studies [Nasef et al., 2000; Kattan et al., 2006].

As for the homopolymerization inhibitor, the AAm grafting was investigated in the presence and absence of a homopolymerization inhibitor, FeCl_3 : the FeCl_3 addition enabled a significant reduction in the AAm homopolymerization. The formation of a hard gel of homopolymerized PAAm in the AAm solution surrounding the AAm-grafted PET film in absence of FeCl_3 made the separation of the AAm-grafted PET surface from the ungrafted AAm monomers laborious. Conversely, in the presence of FeCl_3 , the surrounding AAm solution formed a soft gel (for high AAm concentration) or remained liquid (for low AAm concentration), and consequently, the separation between the AAm-grafted PET surface and the ungrafted AAm monomers became easier. The facile separation of the grafted product from the monomers is an important consideration for practical application of the graft copolymerization method. Due to the reduction of the homopolymerization, larger amounts of AAm monomers are estimated to be available for the AAm-grafting on PET and the graft yield is thought to increase. In the present study, the graft yield increased over the

AAM-monomer concentration range from 25 to 50 wt % without homopolymerization, while the yield decreased above 50 wt % where noticeable homopolymerization was observed.

We also investigated the total- γ -ray-dose dependence of the graft yield over the range from 20 to 100 kGy. The graft yield increased linearly in the lower dose region and showed saturation at higher doses. This saturation feature could be due to an increase in the obstruction of the AAm-monomer permeation during the γ -ray irradiation due to the growing and extending mass of γ -grafted AAm on the PET surface. In addition to this saturation feature of the dose dependence, the graft yield also showed a similar behavior in the dependence on the γ -ray dose rate from 1.02 to 2.40 kGy/h. One might think the phenomenon also originates from the above mentioned homopolymerization: the graft yield could become lower in the above mentioned homopolymerizing system because the dose-rate increase would promote the AAm homopolymerization, which would increase the solution viscosity and restrict monomer diffusion. However, such an adverse effect was not expected in the present case because the AAm solution was incorporated into the DMSO-pretreated PET films before irradiation. Additionally, the FeCl_3 should reduce the homopolymerization during the γ -ray irradiation.

CHAPTER 3

Selective Hg(II) adsorption from aqueous solutions of Hg(II) and Pb(II) by hydrolyzed acrylamide-grafted PET films

3.1. Introduction

In recent years, discharge of heavy metals in industrial effluent has become a great concern and has been regulated in almost all countries because of its potential threat to human life and health and the environment as mentioned in chapter 1 (section 1.1, 1.2). Mercury and lead are commonly used in many industries as raw materials or additives, and have been classified as priority pollutants by the US Environmental Protection Agency [Molinari et al., 2004]. A special characteristic of mercury is that it can be enriched by organisms and can be converted to highly toxic metal-organic complexes. The environmental destruction caused by mercury at Minamata, Japan and Iraq are well known [Bockris, 1997]. Immediate removal of mercury from industrial effluent by appropriate treatment is necessary to prevent formation of highly toxic products.

Mercury and lead both appear in industrial effluent, and are structurally very similar and considered soft acids. Consequently, separation of Hg(II) from Pb(II) can be more difficult than from other heavy metals such as Cu(II) or Zn(II). The high

affinity of Hg(II) for functional groups containing active hydrogen, such as thiol, thioether, amine, and amide groups, is often used in the removal of Hg(II) [Shah et al., 1996; Chiarle, 2000; Zhu et al., 2005]. Hg(II) can form covalent bonds with amide groups, [Sonmez et al., 2002] but because of the presence of electron-withdrawing carbonyl groups, the amide nitrogen atoms are typically not suitable to form coordination bonds with transition metal ions. Therefore, amide group-functionalized copolymers have been studied for selective Hg(II) adsorption [Li et al., 2005; Ştefan et al., 2008; Sonmez et al., 2003]. In chapter 2 dimethyl sulfoxide (DMSO)-assisted graft copolymerization of acrylamide (AAM) on PET films by γ irradiation is described. This chapter describes the potential of selective Hg(II) adsorption by hydrolyzed AAM-grafted PET films from mixtures of Hg(II) and Pb(II). The kinetics of competitive adsorption of Hg(II) and Pb(II) are studied and the selective Hg(II) adsorption kinetic data are fitted with pseudo-first-order and pseudo-second-order equations. Competitive adsorption isotherms of Hg(II) and Pb(II) are studied and selective Hg(II) equilibrium adsorption data are fitted with the Langmuir isotherm model. The effect of pH on the selective adsorption and reusability of the adsorbent is also studied.

3.2. Experimental

3.2.1. Materials and reagents

Commercial PET films (Teijin DuPont films, G2) with a thickness of 50 μm were kindly provided by Teijin Co. Ltd (Osaka, Japan). The PET films were cut into

small pieces (2×2 cm), washed with acetone, and dried in a vacuum oven before use. AAm and FeCl₃ were procured from Sigma Aldrich. DMSO and KOH were supplied by Wako Pure Chemical Industries, Ltd. Hg(II) acetate and basic Pb(II) acetate (anhydrous, Chameleon Reagent) and Hg(II) and Pb(II) standard solutions (Merck) were used as the source of the adsorbate and for the calibration of metal concentrations, respectively.

3.2.2. Instruments and apparatus

The PET films were analyzed by Fourier transform infrared (FTIR) spectroscopy (Jasco, FTIR 620) in the wavenumber range of 400–4000 cm⁻¹. Scanning electron microscopy (SEM) observation of the carbon-coated PET films was performed using an SEM (Zeiss, Ultra55) operating at 3 keV. The concentrations of metal ions in the solutions were analyzed by inductively coupled plasma-mass spectrometry (Agilent7700x ICP MS).

3.2.3. Grafting of AAm onto the PET films by γ -ray irradiation

The dry PET films weighing W_{pristine} were soaked in DMSO for 0.5 h at 140 °C. As described in chapter 2, section 2.2.3, the grafting of AAm onto the DMSO treated PET film was carried out and the graft yield was determined from the percent increase in weigh.

3.2.4. Hydrolysis of AAm-grafted PET films

An AAm-grafted PET film with a graft yield of 14% (obtained using 50 wt% AAm and γ -ray dose of 50 kGy) was hydrolyzed in 10% KOH at 60 °C for 1 h. The percentage of amide groups hydrolyzed to carboxylate groups were determined as described in chapter 2, section 2.2.9.1.

3.2.5. Metal ion adsorption by the hydrolyzed AAm-grafted PET film

Hydrolyzed AAm-grafted films (20 mg) were soaked in aqueous solutions (5 mL) containing equal amounts of Hg(II) and Pb(II) with different known initial metal ion concentrations and pH for 40 min at room temperature (25 °C). The initial pH of the solution was adjusted using HCl or NaOH solution. No effort was made to control the solution pH during the experiments. Metal-loaded films were washed and dried prior to examination.

3.2.6. Determination of metal ion uptake capacity

The metal ion uptake capacity of the film was calculated as follows:

$$Q = V(C_1 - C_2)/W, \quad \dots\dots\dots (3.1)$$

where Q is the adsorption amount (mg/g), W is the weight of the film (g), V is the volume of the solution (L), and C_1 and C_2 are the concentrations (mg/L) of metal ion before and after adsorption, respectively.

3.2.7. Desorption of metal ions

The desorption of Hg(II) and Pb(II) ions from the modified PET films was achieved by treatment in an aqueous solution of HCl (2 M) for 30 min. The percent desorption was calculated using the following equation:

$$\text{Percent desorption} = \left(\frac{\text{Amount of ions (mg) desorbed}}{\text{Adsorbed amount of ions (mg) by adsorbent}} \right) \times 100. \quad \dots\dots\dots (3.2)$$

3.3. Results and discussion

3.3.1. Preparation and characterization of the adsorbent film

AAm-grafted PET films were prepared by graft copolymerization induced by γ -rays using DMSO as a swelling agent. AAm-grafted PET films with a graft yield of 14% were hydrolyzed by treatment in KOH to convert some $-\text{CONH}_2$ groups to ionic $-\text{COOK}$ ones (30% hydrolysis) to reduce the hydrogen bonding between $-\text{CONH}_2$ groups and facilitate the access of metal ions to the amide groups [Gupta et al., 2003; Rahman et al., 2013]. The adsorption capacity of the AAm-grafted PET films for Hg(II) ions increased from 15 to 70 mg/g after hydrolysis. The Hg(II) adsorption capacity of the hydrolyzed AAm-grafted PET film is much higher than that of the only PET-based adsorbent showing selective adsorption of Hg(II) over Pb(II) reported to date [Temoçin et al., 2010]. Some other adsorbents such as activated carbon obtained from palm oil byproducts, [Wahi et al., 2009] modified starch adsorbents, [Huang et al., 2011] and poly(2-hydroxyethyl methacrylate (HEMA)/chitosan) membranes

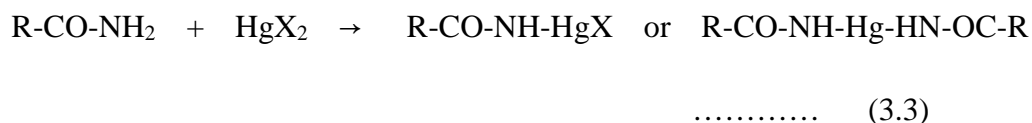
[Bayramoglu et al., 2007] have been reported to show similar affinities for Hg(II) and Pb(II). The adsorption capacities of these adsorbents are compared in Table 3.1.

Table 3.1. Hg(II) and Pb(II) adsorption capacity of AAm-grafted PET and hydrolyzed AAm-grafted PET compared with those of other adsorbents (from single metal solutions)

Adsorbent	Hg(II) adsorption capacity (mg/g)	Pb(II) adsorption capacity (mg/g)
Pristine PET film [present study]	0 ^a	0 ^a
AAm-grafted PET film [present study]	15.0 ^a	1.3 ^a
Hydrolyzed AAm-grafted PET film [present study]	70.0 ^a	8.0 ^a
4-Vinyl pyridine/2-hydroxyethylmethacrylate-grafted PET fiber [Temoçin et al., 2010]	15.72 ^b	1.21 ^b
Activated carbon obtained from palm oil by products [Wahi et al., 2009]	52.67 ^b	48.96 ^b
Modified starch-based adsorbent [Huang et al., 2011]	131.2 ^b	123.2 ^b
Poly(HEMA/chitosan) membranes [Bayramoglu et al., 2007]	~39.5 ^a	~37.0 ^a

^aexperimental value, ^bcalculated from the Langmuir model

To investigate the chemical interactions in the modified films, FTIR spectra of an ungrafted PET film, AAm-grafted PET film, hydrolyzed AAm-grafted PET film, and Hg(II)-loaded hydrolyzed AAm-grafted PET film were measured (Figure 3.1). The FTIR spectrum of the PET film exhibited peaks characteristic of the chemical structure of PET with OH stretching at 3430 cm⁻¹, aromatic C-H stretching at 3054 cm⁻¹, and aliphatic C-H stretching at 2969 and 2907 cm⁻¹. The spectrum of the grafted film showed strong peaks at 3200 and 3350 cm⁻¹ that are assigned to the -NH₂ group of AAm, and were absent from the spectrum of the ungrafted PET film [Coşkun et al., 2006; Gupta et al., 2003]. The intensity of these peaks decreased slightly after hydrolysis. However, the intensity of these peaks was very low in the spectrum of the Hg(II)-loaded hydrolyzed AAm-grafted PET film, which confirms the involvement of grafted AAm groups in Hg(II) binding. It is known that amide compounds react with mercuric ions under typical conditions to form monoamido-mercury or diamido-mercury compounds, as shown in eq. 3.3. Similar compounds might have formed upon adsorption of Hg(II) onto the hydrolyzed AAm-grafted PET film.



The surface morphology of the hydrolyzed AAm-grafted PET film before and after Hg(II) loading was investigated (Figure 3.2). The SEM image of the film before Hg(II) loading [Figure 3.2(a)] showed some pores on its surface, and these pores were almost closed after Hg(II) loading [Figure 3.2(b)] through some type of crosslinking. Such a crosslinking effect between Hg(II) and grafted polyacrylamides has been observed previously [Sonmez et al., 2002].

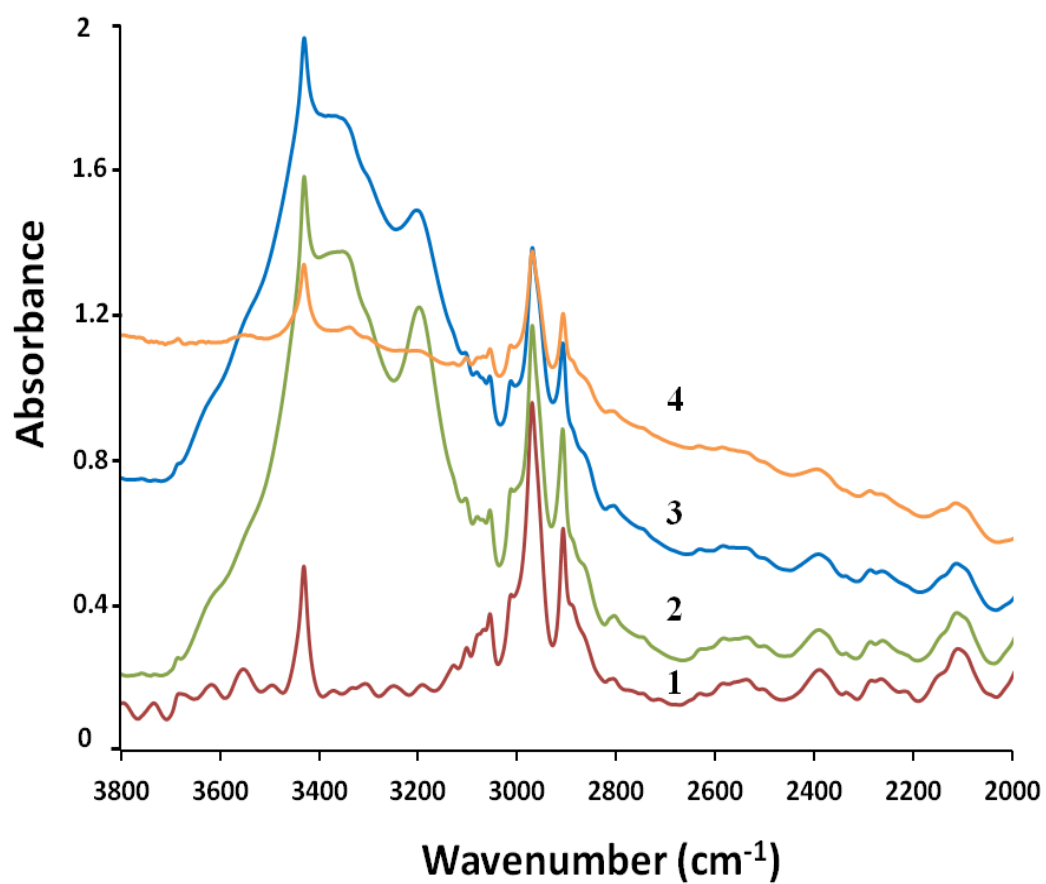
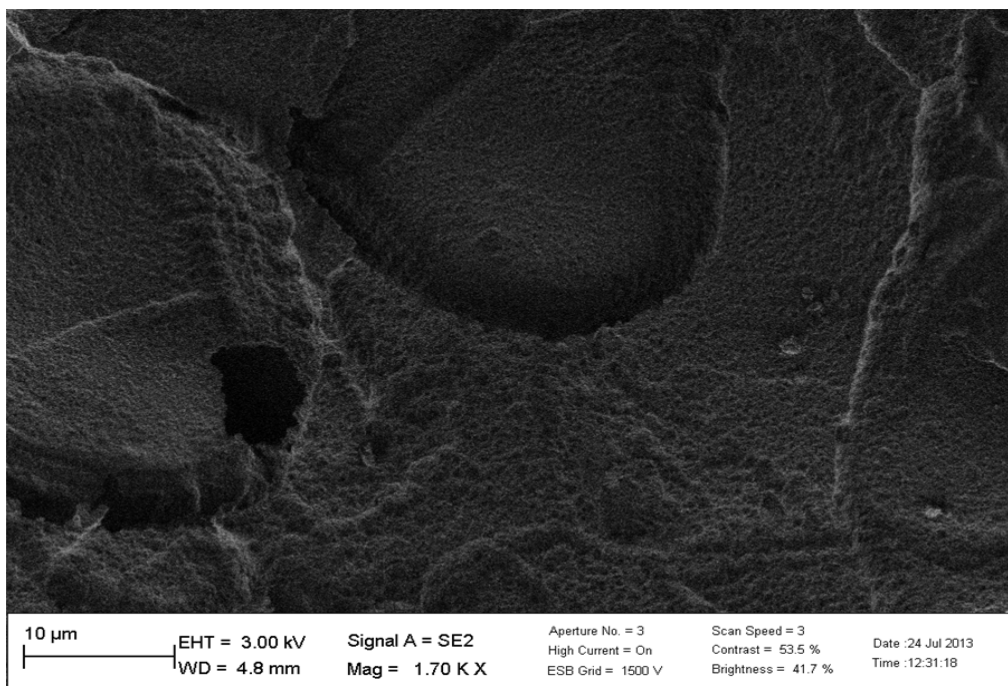


Figure 3.1. FTIR spectra of (1) ungrafted PET film, (2) AAm-grafted PET film, (3) hydrolyzed AAm-grafted PET film, and (4) Hg(II)-loaded hydrolyzed AAm-grafted PET film.

(a)



(b)

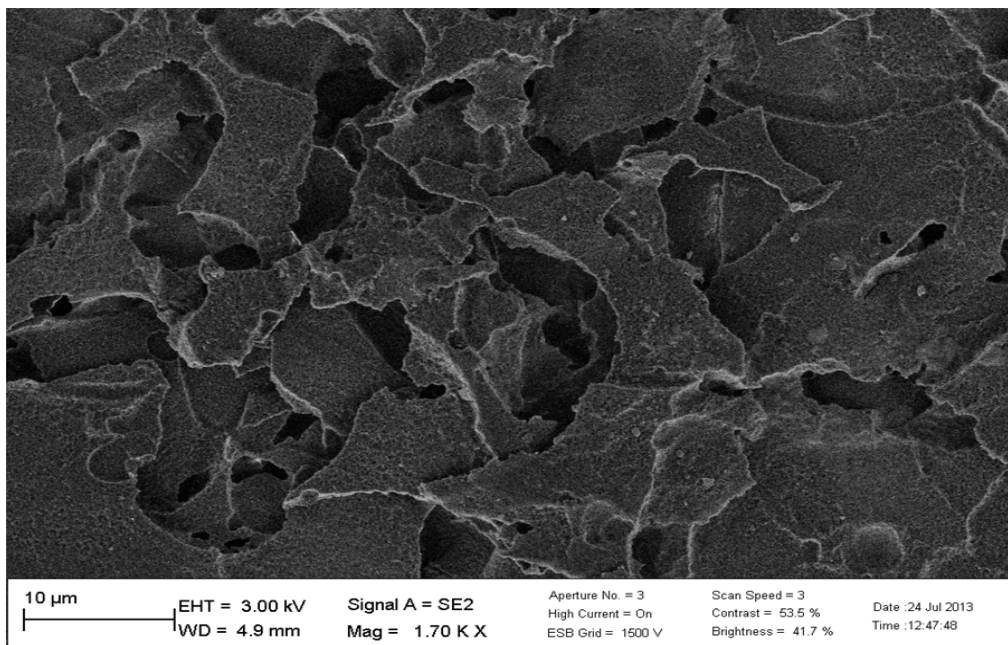


Figure 3.2. SEM images of hydrolyzed AAm-grafted PET films (a) before Hg(II) loading, and (b) after Hg(II) loading.

3.3.2. Selective adsorption of Hg(II) ions by the adsorbent film from aqueous solutions containing Hg(II) and Pb(II)

The hydrolyzed AAm-grafted film adsorbed 24 and 5 mg/g of Hg(II) and Pb(II), respectively, from a binary solution containing Hg(II) and Pb(II) with the same initial concentration of 100 mg/L at pH 4.5. The selectivity of an adsorbent is often represented by the selectivity coefficient, α , which is measured from the distribution coefficient (K_d). K_d refers to the affinity of an adsorbent for a particular ion in the presence of interfering ions, and can be calculated using eq. (3.4) [Yan et al., 2011].

$$K_d = V(C_0 - C_f)/C_f W, \quad \dots\dots\dots (3.4)$$

where K_d is the distribution coefficient (mL/g), C_0 and C_f (mg/mL) are the initial and equilibrium concentrations of a metal species, respectively, V (mL) is the volume of the testing solution, and W (g) is the amount of adsorbent.

The selectivity coefficient, α (dimensionless), for a specific metal ion in the presence of competitor ions can be calculated by Eq. (3.5):

$$\alpha = K_d(T)/K_d(I), \quad \dots\dots\dots (3.5)$$

where $K_d(T)$ is the K_d value of the target metal (Hg(II) ions in this case), and $K_d(I)$ is the K_d value of the other metal in the mixed metal solution (Pb(II) ions here). The calculated selectivity coefficient for the hydrolyzed AAm-grafted PET film to bind Hg(II) over Pb(II) is $\alpha_{(\text{Hg/Pb})} = 19.2$ for an initial concentration of 100 mg/L and pH of 4.5. The reason behind this high selectivity is that the amide groups of the hydrolyzed AAm-grafted PET film can easily form covalent bonds with the Hg(II) ions, but because of the presence of electron-withdrawing carbonyl groups, the amide nitrogen atoms cannot easily form coordination bonds with the Pb(II) ions.

3.3.3. Adsorption kinetics of selective Hg(II) adsorption

The kinetics of selective Hg(II) adsorption studied at an initial concentration of 100 mg/L and initial pH of 4.5 are presented in Figure 3.3. Adsorption occurred rapidly and reached equilibrium after 40 min, at which point the ratio of the final to initial concentration of Hg(II) in solution was almost zero (0.04). The adsorption of Pb(II) was negligible with respect to that of Hg(II). This result indicates the effectiveness of the adsorbent for quick and selective removal of Hg(II) from a dilute solution. Conventional methods for metal removal such as precipitation, membrane filtration, and ion exchange are much less efficient than our PET-based films at low concentration [Zhang et al., 2004].

The experimental data for selective Hg(II) adsorption was fitted with two commonly used kinetic models, the pseudo-first-order and pseudo-second order models [Ho et al., 2006]. The pseudo-first-order equation can be expressed as

$$dQ_t/dt = k_1 (Q_e - Q_t), \quad \dots\dots\dots (3.6)$$

where Q_t and Q_e are the amount of ions adsorbed (mg/g) at any specific time and equilibrium time, respectively, and k_1 is the rate constant (min^{-1}) of first-order adsorption. Integration of Eq. (3.6) by applying boundary conditions and rearrangement to linear form gives

$$\log (Q_e - Q_t) = \log Q_e - (k_1/2.303) t. \quad \dots\dots\dots (3.7)$$

The pseudo-first-order rate constants can thus be determined experimentally by plotting $\log (Q_e - Q_t)$ against t as shown in Figure 3.4.1. The experimental and theoretical Q_e values, first-order rate constant and correlation coefficients (R^2) are given in Table 3.2.

The pseudo-second-order equation is expressed as

$$dQ_t/dt = k_2 (Q_e - Q_t)^2, \quad \dots\dots\dots (3.8)$$

where k_2 ($\text{g min}^{-1} \text{mg}^{-1}$) is the rate constant of second-order adsorption. Integration of eq. (3.8) by applying boundary conditions and rearrangement to linear form gives

$$t/Q_t = (1/k_2 Q_e^2) + t/Q_e. \quad \dots\dots\dots (3.9)$$

The pseudo-second-order rate constants were determined experimentally by plotting t/Q_t against t , as illustrated in Figure 3.4.2. The second-order kinetic parameters for selective Hg(II) adsorption are listed in Table 3.2. The kinetic parameters indicate that the pseudo-second-order kinetic model interprets experimental kinetic data better than the pseudo-first-order one. The pseudo-first-order equation (eq. (3.6)) suggests that the adsorbing molecule interacts with one adsorption site, whereas the pseudo-second-order equation (eq. (3.8)) implies that the adsorbing molecule reacts with two adsorption sites. The obtained results indicate that most of the Hg(II) ions reacted with two amide groups of the hydrolyzed AAm-grafted PET film to form diamido-mercury species.

Table 3.2. Pseudo-first-order and pseudo-second-order rate constants for selective Hg(II) adsorption

Q_e (exp) (mg/g)	Pseudo-first-order rate constant			Pseudo-second-order rate constant		
	Q_e (theo) (mg/g)	k_1 (min^{-1})	R^2	Q_e (theo) (mg/g)	k_2 (g min^{-1} mg^{-1})	R^2
24	16.68	0.0652	0.965	28.81	0.0038	0.998

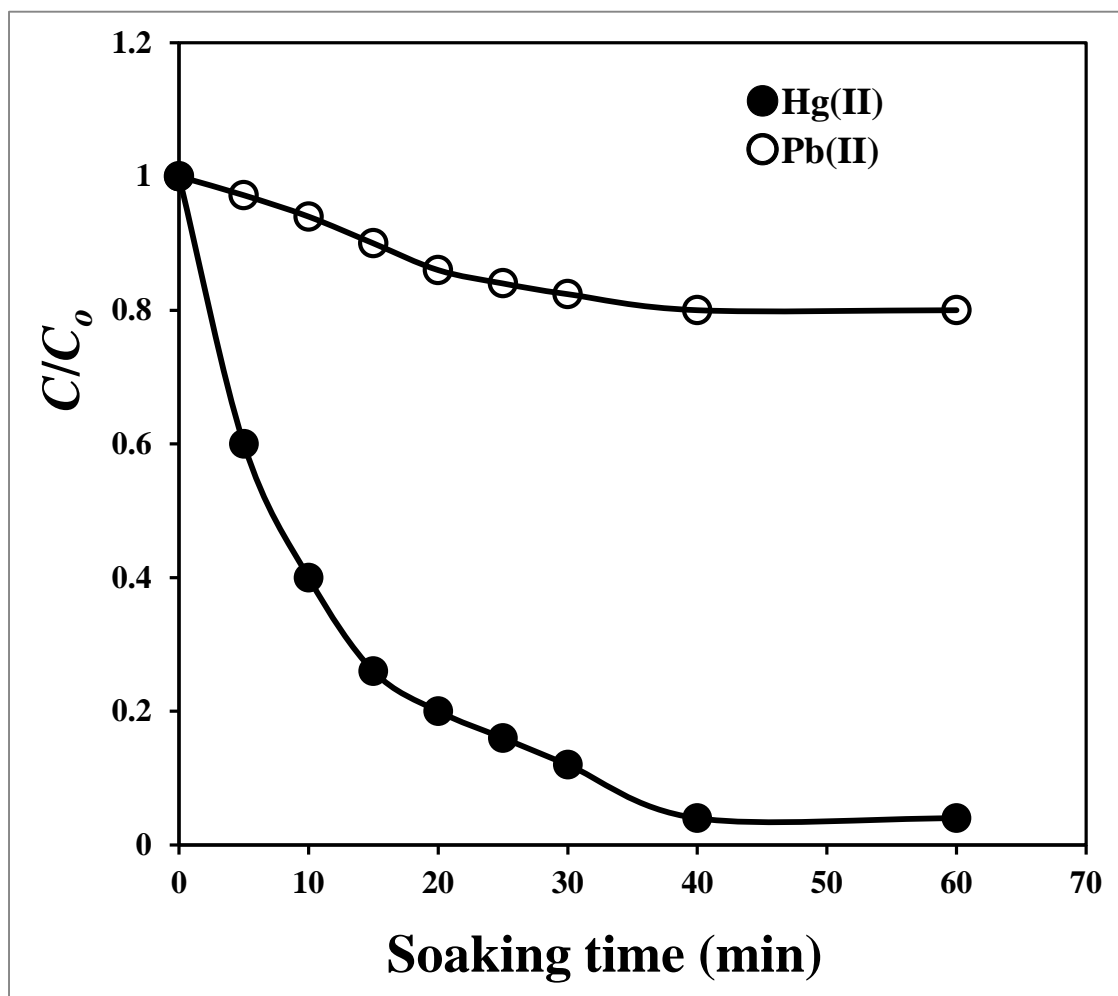


Figure 3.3. Adsorption kinetics for competitive adsorption of Hg(II) and Pb(II) by hydrolyzed AAm-grafted films with the same initial concentration of metal ions (pH 4.5; initial concentration = 100 mg/L).

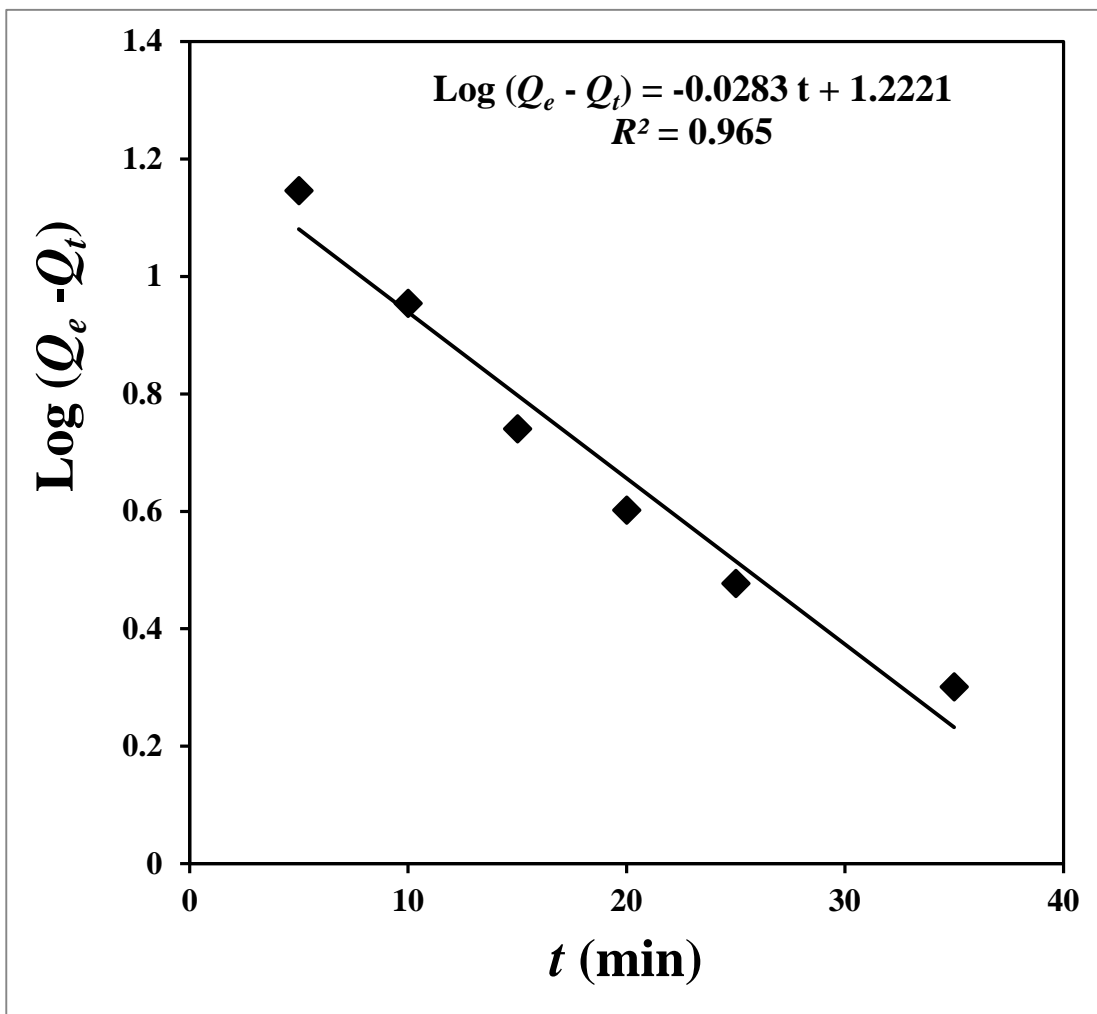


Figure 3.4.1. Pseudo-first-order plot for selective Hg(II) adsorption.

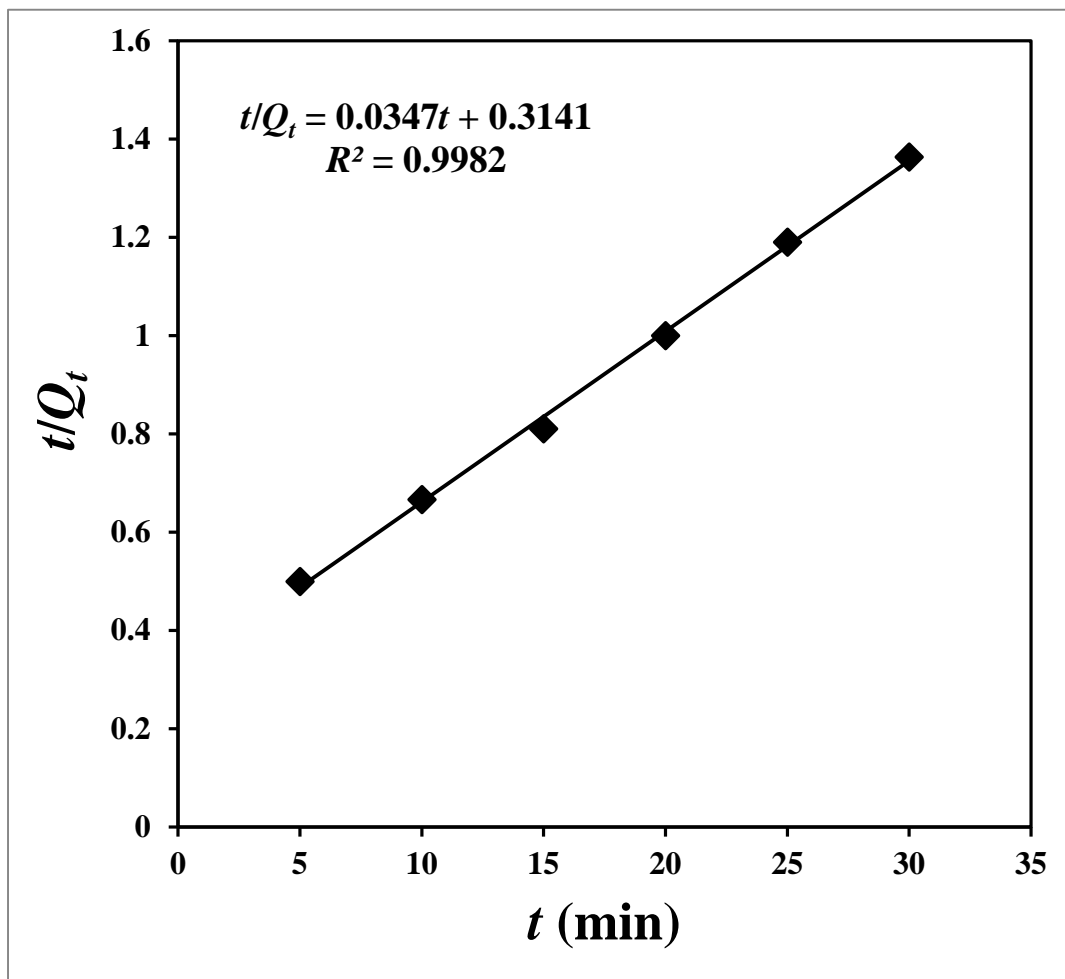


Figure 3.4.2 Pseudo-second-order plot for selective Hg(II) adsorption.

3.3.4. Equilibrium adsorption isotherms of selective Hg(II) adsorption

Adsorption isotherms for competitive adsorption of Hg(II) and Pb(II) with the same initial concentrations are shown in Figure 3.5. As the equilibrium concentration increases, adsorption of Hg(II) increases gradually to reach a saturated level, and the adsorption of Pb(II) showed a slight increase. Results indicated high selectivity of the adsorbent for Hg(II) over the entire initial concentration range studied (100–500 mg/L).

The well-established Langmuir isotherm model [Langmuir et al., 1918] was used to predict the selective Hg(II) adsorption data. The Langmuir model is based on the assumption of monolayer adsorption of an adsorbate by identical adsorption sites of a structurally homogeneous adsorbent. The linear form of the Langmuir isotherm is

$$C_e/Q_e = C_e/Q_o + (1/Q_o b), \quad \dots\dots\dots (3.10)$$

where C_e is the equilibrium concentration (mg/L), Q_o is the monolayer saturation adsorption capacity of the adsorbent (mg/g), Q_e is the equilibrium adsorption capacity, and b is the Langmuir adsorption constant (L/mg). With the experimental data given in Figure 3.6, a plot of C_e/Q_e versus C_e was drawn; it is shown in Figure 3.6. The linear relationship between C_e/Q_e and C_e indicates that the adsorption behavior follows the Langmuir adsorption isotherm and suggests that selective Hg(II) adsorption involved formation of a monolayer on the surface of the hydrolyzed AAm-grafted PET films. Values of b , Q_o , and correlation coefficients (R^2) are also given in Figure 3.6.

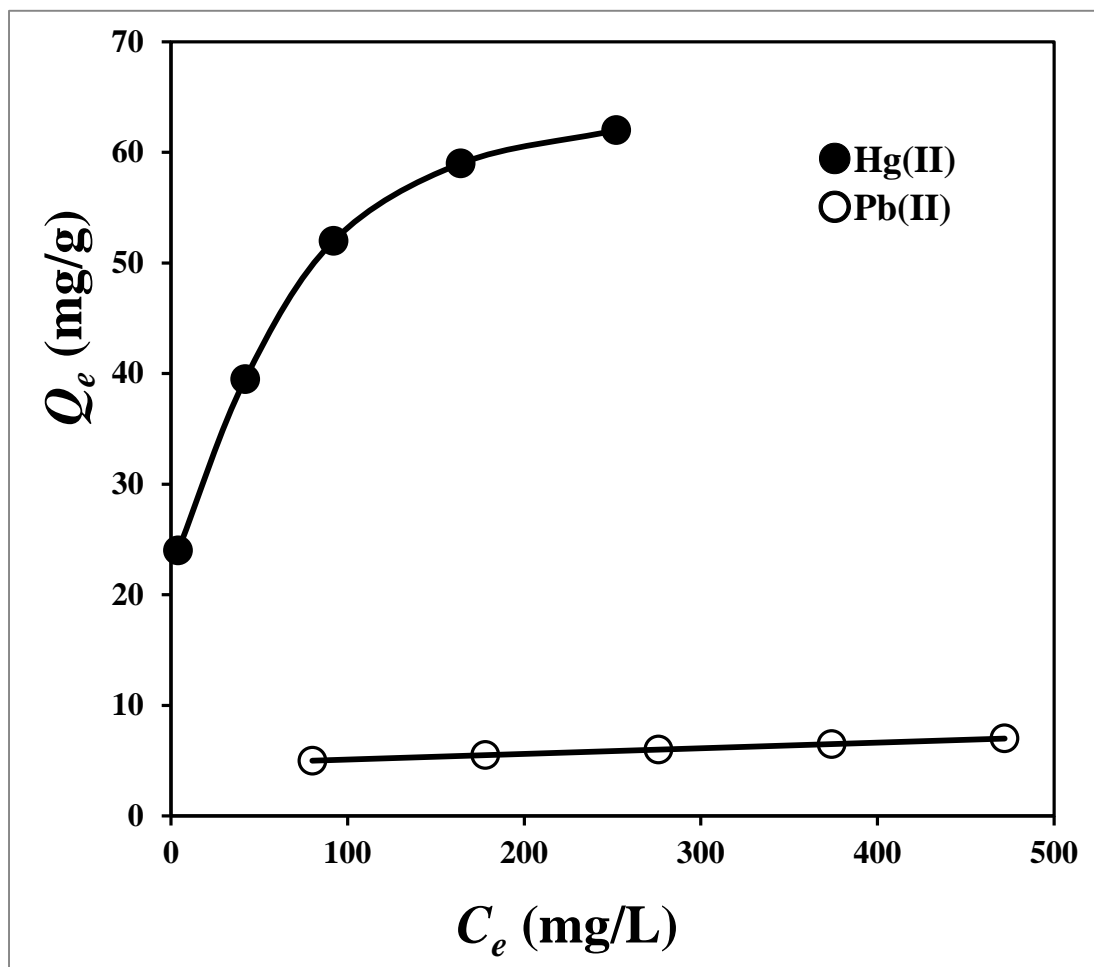


Figure 3.5. Equilibrium adsorption isotherm for competitive adsorption of Hg(II) and Pb(II) by the hydrolyzed AAm-grafted films with the same initial concentrations of metal ions (pH 4.5; $t = 40$ min).

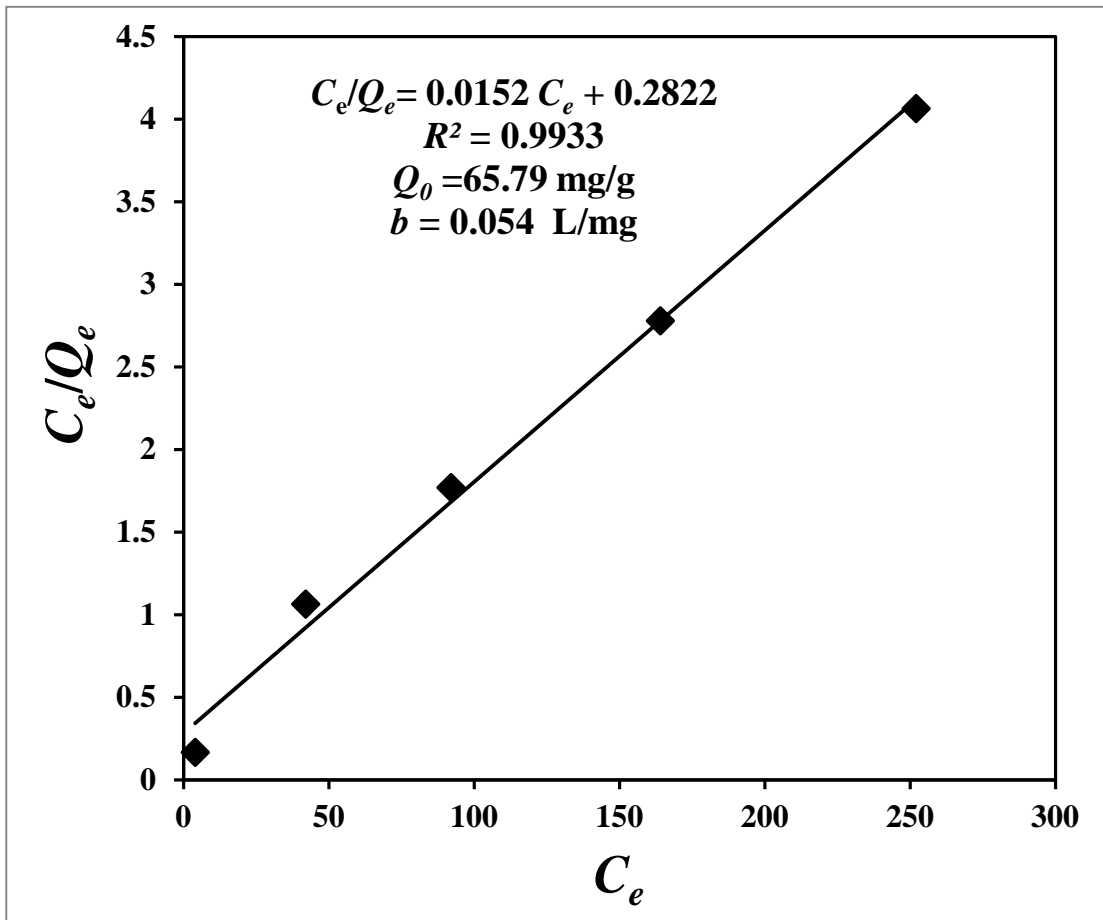


Figure 3.6. Langmuir isotherm plot for selective Hg(II) adsorption.

3.3.5. Effect of pH on selective Hg(II) adsorption

It is known that pH has a substantial influence on the adsorption process because it determines the surface behavior of the adsorbent and the availability of metal ions in solution. Selective adsorption of Hg(II) from mixtures of Hg(II) and Pb(II) with different initial pH were studied. The experimental results for an initial concentration of 500 mg/L are shown in Figure 3.7. At low pH, adsorption of both Hg(II) and Pb(II) was low, which may be caused by protonation of the adsorbent surface. Between pH 4 and 5, the adsorbent showed excellent selective adsorption of

Hg(II). Above pH 5, the Hg(II) adsorption decreased because of formation of a hydrolyzed product such as HgO or other polynuclear hydroxo-bridged species and precipitation of basic salts [Rocha et al., 2009]. For initial concentrations of ≥ 500 mg/L, some yellow precipitate was clearly observed above pH 5, and the decrease of Hg(II) adsorption above pH 5 was considerable for such concentrations. However, hydrolysis and/or precipitation effects were not observed for a low initial concentration of 100 mg/L, and adsorption capacity remained almost unchanged from pH 4.5 to 5.6 at this concentration.

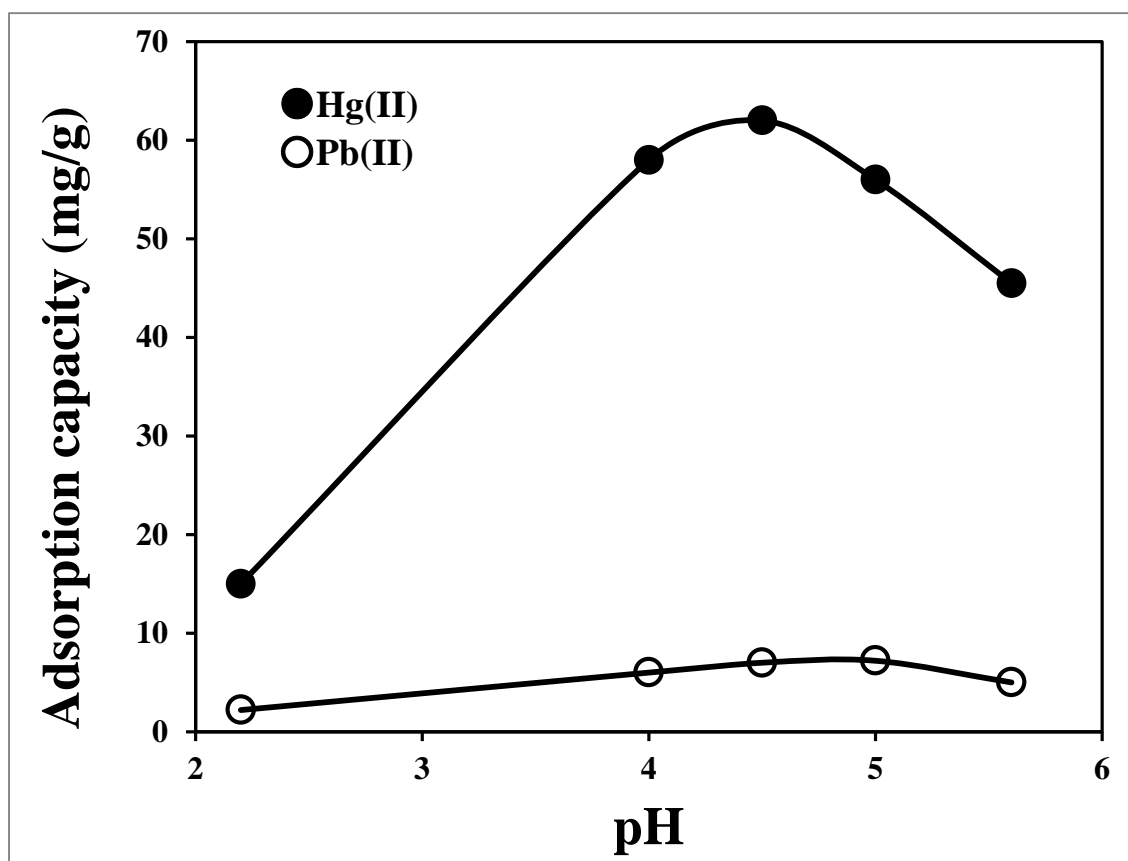


Figure 3.7. Effect of pH on the competitive adsorption of Hg(II) and Pb(II) by the hydrolyzed AAm-grafted films with the same initial concentration of metal ions (initial concentration = 500 mg/L; $t = 40$ min).

3.3.6. Desorption of Hg(II) and reuse of the adsorbent

After the selective adsorption of Hg(II), the adsorbed metal ions were desorbed using 2 M hydrochloric acid. Desorption took place rapidly to reach equilibrium within 10–20 min. The desorption ratio was 98.8%. The regenerated adsorbents were reused for selective Hg(II) adsorption from aqueous solutions containing Hg(II) and Pb(II) for five successive cycles, as shown in Figure 3.8. The sorption capacity of the regenerated adsorbent showed very little decrease, indicating that the regenerated adsorbents are effective for readsorption of Hg(II). Therefore, the adsorbent can be used repeatedly for selective Hg(II) adsorption.

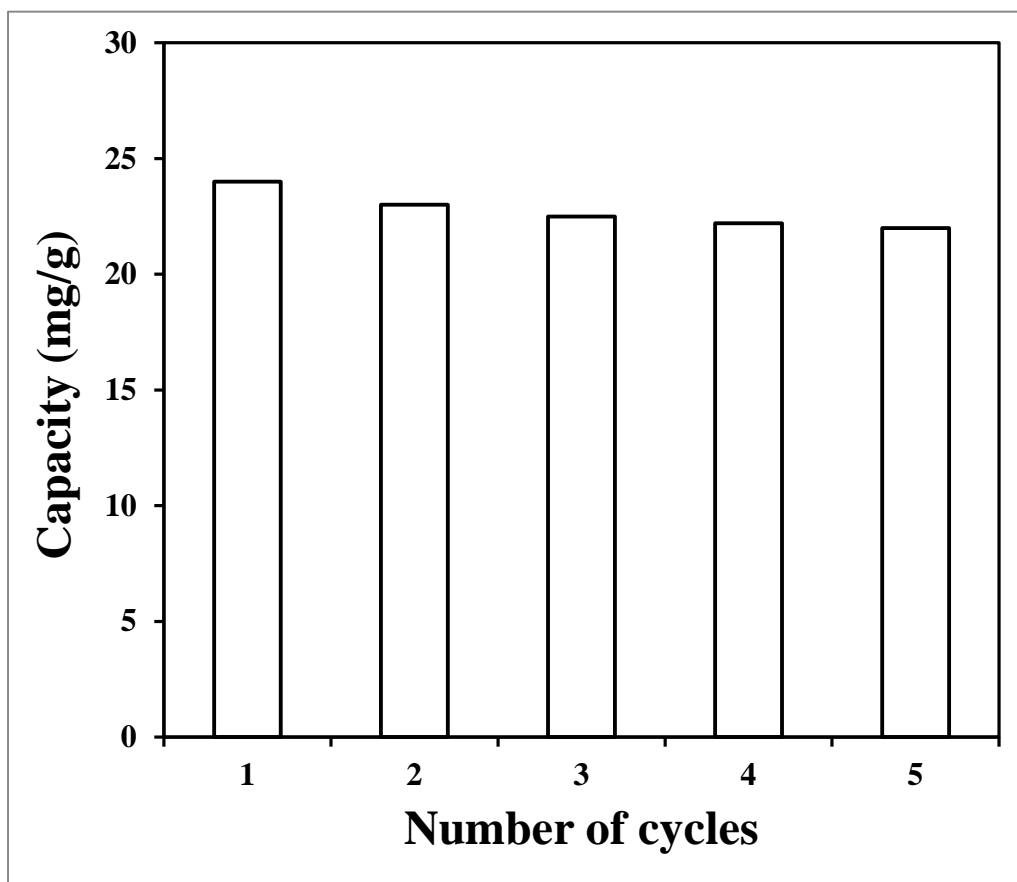


Figure 3.8. Repeated use of a hydrolyzed AAm-grafted film for adsorption of Hg(II) from a mixture of Hg(II) and Pb(II) (pH 4.5; $t = 40$ min; $C_i = 100$ mg/L).

3.4. Conclusion

Hydrolyzed AAm-grafted PET films showed selective Hg(II) adsorption from binary solutions of Hg(II) and Pb(II) throughout the entire initial concentration range (100–500 mg/L) and pH range (2.2–5.6) studied. The selectivity coefficient of Hg(II) adsorption over that of Pb(II) was 19.2 at pH 4.5 and an initial concentration of 100 mg/L. Selective adsorption was achieved because the amide groups of the adsorbent films readily formed covalent bonds with Hg(II) ions, but the weakly electron-donating amide nitrogen atoms did not easily coordinate with Pb(II) ions. Selective Hg(II) adsorption followed the Langmuir isotherm model and a pseudo-second-order equation. The adsorbent film can be used repeatedly for selective Hg(II) sorption from aqueous solutions containing both Hg(II) and Pb(II).

CHAPTER 4

Selective Cu(II) adsorption from aqueous solutions including Cu(II), Co(II) and Ni(II) by modified acrylic acid grafted PET film

4.1. Introduction

In recent years heavy metals have received much public attention as potential hazards for human life and health ignited by the well-known environmental destruction cases: Minamata disease (organic mercury poisoning), Itai-itai disease (cadmium poisoning) and the stricter environmental regulations on the discharge of heavy metals make it necessary to develop efficient and low cost technologies for their removal as discussed in chapter 1 (section 1.1, 1.2).

In this study we attempted to prepare a selective Cu(II) adsorbent by grafting of acrylic acid on PET films. Acrylic acid ($\text{CH}_2=\text{CH}-\text{COOH}$, AAc) has been grafted on different polymers including PET for application in heavy metal recovery. Adsorption of Cu(II) on AAc grafted PET fiber has been investigated and it has been reported that the AAc graft PET fibers have much higher Cu(II) ion adsorption capacity than pure PET fibers [Karakısla, 2003]. Preparation of a chelating fiber with waste PET by grafting of AAc followed by treatment with ethylenediamine has been carried out and the prepared fiber has been studied for fast removal of Cu(II) and Ni(II) from water

[Wang et al., 2012]. AAc grafted nonwoven polypropylene sheet has been prepared by using γ ray irradiation and its applicability for removal of Cu(II), Ni(II) and Co(II) has been investigated [Hegazy et al., 2012]. Highly enhanced adsorption of Pb (II) on chitosan granules functionalized with AAc has been reported [Li et al., 2006]. Grafting of AAc on fungal biomass for enhancement of Cu(II) and Cd(II) biosorption has been studied [Deng et al., 2005]. The competitive removal of Pb(II), Cu(II) and Cd(II) from a ternary solution has been investigated by hydroxyethylcellulose-g-poly(acrylic acid) copolymer and its sodium salt [Çavuş et al., 2006].

Therefore to give the functional properties of AAc to PET, grafting of AAc on PET films were carried out by γ irradiation. But the graft films showed little metal ion adsorption due to compact structure of the graft chains. Therefore the graft films were modified with KOH treatment for expansion of the graft chains to increase the metal ion adsorption. The modified films were used to study the potential of selective Cu²⁺ adsorption from aqueous solution containing Cu²⁺, Co²⁺ and Ni²⁺ focusing with the four main objectives: (1) characterization of modified AAc grafted PET films by FTIR and SEM (2) study the equilibrium adsorption isotherm of selective Cu²⁺ adsorption from ternary metal solutions of Cu²⁺, Co²⁺ and Ni²⁺ and use of Langmuir and Freundlich isotherm models for interpretation of equilibrium adsorption data (3) study the kinetic of selective Cu²⁺ adsorption from ternary metal solutions of Cu²⁺, Co²⁺ and Ni²⁺ and use of pseudo-first-order and pseudo-second-order equations for interpretation of adsorption kinetic data (4) Study the desorption of metal ions from the film and reuse of the film.

4.2. Experimental

4.2.1. Materials and reagents

Commercial PET films (Teijin DuPont films, G2) of thickness 50 μm were kindly provided by Teijin Co. Ltd. These films were cut into small pieces ($3.5 \times 1.5 \text{ cm}^2$), washed with acetone, and dried in vacuum oven before use. AAc and FeCl_3 were procured from Sigma Aldrich. KOH was supplied by Wako pure chemical industries Ltd. Cobalt (II) chloride, nickel (II) chloride and copper (II) chloride (anhydrous, Chameleon Reagent) and cobalt, nickel and copper standard solutions (Fluka) were used as a source of the adsorbate and for the calibration of metal ion concentrations, respectively.

4.2.2. Instrument and apparatus

The PET films were analyzed by a Fourier transform infrared (FTIR) spectrophotometer, Jasco FTIR 620 in the wavenumber range $400\text{--}4000 \text{ cm}^{-1}$ to investigate the chemical and/or physical interactions. Scanning electron microscopy (SEM) image observations of the carbon coated PET films were performed using Zeiss Ultra55 SEM operated at 7-10 keV. The metal-ion concentrations in the solutions were analyzed by an inductively coupled plasma mass spectrometer, Agilent7700 series ICP-MS.

4.2.3. Grafting of AAc onto the PET films by gamma radiation

The dry PET films weighing W_{pristine} were taken into glass bottles containing different concentration (20- 40 wt %) of AAc aqueous solutions. FeCl_3 at a constant concentration (1 wt %) was added to the AAc solutions to minimize homopolymer formation. The contents of the glass bottles were then irradiated with different doses (20-100 kGy) of γ rays with a dose rate of 1.0 kGy/h in air (γ -ray irradiation of the PET films was carried out at the ^{60}Co γ -ray irradiation facility of Research Reactor Institute, Kyoto University). The obtained grafted films were washed in distilled water at 60°C for 24 h to remove the homopolymers. Then the films were dried in a vacuum oven at 60°C for 24 h and were weighed ($W_{\text{AAc grafted}}$). The graft yield was determined by the percent increase in the weight as follows:

Graft yield:

$$\delta W_{\text{AAc grafted}} (\%) = (W_{\text{AAc grafted}} - W_{\text{pristine}}) / W_{\text{pristine}} \times 100 . \quad \dots\dots\dots (4.1)$$

4.2.4. KOH treatment of the AAc grafted film

The AAc grafted films with 40 % graft yield (obtained at 40 % AAc concentration and 100 kGy dose) were modified by treatment with 2.5 % KOH for 2 min at 25 °C.

4.2.5. Metal ion adsorption by the modified AAc grafted PET film

The modified AAc grafted films of 60 mg were soaked into the 10 ml aqueous solutions including of Cu(II), Ni(II) and Co(II) at a definite metal ion concentration and pH for 60 min at room temperature (25 °C). pH of the solutions were adjusted using HCl and NaOH solution. Metal loaded films were washed and dried. The metal-ion concentrations of the solutions were analyzed by ICP-MS.

4.2.6. Determination of metal ion uptake capacity

The metal ion uptake capacity of the film was calculated as described in chapter 3, section 3.2.6.

4.2.7. Desorption of metal ions

The desorption of Cu(II), Ni(II), Co(II) ions from the adsorbent films were carried out by the treatment with 2M aqueous solution of HCl for 30 min. The percent desorption was calculated as presented in chapter 3, section 3.2.7.

4.3. Results and discussion

4.3.1. Preparation and characterization of the adsorbent film

Grafting of AAc onto PET films was carried out by γ irradiation. AAc grafting on PET film might have followed a free radical mechanism where at first primary free radical is formed on PET backbone initiated by γ ray which then reacts with monomer to form graft growing chain and finally the graft copolymer is formed by a termination reaction [Ping et al., 2011]. The prepared AAc grafted films (G- 40 %) were modified by treatment with KOH which increased the metal ion adsorption capacity of the films largely, almost 10 times than the AAc grafted films. The adsorption capacity of Cu^{2+} , Co^{2+} and Ni^{2+} ions obtained in the present study together with that reported in previous studies are presented in Table 4.1. The modified AAc grafted PET films after adsorption of Cu^{2+} , Co^{2+} and Ni^{2+} ions are shown in Figure 4.1.

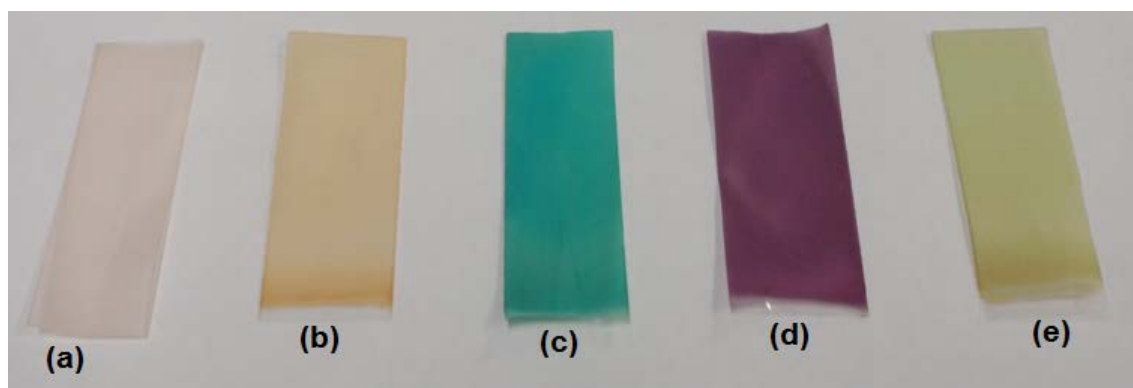


Figure 4.1. (a) AAc grafted PET (b) AAc grafted PET after modification by KOH treatment (c) Modified AAc grafted PET film after Cu(II) loading (d) Modified AAc grafted PET film after Co(II) loading (e) Modified AAc grafted PET film after Ni(II) loading.

Table 4.1. Metal ion adsorption capacity of AAc grafted PET, modified AAc grafted PET compared with some other adsorbents (From single metal solution)

Adsorbent	Cu ²⁺ adsorption capacity (mg/g)	Co ²⁺ adsorption capacity (mg/g)	Ni ²⁺ adsorption capacity (mg/g)
Pristine PET film [present study]	0 ^a	0 ^a	0 ^a
AAc graft PET film [present study]	10.0 ^a	7.0 ^a	8.0 ^a
Modified AAc graft PET film [present study]	100.0 ^a	67.0 ^a	85.0 ^a
Itaconic acid/acrylamide graft PET fiber [Çoşkun et al., 2006, React. Funct. Polym.]	7.73 ^b	14.81 ^b	13.79 ^b
Methacrylic acid/acrylamide graft PET fiber [Çoşkun et al., 2006, Sep. Purif. Technol.]	31.25 ^b	27.17 ^b	43.48 ^b
Cross-linked and non cross-linked chitosan [Schmuhl et al., 2001]	>80 ^a	-	-

a: experimental value, *b*: calculated from the Langmuir model

To understand the change of the PET film after AAc grafting and KOH treatment, the IR spectra of the films were determined. IR spectrum of the PET film (Figure 4.2a) represented the peaks characteristic for poly(ethylene terephthalate) chemical structure (absorption peak for OH stretching at 3430 cm⁻¹, aromatic C-H stretching at 3054 cm⁻¹, aliphatic C-H stretching at 2969 and 2907 cm⁻¹, C=O stretching vibration at 1684 cm⁻¹ and bands associated with the aromatic ring at 1614, 1578 and 1505 cm⁻¹). IR spectrum of the AAc grafted PET film showed new peaks for

carboxyl -OH groups around 2300-3700 cm⁻¹ which was absent in IR spectrum of pristine PET film (Figure 4.2a). The -OH peaks near 2580 and 2900 cm⁻¹ indicates the existence of strong hydrogen bonding between -COOH groups in the AAc grafted PET film [Max et al., 2004; Kobayashi et al., 1998]. After KOH treatment the -OH peak near 2580 cm⁻¹ disappeared (Figure 4.2a) indicating the reduction of hydrogen bonding between the -COOH groups and formation of some -COO⁻K⁺ groups which is confirmed by the appearance of new peak near 1560 cm⁻¹ assigned for carboxylate ion [Macknight et al., 1968] (Figure 4.2b). Therefore it can be said that AAc grafted PET film can show little adsorption of metal ion due to the presence of hydrogen bonded -COOH groups, but after KOH treatment, the films showed greater metal ion adsorption due to the reduction of hydrogen bonding between -COOH groups and presence of some ionized -COO⁻K⁺ groups. The conversion percentage of -COOH groups to -COO⁻K⁺ groups can be calculated from the IR spectra by the following equation

$$\text{Conversion (\%)} = (B - C / B - A) \times 100 \quad \dots\dots\dots (4.2)$$

where A, B, C represents the total area under the IR peaks from 2300-3700 cm⁻¹ (the region where carboxyl -OH peaks appeared) for pristine PET, AAc grafted PET and KOH treated AAc grafted PET respectively. The conversion percentage calculated is 28 %.

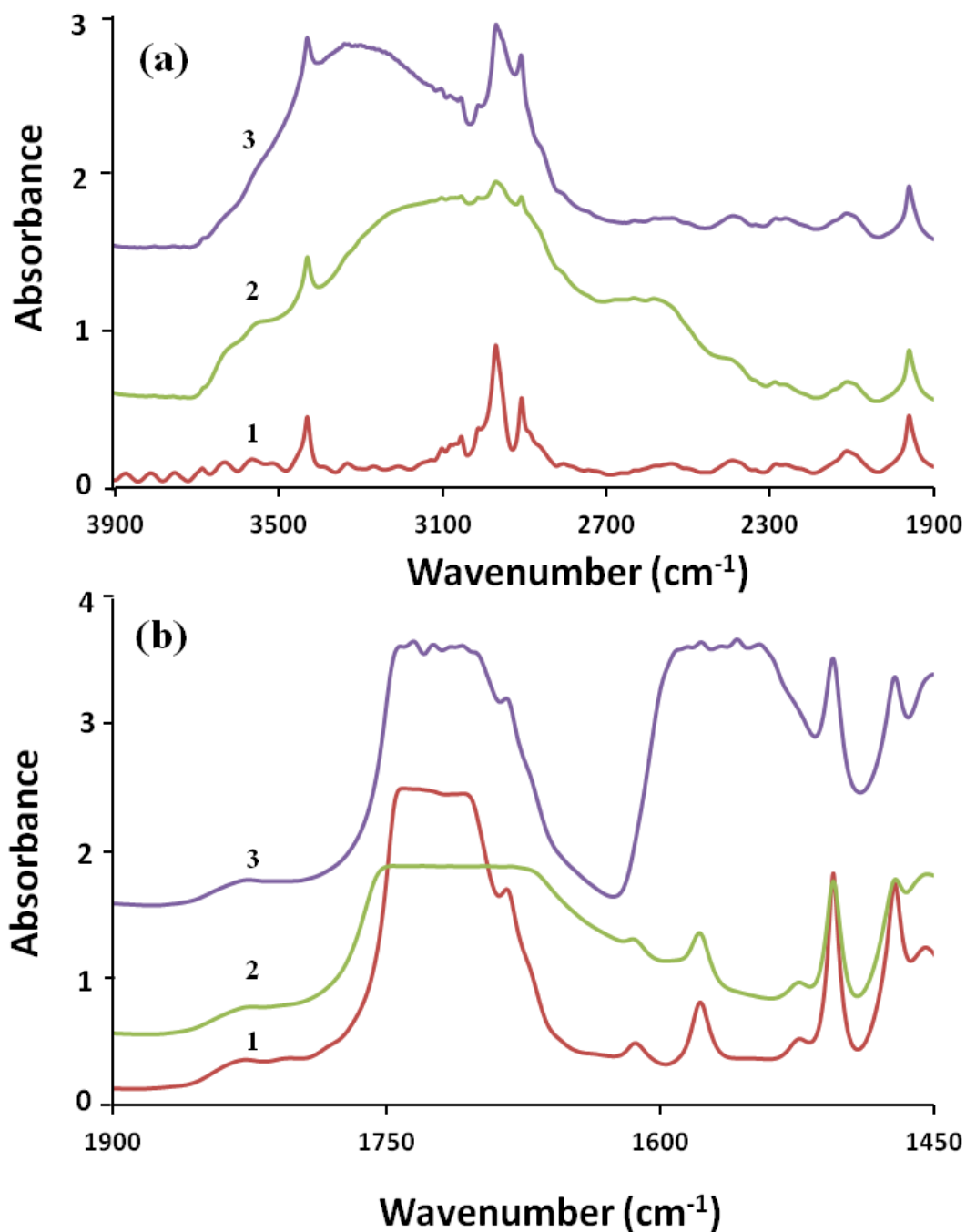


Figure 4.2. FTIR spectra of (1) ungrafted PET film (2) AAc grafted PET film (3) KOH treated film AAc grafted PET film. The spectra are split into the two figures at 1900 cm^{-1} .

The reason behind increase of metal ion adsorption after KOH treatment can be better understood from the SEM image. SEM micrographs of pristine PET film, AAc grafted PET film and modified AAc grafted PET film are shown in Figure 4.3. The effect of KOH treatment is not only conversion of some extent of $-\text{COOH}$ group to $-\text{COOK}$ group, rather the more significant effect is the structural change of the graft film surface after introduction of some $-\text{COOK}$ group. Before KOH treatment the graft chains showed a compact structure in SEM image (Figure 4.3, b) which is due to the attraction between the graft chains because of hydrogen bonding (Figure 4.3, b-1). At this condition many of the functional groups ($-\text{COOH}$) were inaccessible to the metal ions. After KOH treatment, graft chains showed an expanded structure in SEM image (Figure 4.3, c) which is due to the repulsion of graft chains by the electrostatic force of some ionic $-\text{COO}^-$ groups. (Figure 4.3, c-1). At this condition the initial functional groups ($-\text{COOH}$) of the graft films became easily accessible to the metal ions besides the new functional groups ($-\text{COOK}$). The average surface roughness (R_a) calculated from the SEM image of pristine PET, AAc grafted PET and KOH treated AAc graft PET film is 9.6, 10.8 and 20.7 pixel respectively (roughness is calculated by using an image processing program, imageJ). Large increase of surface roughness after KOH treatment provides further proof of the rearrangement of the graft chains from compact structure to expanded structure which facilitated the metal ion adsorption.

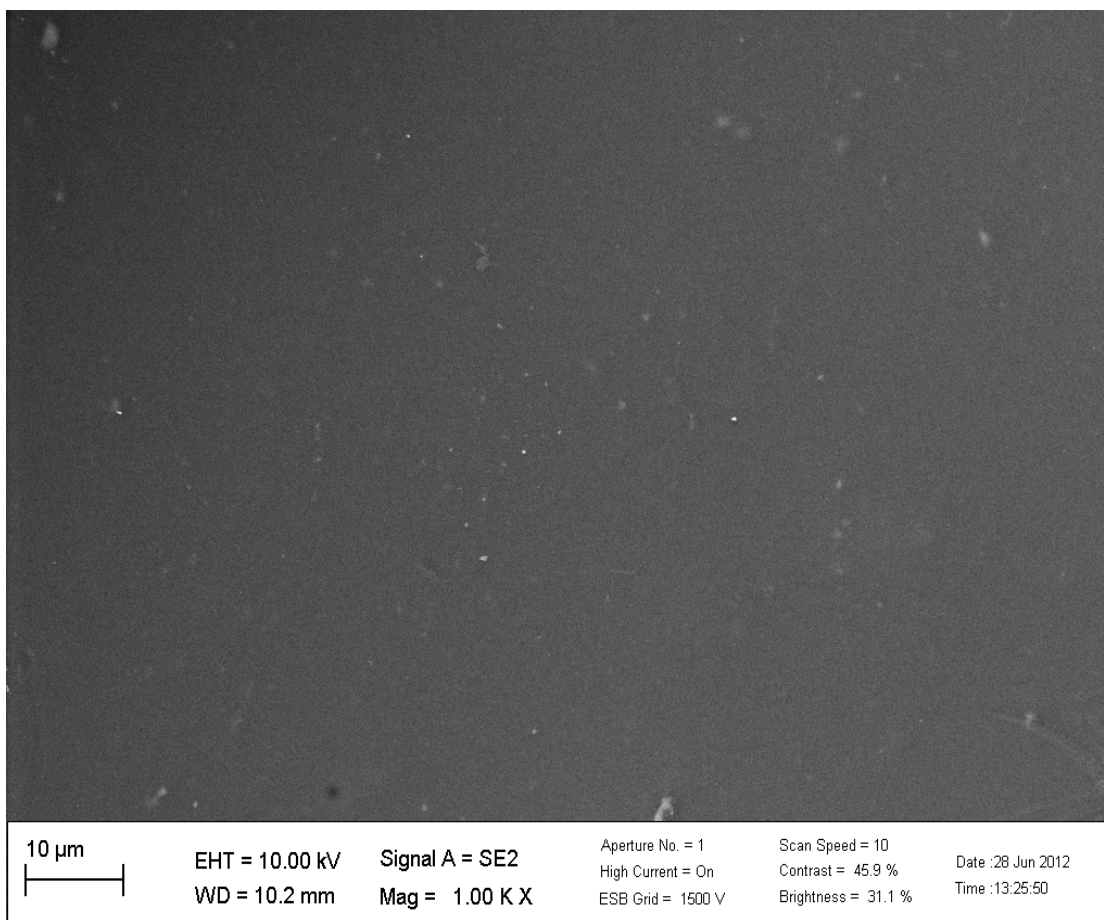


Figure 4.3.(a). SEM micrograph of ungrafted PET film.

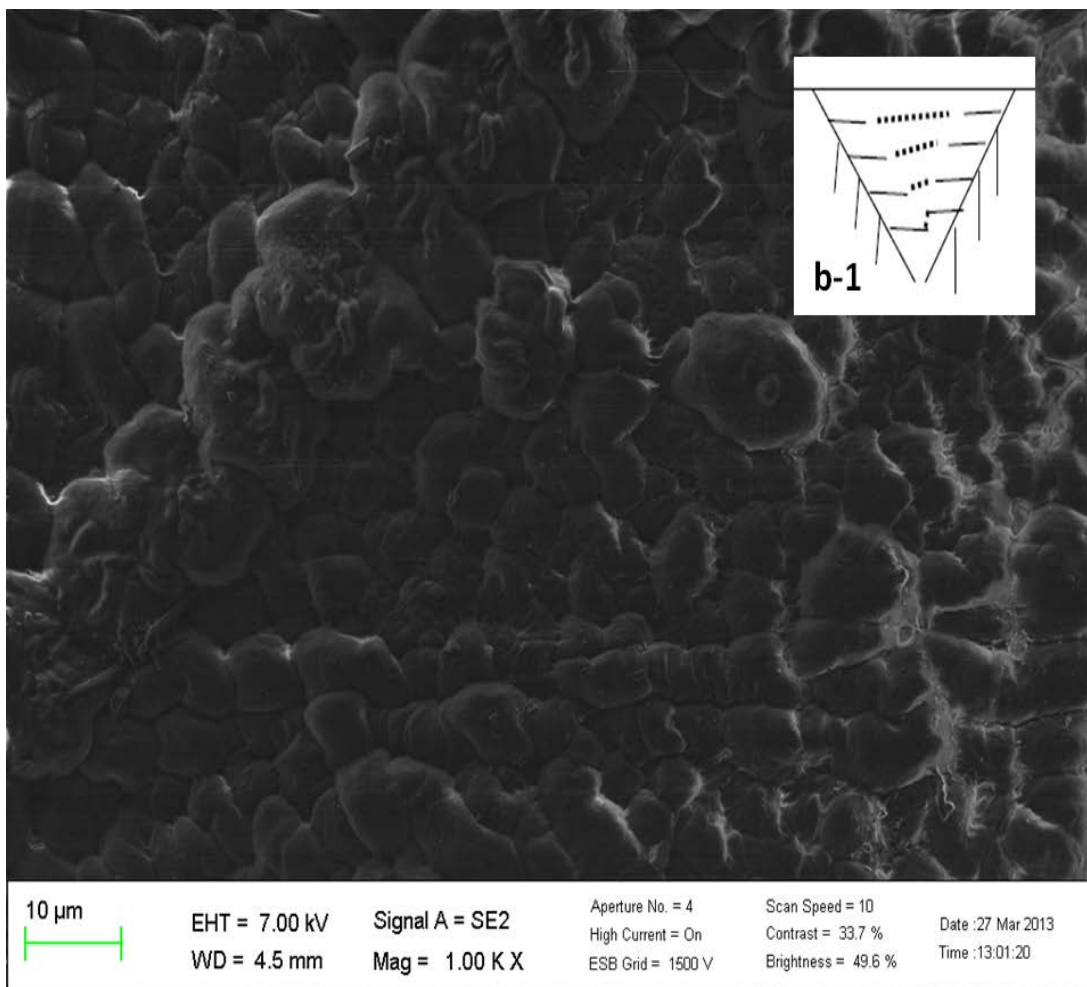


Figure 4.3.(b). SEM micrograph of AAc grafted PET film, (b-1) graft chains are attracted by hydrogen bonding and the functional groups are inaccessible to the metal ions.

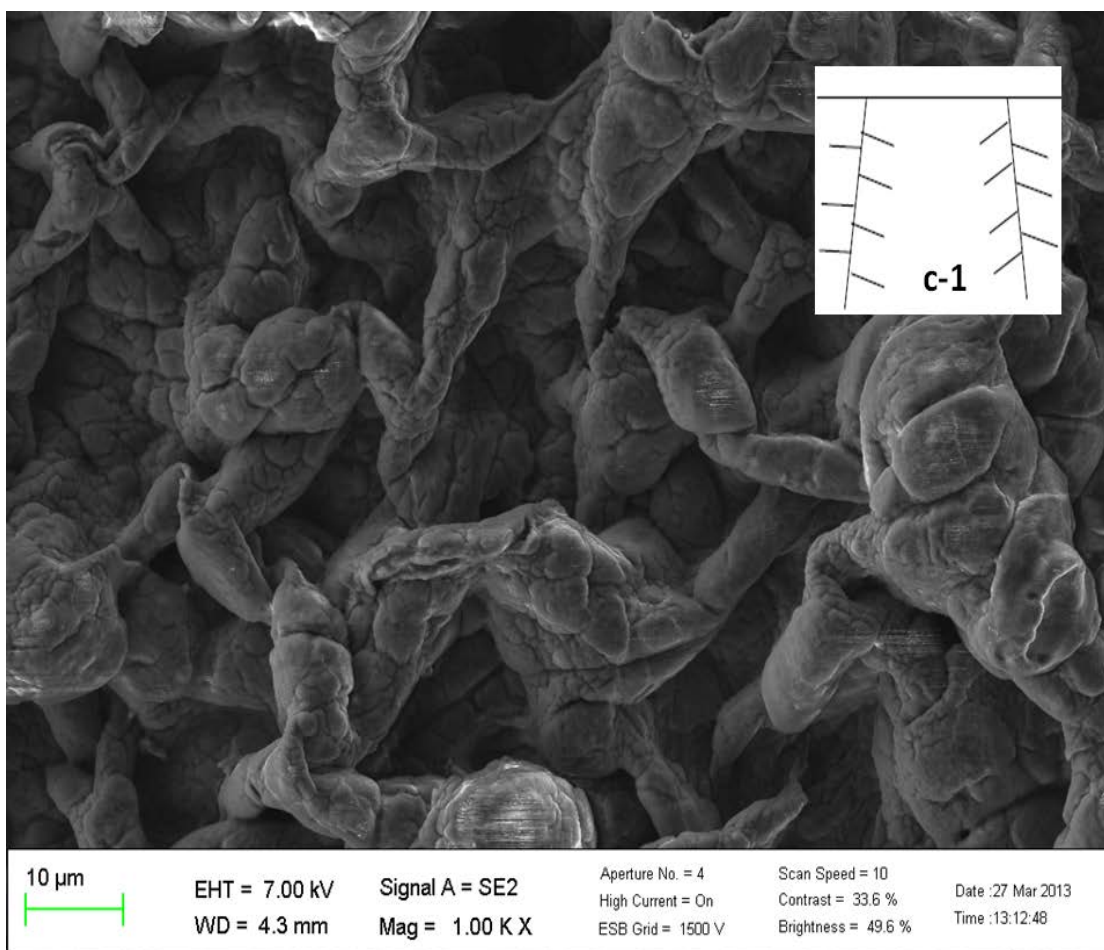


Figure 4.3.(c). SEM micrograph modified AAc grafted PET, (c-1) graft chains are repulsed by electrostatic force of $-\text{COO}^-$ group and the functional groups are accessible to the metal ions

4.3.2. Selective Cu(II) ion adsorption by the adsorbent film

The modified graft film adsorbed 55.6, 9.0 and 7.8 mg/g of Cu(II), Ni(II) and Co(II) respectively from a ternary solutions of Cu(II), Ni(II) and Co(II) under the same initial concentrations of 2000 mg/L of each metal ion at pH 4. The selectivity of an adsorbent is often measured from the distribution coefficient (K_d). The term K_d refers to the affinity of an adsorbent for a particular ion in presence of interfering ions. K_d can be calculated by Eq. (4.3) [Yan et al., 2011]

$$K_d = V(C_0 - C_f) / C_f W \quad \dots\dots\dots (4.3)$$

where, K_d is the distribution coefficient (mL/g), C_0 and C_f (mg mL^{-1}) are the initial and equilibrium concentrations of a metal species, respectively, V (mL) is the volume of the testing solution, and W (g) is the amount of adsorbent.

Now, the selectivity coefficient, α (dimensionless), for a specific metal ion in the presence of competitor ions can be expressed as Eq. (4.4)

$$\alpha = K_d(T) / K_d(I) \quad \dots\dots\dots (4.4)$$

where, $K_d(T)$ is the K_d value of the targeted metal (Cu(II) ions in this case), and $K_d(I)$ is the K_d value of the other metal in the mixed metal solutions (Ni(II) or Co(II) ions in this case). The selectivity coefficient for binding of Cu(II) over Ni(II) and Co(II) calculated (at initial concentrations of 2000 mg/L and pH 4) for modified AAc grafted PET film is $\alpha_{\text{(Cu/Ni)}} = 7$ and $\alpha_{\text{(Cu/Co)}} = 8$ respectively. The selectivity sequence for the modified graft film [Cu(II) > Ni(II) > Co(II)] followed the Irving–Williams series, which refers to the relative stabilities of complexes formed by the transition metal ions with ligands [Irving et al., 1953]. The high selectivity for Cu(II) can be explained in terms of the Pearson's concept of hard- and soft-acids and bases. According to the

concept, the carboxylate groups can be considered as soft bases, on the other hand Cu^{2+} can be considered as a soft acid, while Ni^{2+} and Co^{2+} are relatively hard acids [Rivas et al., 2004]. Generally, hard acids coordinate better with hard bases and soft acids with soft bases. Therefore a strong interaction between Cu^{2+} and carboxylate group bearing adsorbent films are expected.

4.3.3. Equilibrium adsorption isotherm of selective Cu(II) ion adsorption

An adsorption isotherm which represents the relationship between the amount of metal ions adsorbed by the adsorbent and the metal ions concentration remaining in solution is commonly used to study the adsorption process. Adsorption isotherms for competitive adsorption of Cu(II), Ni(II) and Co(II) under the same initial concentrations are shown in Figure 4.4. In case of Cu(II), the adsorption capacity increased with the increase of equilibrium concentration while for Ni(II) and Co(II), the adsorption capacity reached maximum for equilibrium concentration 167 and 172 mg/L respectively and thereafter decreased with increase of equilibrium concentration. This might be due to the high affinity of the adsorbent for Cu(II) than Ni(II) and Co(II) (section 4.3.2), for which with increase of Cu(II) ion concentration with respect to the available adsorption sites, the adsorption of Ni(II) and Co(II) decreased.

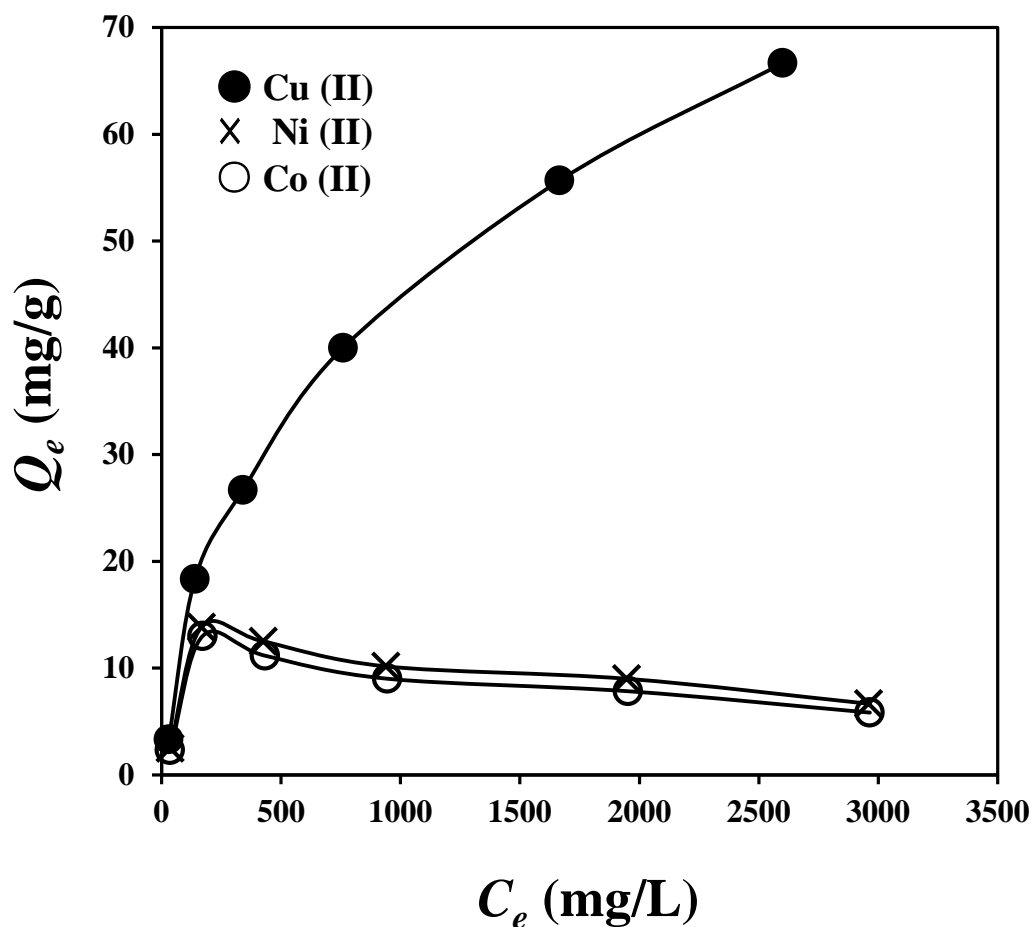


Figure 4.4. Equilibrium adsorption isotherm for competitive adsorption of Cu(II), Ni(II) and Co(II) by the modified graft films under the same initial concentrations of metal ions. (pH 4; t = 60 min; G = 40 %)

For interpretation of the selective Cu(II) adsorption data, the Langmuir [Langmuir et al., 1918] and Freundlich [Freundlich et al., 1906] isotherm models were used. The linear form of the Langmuir isotherm is presented by

$$C_e / Q_e = C_e / Q_0 + 1 / (Q_0 b) \quad \dots\dots\dots (4.5)$$

where C_e is the equilibrium concentration (mg L^{-1}), Q_0 the monolayer saturation adsorption capacity of adsorbent (mg g^{-1}), Q_e is the equilibrium adsorption capacity and b is Langmuir adsorption constant (Lmg^{-1}). The plot of C_e/Q_e versus C_e shown in

Figure 4.5.1. was drawn from the experimental data given in Figure 4.4. The relationship between C_e/Q_e and C_e is linear indicating that the adsorption behavior follows the Langmuir adsorption isotherm. The b , Q_0 , and correlation coefficients (R^2) values are presented in Table 4.2.

The Freundlich isotherm is described by the following equation

$$\log Q_e = \log K_F + 1/n \log C_e \quad \dots\dots\dots (4.6)$$

where C_e is the equilibrium concentration (mg L^{-1}), Q_e is the equilibrium adsorption capacity, K_F the sorption capacity (mg g^{-1}) and n is an empirical parameter. The plot of $\log Q_e$ versus $\log C_e$ shown in Figure 4.5.2. was drawn from the experimental data given in Figure 4.4. The K_F , n , and correlation coefficients (R^2) values are presented in Table 4.2.

Table 4.2: Langmuir and Freundlich isotherm parameters for selective Cu(II) adsorption

Langmuir isotherm parameters			Freundlich isotherm parameters		
Q_0 (mg/g)	b (L/mg)	R^2	K_F (mg/g)	n	R^2
81.30	0.0015	0.986	0.53	1.56	0.942

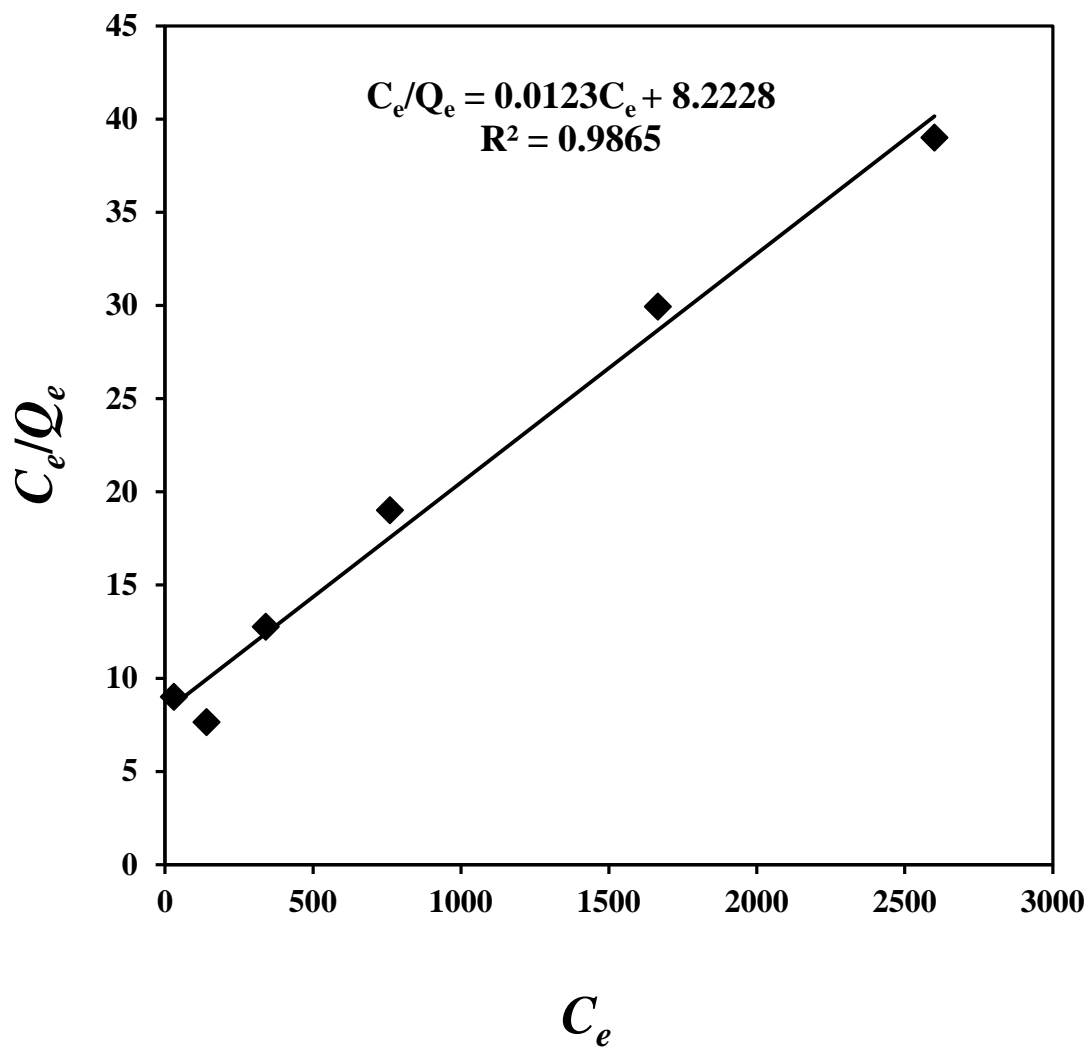


Figure 4.5.1. Langmuir isotherm plot for selective Cu(II) adsorption

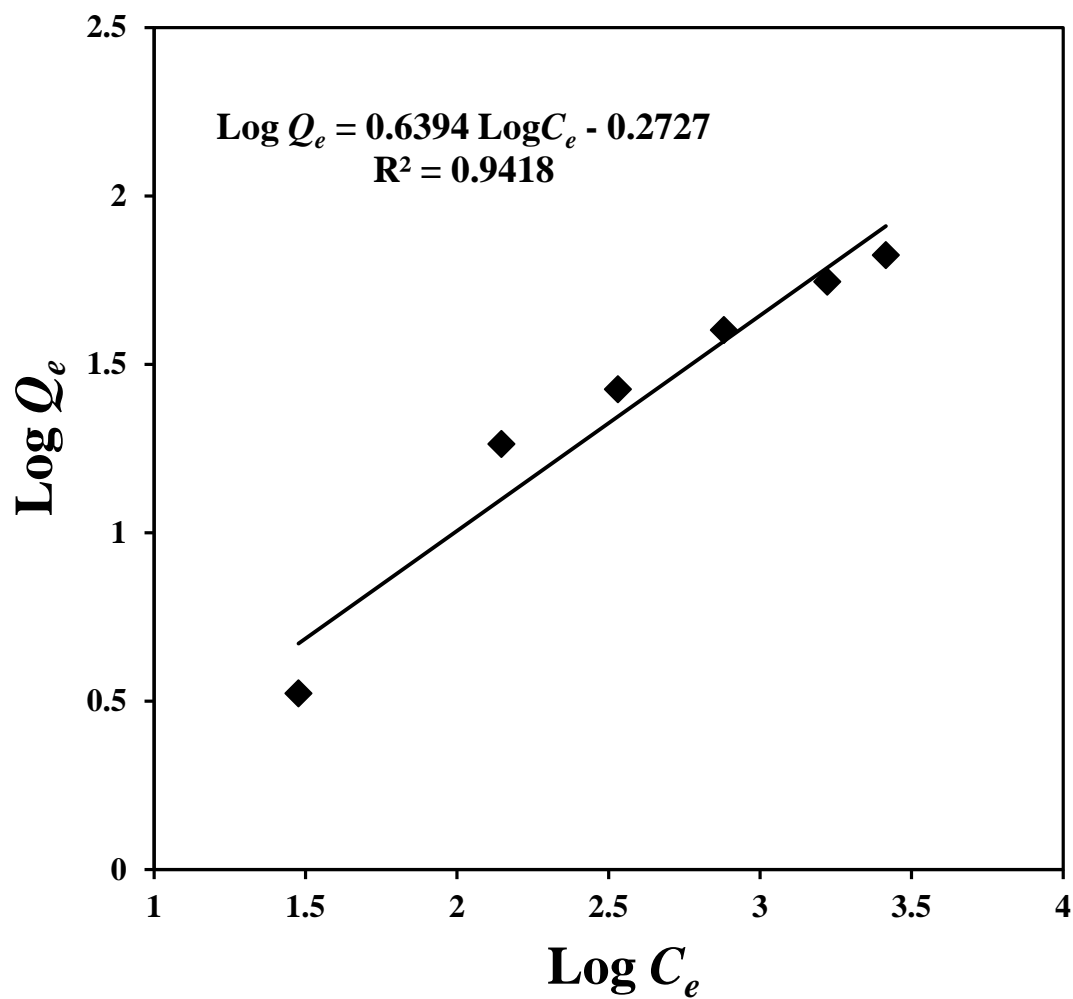


Figure 4.5.2. Freundlich isotherm plot for selective Cu(II) adsorption

The linear plots show that the two studied models, the Langmuir equation and Freundlich equation can give prediction of experimental data. The Langmuir model assumes monolayer adsorption of adsorbate on a structurally homogeneous adsorbent where all adsorption sites are identical. On the other hand the Freundlich model is not restricted to homogeneous system or monolayer adsorption; it can also describe heterogeneous system and multilayer adsorption. Therefore fitting of experimental data with Langmuir model suggest that a mono-layer adsorption of ions on the adsorbent is appropriate to describe the selective Cu (II) adsorption on the modified AAc grafted PET. This also suggest that the adsorption was mainly chemical adsorption and the adsorption sites are identical to the metal ions, in other words surface heterogeneity of apparently heterogeneous surface of the modified AAc grafted PET is not significant in respect of adsorption phenomenon. Similar conclusion has been drawn when the adsorption of metal ions on the rough surface of meranti sawdust followed the Langmuir adsorption isotherm model [Rafatullah et al., 2009].

4.3.4. Adsorption kinetic of selective Cu(II) ion adsorption

Figure 4.6 shows the kinetics of competitive adsorption of Cu(II), Ni(II) and Co(II) under the same initial concentrations of metal ions by modified AAc grafted PET films. It was observed that the adsorption of Cu(II) ions increased with increasing soaking time while adsorption of Ni(II) and Co(II) reached maximum after 10 min and after that decreased with increasing soaking time. This can be explained as the adsorbent-Ni(II) and adsorbent-Co(II) complexes are less stable than adsorbent-Cu(II)

complex (section 4.3.2), therefore with increase of soaking time more stable complexes replace less stable complexes.

The pseudo-first-order and pseudo-second order kinetic models were applied to fit the selective Cu(II) adsorption by the modified AAc grafted PET films. The pseudo-first-order and pseudo-second-order equations [Ho et al., 2006; Namasivayam et al., 1997], are expressed as:

$$\log (Q_e - Q_t) = \log Q_e - (k_1/2.303) t \quad \dots\dots\dots (4.7)$$

$$t/Q_t = 1/ (k_2 Q_e^2) + t/ Q_e \quad \dots\dots\dots (4.8)$$

where Q_t and Q_e are the amount of ions adsorbed (mg g^{-1}) at any time and equilibrium time, respectively, k_1 is the rate constant (min^{-1}) of first-order adsorption and k_2 ($\text{g min}^{-1} \text{mg}^{-1}$) is the rate constant of second-order adsorption. The pseudo-first-order rate constants could be determined experimentally by plotting $\log (Q_e - Q_t)$ against t as shown in Figure 4.7.1.

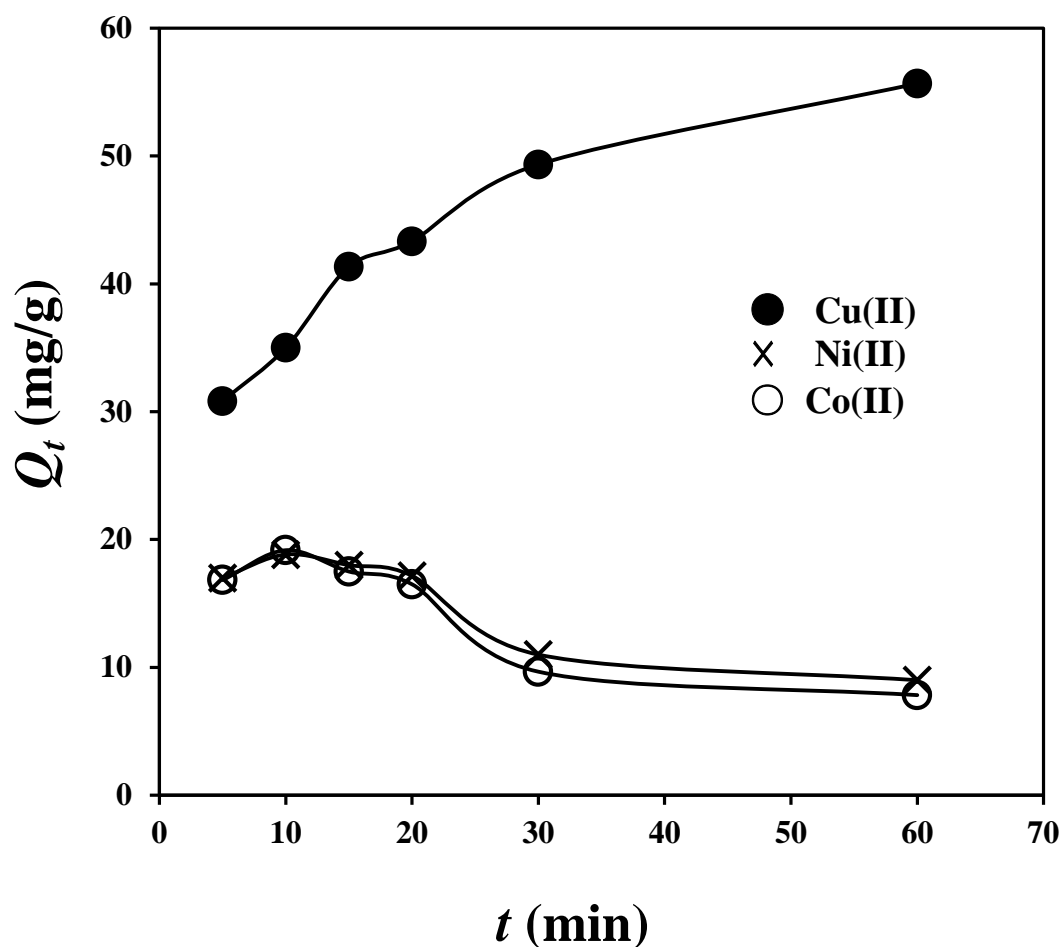


Figure 4.6: Adsorption kinetics for competitive adsorption of Cu(II), Ni(II) and Co(II) by the modified graft films under the same initial concentrations of metal ions. (pH 4; Initial concentration, $C_i = 2000$ mg/L; $G = 40$ %)

The experimental and theoretical Q_e value, first order rate constant and the correlation coefficients (R^2) are given in Table 4.3. It can be seen from the results that the experimental Q_e value and the Q_e value calculated from first order kinetic model are not in agreement with each other. Pseudo second-order rate constants could be determined experimentally by plotting t/Q_t against t as shown in Figure 4.7.2. All the

second order kinetic parameters for selective Cu(II) adsorption are given in Table 4.3. It can be seen that the experimental Q_e and the Q_e value calculated from second order kinetic model are in accordance with each other. Therefore the pseudo-second-order equation can be used to interpret selective Cu (II) adsorption on the modified AAc grafted PET. Pseudo-second-order model fit with the experimental kinetic data indicate that intra-particle diffusion process was the rate-limiting step of the adsorption [Rengaraj et al., 2007] and it also prove that the chelating interaction plays the major role in the adsorption process [Li et al., 2010].

Table 4.3. The pseudo-first-order and pseudo-second-order rate constants for selective Cu(II) adsorption

Q _e (exp.) (mg/g)	Pseudo-first-order rate constant			Pseudo-second-order rate constant		
	Q _e (theor.) (mg/g)	k ₁ (min ⁻¹)	R ²	Q _e (theor.) (mg/g)	k ₂ (g min ⁻¹ mg ⁻¹)	R ²
55.66	34.1	0.0548	0.9877	56.82	0.0034	0.9899

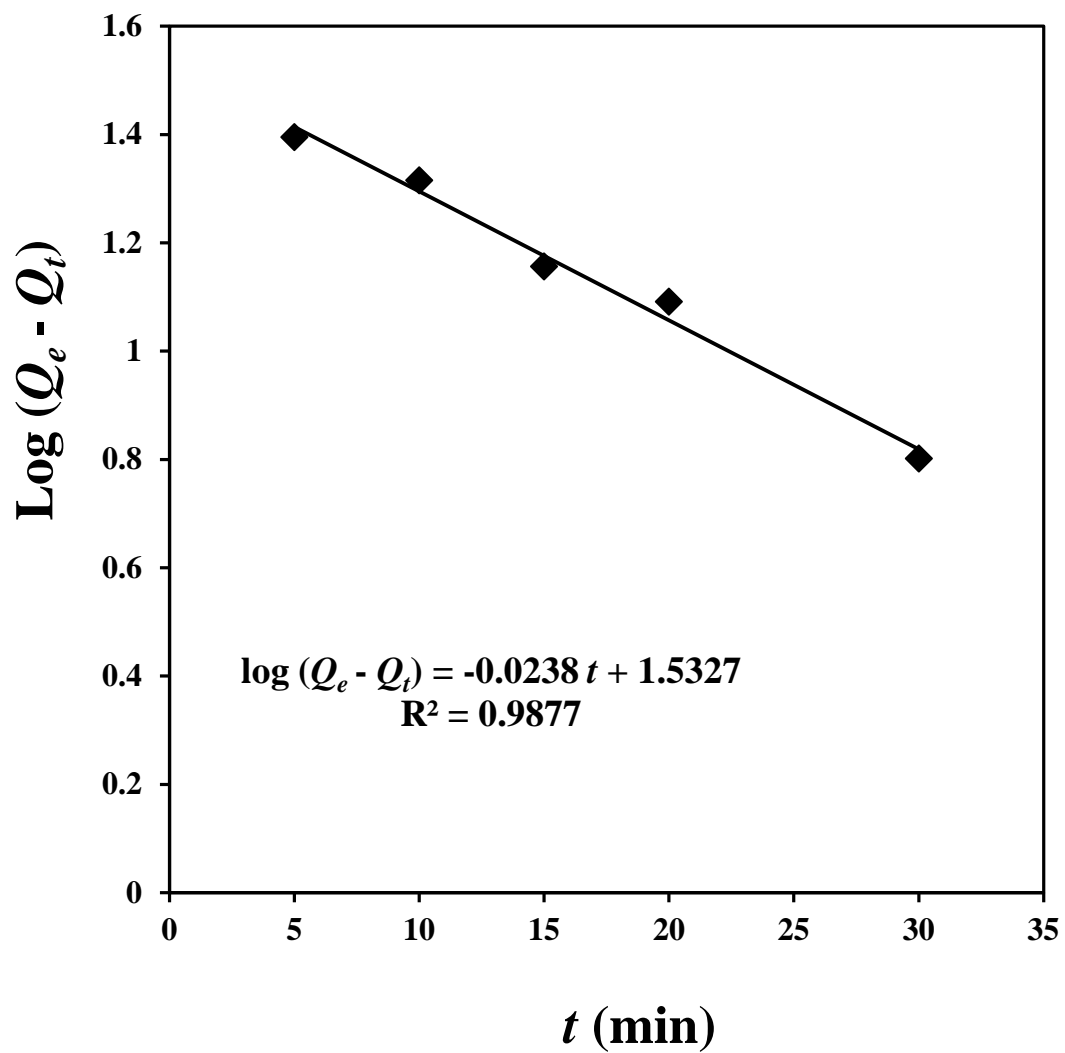


Figure 4.7.1. Pseudo-first order plot for selective Cu(II) adsorption

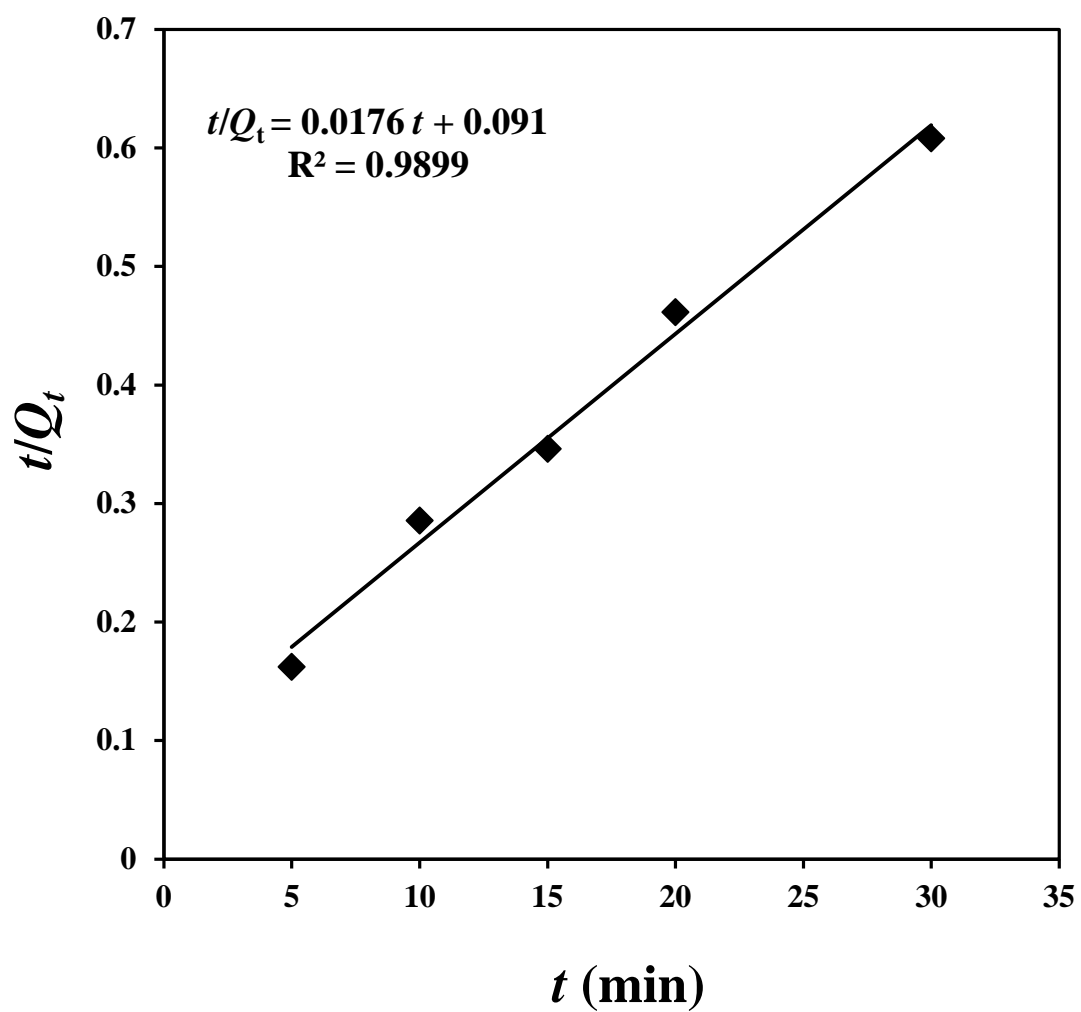


Figure 4.7.2. Pseudo-second order plot for selective Cu(II) adsorption

4.3.5. Effect of pH on selective Cu(II) ion adsorption

Effect of pH on competitive adsorption of Cu(II), Ni(II) and Co(II) by the modified graft films at initial concentration 500 mg/L is shown in Figure 4.8. It can be seen that the adsorbent is highly selective towards for Cu(II) in the pH range 1.5 to 4.5. At low pH, the carboxylate ions are more protonated and therefore adsorption of all metal ions were low. With increase of pH from 1.5 to 4.5 adsorption of all metal ions increased and in the pH range the adsorbent showed selectivity towards Cu(II) due to its high affinity towards Cu(II). But increase of pH after 4.5 caused precipitation of Cu(OH)₂.

4.3.6. Desorption and reuse of the adsorbent

After adsorption of metal ion on the modified AAc grafted PET, the adsorbents were regenerated using 2 M hydrochloric acid. Desorption took place rapidly and the equilibrium achieved within 10-20 min. The desorption ratio was 99 %. During desorption, the hydrogen ions in the solution were exchanged with the metal ions on the sorption sites. The regenerated film (-COOH form) was treated with KOH solution (to convert to -COO⁻K⁺ form) before being reused in subsequent cycles. Because we found that this -COOH form showed much lower metal adsorption than -COO⁻K⁺ form which may be due to the formation of hydrogen bonding again. The sorption capacity of the film for Cu(II) from aqueous solution of Cu(II), Co(II) and Ni(II) in five successive cycles is shown in Figure 4.9. For the 2nd cycle the sorption capacity decreased which may be due to the loss of physically adsorbed homopolymer of AAc

which might have washed out in acid and base solutions [Deng et al., 2005]. However, the sorption capacity not changed that much in subsequent cycles indicating that the film can be used repeatedly for Cu(II) adsorption.

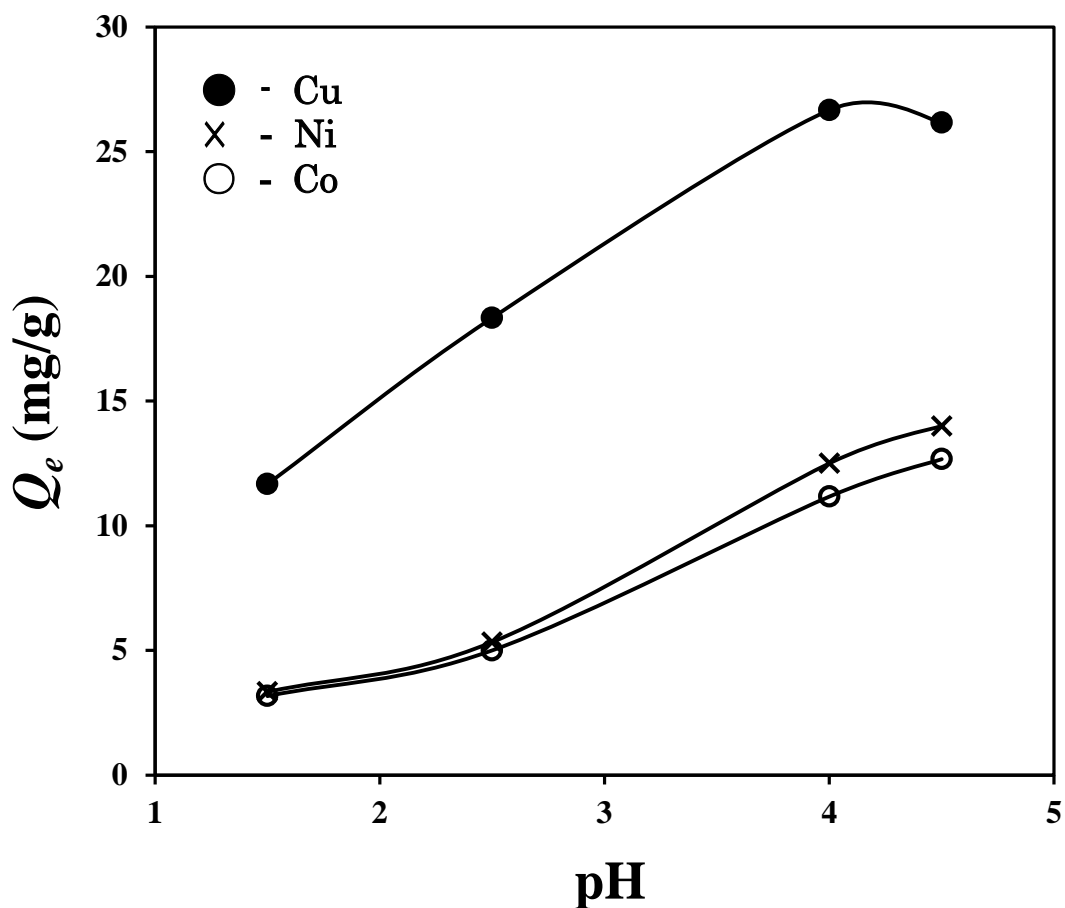


Figure 4.8. Effect of pH on the competitive adsorption of Cu(II), Ni(II) and Co(II) by the modified graft films under the same initial concentrations of metal ions. ($t = 60$ min; Initial concentration = 500 mg/L; $G = 40\%$)

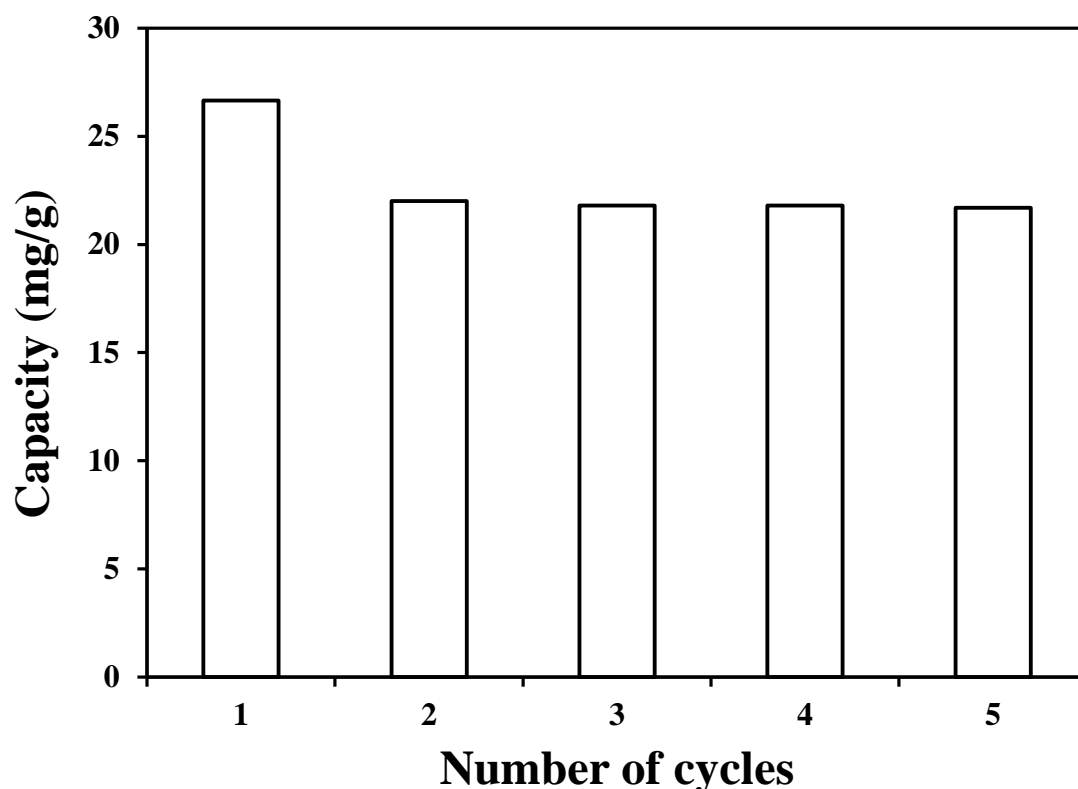


Figure 4.9. Repeated use of modified AAc grafted film for adsorption of Cu(II) from mixture of Cu(II), Co(II) and Ni(II) [pH 4; t = 60 min; $C_i = 500$ ppm; G = 40 %]

4.4. Conclusion

The KOH treated AAc graft PET films containing carboxylate groups can form more stable complex with Cu^{2+} than Co^{2+} or Ni^{2+} and therefore can show selective Cu^{2+} adsorption from aqueous solution containing Cu^{2+} , Co^{2+} and Ni^{2+} with a selectivity coefficient of 7 and 8 for binding of Cu^{2+} over Ni^{2+} and Co^{2+} respectively at pH 4 and initial concentration 2000 mg/L. Langmuir isotherm model and pseudo-second-order equation can be used for interpretation of selective equilibrium and kinetic adsorption data respectively. The adsorbent film can be used repeatedly for Cu^{2+} sorption from aqueous solution of Cu^{2+} , Co^{2+} and Ni^{2+} .

CHAPTER 5

Summary, conclusion and future study

5.1. Summary and conclusive remarks of present study

In the present study γ ray induced grafting of acrylic monomers on PET films were investigated and the selective adsorption of hazardous heavy metals by the prepared acrylic monomer grafted PET films were examined.

In chapter 2 the γ -ray induced grafting of acrylamide (AAM) onto poly(ethylene terephthalate) (PET) films and the resulting changes in properties, including the Hg(II)-capturing functionality, were investigated. No grafting was observed on pristine PET films. Therefore, the films were treated with dimethyl sulfoxide (DMSO) prior to the γ -ray grafting with the goal of facilitating grafting; some of the samples were pretreated at high temperature (100 to 160 °C) and showed a considerable increase in the adsorption of AAM from solution. The highest graft yield obtained in the present study was 15.5 % for the DMSO specimens pretreated at 140 °C and γ -ray irradiated with a 100-kGy total dose (1-kGy/h dose rate) in 50 wt% AAM-monomer solutions in the presence of 1 wt % FeCl₃ (polymerization inhibitor). In addition to the promotion of the graft yield, the formation of micropores in the DMSO-pretreated specimens was found during the optical microscopy investigations. This structural change is hypothesized to assist the adsorption and γ -ray grafting of AAM to PET. The AAM-grafted PET films prepared using DMSO pretreatment

showed high removal efficiency for Hg(II) ions, while the pristine PET film showed no uptake, reflecting these changes. Thus this study represents a new method for γ ray induced grafting of AAm on PET film by treatment with a swelling agent, dimethyl sulfoxide (DMSO) prior to grafting and the highest graft yield (15.5 % / 1125 $\mu\text{g}/\text{cm}^2$) obtained by the present method is much higher than that achieved using conventional γ -ray induced grafting (~ 0 %) and other non-chemical grafting techniques [such as UV irradiation (~ 0.3 %), CO_2 laser irradiation (~ 359 $\mu\text{g}/\text{cm}^2$) and the SI-ATRP (surface-initiated atom transfer radical polymerization) (~ 2.52 %) methods].

In chapter 3 selective Hg(II) adsorption from aqueous solutions of Hg(II) and Pb(II) using hydrolyzed AAm-grafted PET films was examined to explore the potential reuse of waste PET materials. Selective recovery of Hg(II) from a mixture of soft acids with similar structure, such as Hg(II) and Pb(II), is important to allow the reuse of recovered Hg(II). An adsorbent for selective Hg(II) adsorption was prepared by γ -ray-induced grafting of AAm onto PET films followed by partial hydrolysis through KOH treatment. The adsorption capacity of the AAm-grafted PET films for Hg(II) ions increased from 15 to 70 mg/g after partial hydrolysis because of the reduction of hydrogen bonding between $-\text{CONH}_2$ groups and the corresponding improved access of metal ions to the amide groups. The prepared adsorbent was characterized by Fourier transform infrared spectroscopy and scanning electron microscopy. The adsorbent film showed high selectivity for the adsorption of Hg(II) over Pb(II) throughout the entire initial metal concentration range (100–500 mg/L) and pH range (2.2–5.6) studied. The high selectivity is attributed to the ability of Hg(II) ions to form covalent bonds with the amide groups. The calculated selectivity coefficient for the adsorbent binding Hg(II) over Pb(II) was 19.2 at pH 4.5 with an

initial metal concentration of 100 mg/L. Selective Hg(II) adsorption equilibrium data followed the Langmuir model and kinetic data were well fitted by a pseudo-second-order equation. The adsorbed Hg(II) and Pb(II) ions were effectively desorbed from the adsorbent film by acid treatment, and the regenerated film showed no marked loss of adsorption capacity upon reuse for selective Hg(II) adsorption. Thus in this study a new adsorbent hydrolyzed AAm grafted PET is prepared that can show effective and selective adsorption of Hg(II) from mixture of Hg(II) and Pb(II) which favors the reuse of the recovered Hg(II) and Pb(II).

In chapter 4 acrylic acid (AAc) grafted PET films were prepared by γ irradiation for selective adsorption of Cu(II). The graft films showed little metal ion adsorption due to compact structure of the graft chains as shown by the scanning electron microscopy (SEM) images which restricted the access of metal ions to the functional groups. Therefore the graft films were modified with KOH treatment for expansion of the graft chains to facilitate the access of metal ions to the functional groups. The modified films were used to study the selective Cu²⁺ adsorption from aqueous solution containing Cu²⁺, Co²⁺ and Ni²⁺. Langmuir and Freundlich isotherm models were used for interpretation of selective equilibrium adsorption data and Langmuir model showed better fitting with experimental data. Again pseudo-first-order and pseudo-second-order equations were used for interpretation of selective kinetic adsorption data and pseudo-second-order equation showed better prediction of experimental data. The adsorbent film showed high selectivity towards Cu²⁺ in presence of Cu²⁺, Co²⁺ and Ni²⁺ in the pH range 1.5 to 4.5. Desorption and reuse of the adsorbent film were also studied which indicated that the film can be used repeatedly for selective Cu²⁺ sorption from aqueous solution. Thus this study shows

preparation of a new adsorbent hydrolyzed AAc grafted PET that can selectively adsorb Cu(II) from mixture of Cu(II), Co(II) and Ni(II) which allows the recycle of the recovered Cu(II).

It can be concluded that the present study shows successful preparation of new selective adsorbents through γ ray induced grafting of functional monomers on PET film. The prepared adsorbents showed adsorption of specific metal ions selectively and effectively from binary and ternary metal solutions. Thus present study demonstrates the future prospect of re-use of waste PET materials in selective hazardous heavy metal adsorption.

5.2. Suggestion of future study

Present study describes preparation of two adsorbent films: AAm grafted PET film and AAc grafted PET film from PET by γ ray irradiation. Present study also showed the effectiveness of AAm grafted PET film for selective adsorption of Hg(II) from mixture of Hg(II) and Pb(II) and AAc grafted PET film for selective adsorption of Cu(II) from mixture of Cu(II), Co(II) and Ni(II). Extensive study on the effectiveness of the prepared films for all commonly used metal ions such as Cu(II), Co(II), Ni(II), Zn(II), Fe(III), Hg(II), Pb(II), Cr(VI), Cd(II) etc can be useful to find out their applicability in selective adsorption in presence of different metal ions. The prepared adsorbent films can be further chemically modified to add more functionality. Study on preparation of adsorbents by grafting with other acrylic or vinyl monomers or mixture of monomers can be undertaken to prepare new effective adsorbents. The adsorption capacity of the adsorbents were studied by soaking the adsorbent in a

certain amount of metal solution, investigation of the adsorption capacity using column method can be helpful for practical waste water treatment application. We have used commercial PET films for our study, but to reach to the goal of re-use of waste PET, it is necessary to investigate preparation of adsorbent from waste PET materials.

References

- Abdel-Bary E.M., Sarhan A.A., Abdel-Razik H.H. (1986) Effect of graft copolymerization of 2-hydroxyethyl methacrylate on the properties of polyester fibers and fabric, *J. Appl. Polym. Sci.*, 35, 439-448.
- Al-Degs Y.S., El-Barghouthi M.I., Issa A.A., Khraisheh M.A., Walker G.M. (2006) Sorption of Zn(II), Pb(II), and Co(II) using natural sorbent: equilibrium and kinetic studies, *Water Res.*, 40 2645-2658.
- Arslan M., Temoçin Z., Yiğitoğlu M., (2004) Removal of cadmium(II) from aqueous solutions using sporopollenin, *Fresenius Environ. Bull.*, 13, 1-4.
- Arslan M. (2010) Preparation and use of amine-functionalized glycidyl methacrylate-g-poly(ethylene terephthalate) fibers for removal of chromium(VI) from aqueous solution, *Fiber Polym.*, 11, 325-330.
- Bäg H., Türker A. R., Coşkun R., Saçak M., Yiğitoğlu M. (2000) Determination of zinc, cadmium, cobalt and nickel by flame atomic absorption spectrometry after preconcentration by poly_ethylene terephthalate/ fibers grafted with methacrylic acid, *Spectrochim. Acta B*, 55, 1101-1108.
- Bayramoglu G., Arica M. Y., Bektas S. (2007) Removal of Cd(II), Hg(II), and Pb(II) ions from aqueous solution using p(HEMA/Chitosan) membranes, *J. Appl. Polym. Sci.*, 106, 169–177.
- Bhattacharya A., Misra B.N. (2004) Grafting: a versatile means to modify polymers techniques, factors and applications, *Prog. Polym. Sci.*, 29, 767–814.
- Bockris J.O.M. (1997) *Environmental Chemistry*, Plenum Press, New York.
- Borba C.E., Guirardello R., Silva E.A., Veit M.T., Tavares C.R.G. (2006) Removal of

- nickel(II) ions from aqueous solution by biosorption in a fixed bed column: experimental and theoretical breakthrough curves, *Biochem. Eng. J.* 30, 184-191.
- Bozkaya O., Yiğitoğlu M., Arslan M. (2012) Investigation on selective adsorption of Hg(II) ions using 4-vinyl pyridine grafted poly(ethylene terephthalate) fiber, *J. Appl. Polym. Sci.*, 124, 1256-1264.
- Buxbaum L. H. (1968) The Degradation of Poly(ethylene terephthalate), *Angew. Chem. Int. Ed. Engl.*, 7, 182–190.
- Brandrup, J., Immergut, E.H. (1975). *Polymer Handbook* Second ed. John Wiley, New York.
- Campbell D., Araki K., Turner, D.T. (1966) ESR study of free radicals formed by γ -irradiation of poly(ethyleneterephthalate). *J. Polym. Sci. Part A: Polym. Chem.* 4, 2597–2606.
- Çavuş S., Gürdağ G., Yaşar M., Güçlü K., Gürkaynak M. A. (2006) The competitive heavy metal removal by hydroxyethyl cellulose-g-poly(acrylic acid) copolymer and its sodium salt: The effect of copper content on the adsorption capacity, *Polym. Bull.* 57, 445–456.
- Chiarle S., Ratto M., Rovatti M. (2000) Mercury removal from water by ion exchange resins adsorption, *Water Res.*, 34, 2971-2978.
- Controlling transboundary movements of hazardous wastes (2011) printed as part of the 2009-2011 work programme of the Basel Convention Committee by the Publishing Service, United Nations, Geneva, <http://www.basel.int/Portals/4/Basel%20Convention/docs/pub/leaflets/leaflet-control-procedures-en.pdf> (accessed February 2014)

- Coşkun R., Soykan C. (2006) Lead(II) Adsorption from Aqueous Solution by Poly(ethylene terephthalate)-g-Acrylamide Fibers, *J. Polym. Res.*, 13, 1-8.
- Çoşkun R., Soykan C., Saçak M. (2006) Adsorption of copper(II), nickel(II) and cobalt(II) ions from aqueous solution by methacrylic acid/acrylamide monomer mixture grafted poly(ethylene terephthalate) fiber, *Sep. Purif. Technol.*, 49, 107-114.
- Coşkun R., Soykan C., Saçak M. (2006) Removal of some heavy metal ions from aqueous solution by adsorption using poly(ethylene terephthalate)-g-itaconic acid/acrylamide fiber, *React. Funct. Polym.*, 66, 599-608.
- Dadsetan M., Mirzadeh H., Sanjani N.S. (2000) Surface modification of polyethylene terephthalate film by CO₂ laser-induced graft copolymerization of acrylamide, *J. Appl. Polym. Sci.*, 76, 401–407.
- Deng Y., Ting P. (2005) Fungal biomass with grafted poly(acrylic acid) for enhancement of Cu(II) and Cd(II) biosorption, *Langmuir*, 21, 5940-5948.
- Descalzo A.B., Martínez M.R., Radeglia R., Rurack K., Soto. J. (2003) Coupling selectivity with sensitivity in an integrated chemosensor framework: design of a Hg²⁺-responsive probe, operating above 500 nm, *J. Am. Chem. Soc.*, 125, 3418-3419.
- D'Itri F. M., in Cunningham W. P., Cooper T. H., Gorham E. and Hepworth M. T. (Eds.) (1998) Heavy metals and heavy metal poisoning in *Environmental Encyclopedia* (Second edition), Gale Research, Detroit, 511-513.
- El-Arnaouty M.B., Abdel Ghaffar A.M., El Shafey H.M. (2008) Radiation-induced graft copolymerization of acrylic acid/acrylonitrile onto LDPE and PET films and its biodegradability. *J. Appl. Polym. Sci.*, 107, 744–754.

- El-Gendy E. H., Ali N. M., El-Shanshoury I.A. (2006) Processes involved during radiation grafting of N-vinyl pyrrolidone onto poly(ethylene terephthalate) fabric. *J. Appl. Polym. Sci.*, 101, 3009–3022.
- Faterpeker S.A., Potnis S.P. (1981) Radiation grafting of poly(Ethylene terephthalate) (PET) fibre, II hydrolysis of grafted poly(vinyl acetate) to poly(vinyl alcohol), *Angew. Makromol. Chem.* 93, 111 - 129 (Nr. 1425).
- Fu F., Wang, Q. (2011) Removal of heavy metal ions from wastewaters: A review, *Journal of Environmental Management* 92, 407-418.
- Freundlich H. M. F. (1906) Über die adsorption in lösungen”, *Zeitschrift für Physikalische Chemie (Leipzig)*, 57A, 385-470.
- Goel N. K., Bhardwaj Y. K., Manoharan R., Kumal V., Dubey K. A., Chaudhari C. V., Sabharwal S. (2009) Physicochemical and electrochemical characterization of battery separator prepared by radiation induced grafting of acrylic acid onto microporous polypropylene membranes, *Express Polymer Letters*, 3, 268–278.
- Gupta B., Anjum N. (2003) Preparation of ion-exchange membranes by the hydrolysis of radiation-grafted polyethylene-g-polyacrylamide films: properties and metal-ion separation, *J. Appl. Polym. Sci.*, 90, 3747-3752.
- Gupta B., Grover N., Singh H. (2009) Radiation grafting of acrylic acid onto poly(ethylene terephthalate) fabric. *J. Appl. Polym. Sci.*, 112, 1199–1208.
- Gupta B., Grover N., Mohanty S., Jain K.G., Singh H. (2010) Radiation grafting of acrylic acid/N-vinyl pyrrolidone binary mixture onto poly(ethylene terephthalate) fabric and growth of human mesenchymal stem cell. *J. Appl. Polym. Sci.* 115, 116–126.
- Gupta B., Mishra S., Saxena S. (2008) Preparation of thermosensitive membranes by

- radiation grafting of acrylic acid/N-isopropyl acrylamide binary mixture on PET fabric. *Radiat. Phys. Chem.*, 77, 553–560.
- Hamada H., Razik A., Kenawy E. R. (2012) Synthesis, characterization, and amidoximation of diaminomaleodinitrile-functionalized polyethylene terephthalate grafts for collecting heavy metals from wastewater, *J. Appl. Polym. Sci.*, 125, 1136-1145.
- Hara K., Iida M., Yano K., Nishida T. (2004) Metal ion absorption of carboxymethylcellulose gel formed by γ -ray irradiation For the environmental purification, *Colloids Surf., B.*, 38, 227–230.
- Hegazy, E.A., Kamal, H., Maziad, N., Dessouki. A. (1999) Membranes prepared by radiation grafting of binary monomers for adsorption of heavy metals from industrial wastes. *Nucl Instrum Meth Phys Res B*, 151, 386–92.
- Hegazy D.E.S. (2012) Selectivity of acrylic acid radiation grafted non-woven polypropylene sheets towards some heavy metals ions, *Open Journal of Polymer Chemistry*, 2, 6-13.
- Ho Y.S. (2006) Review of second-order models for adsorption systems, *J. Hazard. Mater.*, 136, 681-689.
- Ho Y.S., Ng J.C.Y., McKay G. (2001) Removal of Lead(II) from effluents by sorption on peat using second-order kinetics, *Separ. Sci. Technol.*, 36, 241-261.
- Huang L., Xiao C., Chen B. (2011) A novel starch-based adsorbent for removing toxic Hg(II) and Pb(II) ions from aqueous solution, *J. Hazard. Mater.*, 192, 832– 836
- Ho Y.S. (2006) Review of second-order models for adsorption systems, *J. Hazard. Mater.* 136, 681-689.
- Hsieh Y. L., Shinawatra M., Castillo M.D. (1986) Postirradiation polymerization of

- vinyl monomers on poly(ethylene terephthalate). *J. Appl. Polym. Sci.*, 31, 509-519.
- Ibrahim S.M., El-Salmawi K.M., El-Naggar A.A. (2006) Use of radiation grafting of polyethylene-coated polypropylene nonwoven fabric by acrylamide for the removal of heavy metal ions from wastewaters, *J. Appl. Polym. Sci.*, 102, 3240–3245.
- Irving H., Williams R.J.P. (1953) The stability of transition-metal complexes, *J. Chem. Soc.*, 3192–3210.
- Jin L., Bai R.B. (2002) Mechanisms of lead adsorption on chitosan/PVA hydrogel beads, *Langmuir*, 18, 9765-9770.
- Kattan M., El-Nesr E. (2006) γ -Radiation-induced graft copolymerization of acrylic acid onto poly(ethyleneterephthalate) films: a study by thermal analysis. *J. Appl. Polym. Sci.*, 102, 198–203.
- Karakısla M. (2003) The Adsorption of Cu(II) Ion from aqueous solution upon acrylic acid grafted poly(ethylene terephthalate) fibers, *J. Appl. Polym. Sci.*, 87, 1216-1220.
- Khezami L., Capart R. (2005) Removal of chromium(VI) from aqueous solution by activated carbons: kinetic and equilibrium studies, *J. Hazard. Mater.*, 123, 223-231.
- Knox B.H., Weigmann H.D., Scott M.G., Rebenfeld L. (1981) The Effects of an aqueous medium on the structure and physical properties of a polyester yarn, *Text. Res. J.*, 51(8), 549–558.
- Kobayashi T., Wang H. Y., Fujii N. (1998) Molecular imprint membranes of polyacrylonitrile copolymers with different acrylic acid segments, *Anal. Chim.*

Acta, 365, 81-88.

Ku, Y., Jung, I.L. (2001) Photocatalytic reduction of Cr(VI) in aqueous solutions by UV irradiation with the presence of titanium dioxide, *Water Res.* 35, 135-142.

Langmuir I. (1918) The adsorption of gases on plane surfaces of glass, mica and platinum, *J. Am. Chem. Soc.*, 40, 1361-1403.

Latha A.G., George B.K., Kannam K.G., Ninan K.N. (1991) Synthesis of a Polyacrylamide Chelating Resin and Applications in Metal Ion Extractions, *J. Appl. Polym. Sci.*, 43, 1159-1163.

Li N., Bai R. (2006) Highly Enhanced Adsorption of Lead Ions on Chitosan Granules Functionalized with Poly(acrylic acid), *Ind. Eng. Chem. Res.*, 45, 7897-7904.

Liu C., Huang Y., Naismith N., Economy J., Talbott J. (2003) Novel polymeric chelating fibers for selective removal of mercury and cesium from water, *Environ. Sci. Technol.* 37, 4261-4268.

Li Y., Yue Q.Y., Gao B.Y. (2010) Adsorption kinetics and desorption of Cu(II) and Zn(II) from aqueous solution onto humic acid, *J. Hazard. Mater.*, 178, 455-461.

Macknight W.J., Mckenna L.W., Read B.E., Stein R. S. (1968) Properties of ethylene methacrylic acid copolymers and their sodium salts: infrared studies, *J. Phys. Chem.*, 72, 1122-1126.

Martinovich V. I. and Polikarpov A. P. (2006) Effect of heat and solvent treatment on radiation grafting of acrylic acid to poly(ethylene terephthalate), *High Energ. Chem.*, 40, 149-153.

Max J. J., Chapados C. (2004) Infrared spectroscopy of aqueous carboxylic acids: comparison between different acids and their salts, *J. Phys. Chem.*, 108,

3324-3337.

Maziad N.A., Sayed M.S., Hegazy E.A. (2002) Use of radiation grafted PVC–acrylamide membranes in radioactive waste treatment, *Polym. Int.* 51, 155-155.

Molinari R., Poerio T., Cassano R., Picci N., Argurio P. (2004) Copper(II) removal from wastewaters by a new synthesized selective extractant and SLM viability, *Ind. Eng. Chem. Res.* 43, 623-628.

Namasivayam C., Kadirvelu K. (1999) Uptake of mercury (II) from wastewater by activated carbon from unwanted agricultural solid by-product: coirpith, *Carbon* 37, 79-84.

Nasef M.M. (2000) Gamma radiation-induced graft copolymerization of styrene onto poly(ethylene terephthalate) films, *J. Appl. Polym. Sci.*, 77, 1003–1012.

Naseem R., Tahir S.S. (2001) Removal of Pb(II) from aqueous solution by using bentonite as an adsorbent, *Water Res.* 35, 3982-3986.

National effluent standards, Ministry of the Environment, Government of Japan, <http://www.env.go.jp/en/water/wq/nes.html>

Oyaro N., Juddy O., Murago E.N.M., Gitonga E. (2007) The contents of Pb, Cu, Zn and Cd in meat in Nairobi Kenya, *Int. J. Food Agric. Environ.* 5, 119-121.

Paulino A.T., Minasse F.A.S., Guilherme M.R., Reis A.V., Muniz E.C., Nozaki J. (2006) Novel adsorbent based on silkworm chrysalides for removal of heavy metals from wastewaters, *J. Colloid Interface Sci.* 301, 479-487.

PET bottle recycling in Japan, the council for PET bottle recycling, CPBR, Japan, (2012) http://www.petbottle-rec.gr.jp/english/pdf/reports/0_All_pages.pdf (accessed February 2014).

- Ping X., Wang M., Ge X. (2011) Radiation induced graft copolymerization of n-butyl acrylate onto poly(ethylene terephthalate) (PET) films and thermal properties of the obtained graft copolymer. *Radiat. Phys. Chem.*, 80, 632-637.
- Ping X., Wang M., Ge X. (2010) The study on grafting comonomer of n-butyl acrylate and styrene onto poly(ethylene terephthalate) film by gamma-ray induced graft copolymerization. *Radiat. Phys. Chem.*, 79, 941-946.
- Rao K.N., Rao M.H., Lokhande H.T., Mody N.R. Jog A.G. (1979) Grafting onto polyester fibers. II. Kinetics of grafting of acrylic acid, acrylonitrile, and vinyl acetate onto polyester fibers, *J. Appl. Polym. Sci.*, 23, 2133-2138.
- Rahman N., Sato N., Yoshioka S., Sugiyama M., Okabe H., Hara K. (2013) Selective Cu(II) adsorption from aqueous solutions including Cu(II), Co(II) and Ni(II) by modified acrylic acid grafted PET film, *ISRN Polym. Sci.*, 2013, Article ID 536314, 9 pages.
- Rafatullah M., Sulaiman O., Hashim R., Ahmad A. (2009) Adsorption of copper (II), chromium (III), nickel (II) and lead (II) ions from aqueous solutions by meranti sawdust, *J. Hazard. Mater.*, 170, 969-977.
- Raji C., Anirudhan T.S. (1998) Batch Cr(VI) removal by polyacrylamide grafted sawdust: kinetics and thermodynamics, *Wat. Res.* 32, 3772-3780.
- Rengaraj S., Yeon J.W., Kim Y., Jung Y., Ha Y.K., Kim W.H. (2007) Adsorption characteristics of Cu(II) onto ion exchange resins 252H and 1500H: kinetics, isotherms and error analysis, *J. Hazard. Mater.*, 143, 469-477.
- Rivas B.L., Schiappacasse L.N., Pereira U.E. Moreno-Villoslada I. (2004) Interactions of polyelectrolytes bearing carboxylate and/or sulfonate groups with Cu(II) and Ni(II), *Polymer.*, 45, 1771-1775.

- Ribnick A.S., Weigmann H.D., Rebenfeld L. (1972) Interactions of nonaqueous solvents with textile fibers: part I: effect of solvents on the mechanical properties of a polyester yarn, *Text. Res. J.*, 42(12), 720–726.
- Rocha C.G., Zaia D.A.M., Alfaya R.V.S., Alfaya A.A.S. (2009) Use of rice straw as biosorbent for removal of Cu(II), Zn(II), Cd(II) and Hg(II) ions in industrial effluents, *J. Hazard. Mater.*, 166, 383–388.
- Saçak M., Oflaz F. (1993) Benzoyl-peroxide-initiated graft copolymerization of poly(ethylene terephthalate) fibers with acrylic acid. *J. Appl. Polym. Sci.*, 50, 1909-1916.
- Saçak M., Sertkaya F., Talu M. (1992) Grafting of poly(ethylene terephthalate) fibers with methacrylic acid using benzoyl peroxide. *J. Appl. Polym. Sci.* 44, 1737-1742.
- Şanlı O., Aytemiz S., Ünal H.İ. (1997) Graft Copolymerization of acrylamide on swollen poly(ethylene Terephthalate) fibers using cerium ammonium nitrate initiator, *J. Macromol. Sci. Pure Appl. Chem.* 34, 1003-1015.
- Sciban, M., Klasnja, M., Skrbic B. (2006) Modified softwood sawdust as adsorbent of heavy metal ions from water, *J. Hazard. Mater.* 136, 266-271.
- Schmuhl R., Krieg H.M., Keizer K. (2001) Adsorption of Cu(II) and Cr(VI) ions by chitosan: kinetics and equilibrium studies, *Water SA*, 27, 1-7.
- Shah R., Devi S. (1996) Preconcentration of mercury(II) on dithizone anchored poly(vinyl pyridine) support, *React. Funct. Polym.*, 31,1-9.
- Shukla S.R., Sakhardande V.D. (1992) Column studies on metal ions removal by dyed cellulosic materials, *J. Appl. Polym. Sci.*, 44, 903-910.
- Sonmez H.B., Senkal B.F., Sherrington D.C., Bicak N. (2003) Atom transfer radical

- graft polymerization of acrylamide from *N*-chlorosulfonamidated polystyrene resin, and use of the resin in selective mercury removal, *React. Funct. Polym.*, 55, 1–8.
- Sonmez H.B., Senkal B.F., Sherrington D.C., Bıcak N. (2002) Poly(acrylamide) grafts on spherical bead polymers for extremely selective removal of mercuric ions from aqueous solutions, *J. Polym. Sci. Polym. Chem.*, 40, 3068–3078.
- Srivastava N.K., Majumder C.B. (2008) Novel biofiltration methods for the treatment of heavy metals from industrial wastewater, *J. Hazard. Mater.* 151, 1-8.
- Ştefan D.S., Untea I., Neagu V., Luca C., Ştefan M. (2008) Selective retention of Hg²⁺ ions from aqueous solutions by various amide groups-functionalized copolymers, *Rev. Roum. Chim.*, 53, 617–622.
- Sud D., Mahajan G, Kaur M.P. (2008) Agricultural waste material as potential adsorbent for sequestering heavy metal ions from aqueous solutions – A review, *Bioresour. Technol.* 99 (2008) 6017–6027
- Temoçin Z., Yiğitoğlu M. (2010) Studies on selective uptake behavior of Hg(II) and Pb(II) by functionalized poly(ethylene terephthalate) fiber with 4-vinyl pyridine/2-hydroxyethylmethacrylate, *Water Air Soil Pollut.*, 210, 463–472.
- The world in transition, and Japan's efforts to establish a sound material-cycle Society, Ministry of Environment Government of Japan, (2008) http://www.env.go.jp/en/recycle/smcs/a-rep/2008gs_full.pdf (accessed February 2014).
- Tuhin M. O., Rahman N., Haque M.E., Khan R.A., Dafader N.C., Islam R., Nurnabi M., Tonny W. (2012) Modification of mechanical and thermal property of chitosan–starch blend films, *Radiat. Phys. Chem.*, 81, 1659–1668.

- Uchida E., Uyama Y. and Ikada Y. (1990) A novel method for graft polymerization onto poly (ethylene terephthalate) film surface by UV irradiation without degassing, *J. Appl. Polym. Sci.*, 41,677-687.
- Ui J. (Ed.) (1992) *Industrial Pollution in Japan (The Japanese Experience Series)*, United Nations University Press, Tokyo. (Full text is also available at <http://www.unu.edu/unupress/unupbooks/uu35ie/uu35ie00.htm>).
- Ünlü N., Ersöz M. (2006) Adsorption characteristics of heavy metal ions onto a low cost biopolymeric sorbent from aqueous solutions, *J. Hazard. Mater.*, 136, 272-280.
- Wahi R., Ngaini Z., Usun Jok V. (2009) Removal of mercury, lead and copper from aqueous solution by activated carbon of palm oil empty fruit bunch, *World Appl. Sci. J.*, 5, 84-91.
- Wang J., Xu L., Cheng C., Meng Y., Li A. (2012) Preparation of new chelating fiber with waste PET as adsorbent for fast removal of Cu^{2+} and Ni^{2+} from water: Kinetic and equilibrium adsorption studies, *Chem. Eng. J.*, 193–194, 31–38.
- Wikipedia, the free encyclopedia, http://en.wikipedia.org/wiki/Polyethylene_terephthalate
- Wirse'n A., Sun H., Albertsson A. C. (2005) Solvent-free vapor-phase photografting of acrylamide onto poly(ethylene terephthalate), *Biomacromolecule*, 6, 2697-2702.
- Yan H., Dai J., Yang Z., Yang H., Cheng R. (2011) Enhanced and selective adsorption of copper(II) ions on surface carboxymethylated chitosan hydrogel beads, *Chem. Eng. J.*, 174, 586– 594.
- Yao Z.P. and Ranby B. (1990) Surface modification by continuous graft copolymerization. III. Photoinitiated graft copolymerization onto poly

- (ethylene terephthalate) fiber surface, *J. Appl. Polym. Sci.*, 41, 1459-1467.
- You-Lo H., Pugh C., Ellison M.S. (1984) The Effects of Selected Organic Solvents on the Polymerization of Acrylic Acid to Poly(ethylene Terephthalate) by Glow Discharge, *J. Appl. Polym. Sci.*, 29, 3547-3560.
- Yiğitoğlu M., Arslan M. (2005) Adsorption of hexavalent chromium from aqueous solutions using 4-vinyl pyridine grafted poly(ethylene terephthalate) fibers, *Polym. Bull.*, 55, 259–268.
- Yiğitoğlu M., Arslan, M. (2009) Selective removal of Cr(VI) ions from aqueous solutions including Cr(VI), Cu(II) and Cd(II) ions by 4-vinyl pyridine/2-hydroxyethylmethacrylate monomer mixture grafted poly(ethylene terephthalate) fiber, *J. Hazard. Mater.*, 166, 435–444.
- Zhang H., Du Z., Jiang Y., Yu Q. (2012) Preparation and characterization of grafting polyacrylamide from PET films by SI-ATRP via water-borne system, *J. Appl. Polym. Sci.*, 126, 1941-1955.
- Zhang F., Nriagu J.O., Itoh H. (2004) Photocatalytic removal and recovery of mercury from water using TiO₂-modified sewage sludge carbon, *J. Photochem. Photobiol.*, 167, 223–228.
- Zhou C., Zhang H.W., Jiang Y., Wang W.J., Yu Q. (2011) Grafting of polyacrylamide from poly(ethyleneterephthalate) films, *J. Appl. Polym. Sci.*, 121, 1254–1261.
- Zhu X., Alexandratos S.D. (2005) Affinity and selectivity of immobilized *N*-methyl-D-glucamine for mercury(II) ions, *Ind. Eng. Chem. Res.*, 44, 7490-7495.

APPENDIX A

Abbreviated words

PET	Polyethylene terephthalate
AAm	Acrylamide
AAc	Acrylic acid
DMSO	Dimethyl sulfoxide
PIT	Preirradiation technique
SIT	Simultaneous irradiation technique.
St	Styrene
AN	Acrylonitrile
NIPAAm	N-isopropylacrylamide
NVP	N-vinylpyrrolidone
MEK	Methyl ethyl ketone
DMF	N,N-Dimethylformamide
THF	Tetrahydrofuran
DCM	Dichloromethane
MAA	Methacrylic acid
IA	Itaconic acid
GMA	Glycidyl methacrylate
4-VP	4-vinyl pyridine

HEMA	2-hydroxyethylmethacrylate
SI-ATRP	Surface-initiated atom transfer radical polymerization
UV	Ultraviolet

Symbols

Hg	Mercury
Pb	Lead
Cu	Copper
Co	Cobalt
Ni	Nickel
Cr	Chromium
Cd	Cadmium
Zn	Zinc

List of Publications

CHAPTER 2

- a) Nazia Rahman, Nobuhiro Sato, Masaaki Sugiyama, Yoshiki Hidaka, Hirotaka Okabe, and Kazuhiro Hara, The effect of hot DMSO treatment on the γ -ray induced grafting of acrylamide onto PET films, Published online in polymer Journal ; doi:10.1038/pj.2014.12.
- b) Nazia Rahman, Nobuhiro Sato, Satoru Yoshioka, Masaaki Sugiyama, Hirotaka Okabe, and Kazuhiro Hara, “DMSO-Assisted Grafting of Acrylamide onto PET Film by γ Irradiation”, KURRI Progress Report 2012, pp 218.

CHAPTER 3

- a) Nazia Rahman, Nobuhiro Sato, Masaaki Sugiyama, Yoshiki Hidaka, Hirotaka Okabe, and Kazuhiro Hara, Selective Hg(II) adsorption from aqueous solutions of Hg(II) and Pb(II) by hydrolyzed acrylamide-grafted PET films, Journal of environmental science and health, Part A, (2014) 49, 798–806, DOI: 10.1080/10934529.2014.882209.

CHAPTER 4

- a) Nazia Rahman, Nobuhiro Sato, Satoru Yoshioka, Masaaki Sugiyama, Hirotaka Okabe, and Kazuhiro Hara, Selective Cu(II) adsorption from aqueous solutions including Cu(II), Co(II), and Ni(II) by modified acrylic acid grafted PET film, ISRN Polymer Science, Vol. 2013, Article ID 536314, 9 pages.
<http://dx.doi.org/10.1155/2013/536314>

Acknowledgments

Firstly, all praise and thanks to Allah, the almighty, for making my efforts fruitful and giving me the opportunity to complete the doctoral study successfully. I would like to express my sincere gratitude to all the people who have supported and encouraged me in this study.

I would like to express the deepest appreciation to my principal supervisor Professor Dr. Kazuhiro Hara of Kyushu University for his continuous encouragement and support throughout my PhD study especially without his active guidance, patience, motivation and knowledge this thesis would not have been possible. His kind support on both research and personal level has been precious.

I would like to share the credit of my PhD research work with the collaborating co-supervisor Dr. Nobuhiro Sato of Research Reactor Institute, Kyoto University for the continuous insight discussions and sharing ideas through e-mails that really supported me a lot to make this contribution.

I would like to acknowledge the supervisors of my PhD committee.

I highly appreciate Dr. Hirotaka Okabe of Kyushu University for his kind support in various aspects during my study period. Special thanks go to Dr. Yoshiki Hidaka and Dr. Satoru Yoshioka of Kyushu University for their kind co-operation. Also I would like to thank Dr. Masaaki Sugiyama of Research Reactor Institute, Kyoto University for helpful suggestions.

Enormous thanks go to all the members of Hara laboratory for their warm support, particularly I would like to thank Mr. Sano Takahiro, Keigo Tsuru, Seiya Fuziwara, Tomo Yanagino and Mr. Masaki Yuji for their helpful co-operation in

performing different experiments and Mr. Takashi Nishimoto, Ahmad Hassan Sallehudin Bin Mohd Sarif, Kyohei Iwamoto, Miyazaki Tomohiro and Ms. Iino Misato for their friendly company in my Kyushu University life.

I wish to acknowledge the useful support of the ^{60}Co γ -ray irradiation facility of Research Reactor Institute, Kyoto University. The financial support from the Ministry of Education, Culture, Sports, Science and Technology, Japan under the MONBUKAGAKUSHO Scholarship is appreciatively acknowledged. This research was also supported by JSPS KAKENHI Grant Number 24360398.

Words cannot express how grateful I am to my Parents, Dr. Mafizur Rahman and Shahnaz Rahman who supported me in every step of my life. Their prayer carried me to this stage. Thanks also to all my relatives for their sincere encouragement.

I am indebted to my husband Md. Shamsuzzaman who helped me to realize my potential and supported me practically and emotionally from my undergraduate study. A special thanks to my son Sazid Bin Zaman for his enormous love that encouraged me in this study.